ABSTRACT

PHELPS, DRAKE WILLIAM. Investigating the Neutrophil Respiratory Burst as a Target of Xenobiotics. (Under the direction of Dr. Jeffrey Yoder).

Innate immune cells are often referred to as the "first responders" of the immune system, as they work on the scale of minutes to hours in order to protect the host from pathogenic invasion. In contrast, adaptive immune cells, while much more specific, need days to weeks to mount their response. Despite this, tiered functional adaptive immunity assays in low-throughput rodent models serve as the "gold standard" for immunotoxicity testing of xenobiotics. Testing guidelines from the United States Environmental Protection Agency fail to mention key cells of the innate immune system, such as neutrophils, in their testing paradigms for hazard identification of immunotoxic compounds. Neutrophils are the most abundant leukocyte in circulation, making them a large target for xenobiotic exposure. In this Dissertation, I sought to fill this wide gap by asking if xenobiotics with known and unknown immunotoxicity profiles inhibit one critical function of neutrophils – the respiratory burst. The respiratory burst is the rapid induction of reactive oxygen species (ROS) that are created to kill invading pathogens while also amplifying the immune response, and inhibition of this process may confer susceptibility to infectious disease.

In Chapter 1, I explore the current literature of one large class of chemicals, per- and polyfluoroalkyl substances (PFASs) and the data surrounding their immunotoxic properties in the innate immune system. Several reviews of the immunotoxic effects of PFASs have been published, but they remained focused on the adaptive immune system. While data exist for some of these compounds' effects on innate immunity, many of those data conflict across multiple studies depending on the PFASs and endpoints of interest. In this Chapter, I discuss these

reported contradictions across humans, experimental animals, and wildlife while exposing the data gaps that still surround these compounds' immunotoxicity.

In Chapter 2, I asked whether larval zebrafish can be used to screen compounds for immunotoxicity by assessing respiratory burst *in vivo* after xenobiotic exposure. Larval zebrafish offer an excellent model of human and ecotoxicological immunological health; they also do not possess a functional adaptive immune system, allowing study of the innate immune system with no influence from adaptive immune cells. In this chapter, I show that five compounds suppress the respiratory burst of larval zebrafish: benzo[a]pyrene, 17β-estradiol, lead acetate, methoxychlor, and phenanthrene. Each of these compounds have known immunotoxicity in mammalian models, thus validating the use of the zebrafish model for hazard identification of immunotoxic xenobiotics.

In Chapter 3, I return to the impacts of PFASs on innate immunity by screening nine environmentally relevant PFASs for their ability to suppress the respiratory burst. Perfluorohexanoic acid (PFHxA) and ammonium perfluoro(2-methyl-3-oxahexanoate) (GenX) were identified as PFASs with the ability to suppress the respiratory burst in larval zebrafish. These results were recapitulated in a human neutrophil-like cell line *in vitro*, validating the use of the zebrafish for human health. Finally, I showed that GenX suppressed the neutrophil respiratory burst in primary human neutrophils exposed *ex vivo*. I am the first to show that these two compounds suppress neutrophil function in any species, and this work supports the notion from Chapter 1 that PFASs can functionally inhibit innate immunity.

Finally, in Chapter 4, I synthesize all the data from this Dissertation to give context on what they may mean for the field of immunotoxicology at large. I also provide insight into where I think these data should lead future researchers who seek to expand upon my work through

investigations of mechanism, transcriptomics and metabolomics, and other high-throughput assays. Ultimately, this work serves as a starting point for utilizing high-throughput methodologies for identifying immunotoxic compounds that inhibit innate immune function.

Investigating the Neutrophil Respiratory Burst as a Target of Xenobiotics

by
Drake William Phelps

A dissertation submitted to the Graduate Faculty of
North Carolina State University
in partial fulfillment of the
requirements for the degree of
Doctor of Philosophy

Comparative Biomedical Sciences

Raleigh, North Carolina
2022

APPROVED BY:

_____	_____
Dr. Jeffrey Yoder Committee Chair	Dr. James Bonner
_____	_____
Dr. Heather Patisaul	Dr. David Reif
_____	
Dr. Mary Sheats	

DEDICATION

I dedicate this work to all the communities around the world who are grappling with contamination of their water, food, and air because of corporate greed and pollution. May you find the justice you deserve and the answers necessary to protect the health of you and your loved ones.

BIOGRAPHY

Drake William Phelps is the only child of William and Kelly Phelps. He was born and raised in Danville, Virginia. His passion for science was always encouraged by his parents, science educators, and friends. Drake graduated as valedictorian of the Class of 2012 from Chatham High School. He also attended Piedmont Governor's School for Math, Science, and Technology to further foster his love for science. His first research experience occurred here under the guidance of Dr. Yinghui Dan. He also obtained his Associate's Degree from Danville Community College in 2012. Drake then attended North Carolina State University to obtain his undergraduate degree. Here, he majored in Microbiology while minoring in Biotechnology and French Language. While obtaining his degree, he worked alongside then-doctoral candidate Tiffany Garbutt, under direction of Dr. David Aylor, and Dr. Bryan Troxell, under direction of Dr. Hosni Hassan. It was also at this time where he would meet his future partner, Clinton Willis. Upon graduating in December of 2015, Drake joined the lab of Dr. Tamara Tal at the United States Environmental Protection Agency. This research experience was formative for Drake's identity as a toxicologist who cares passionately about protecting human and environmental health from toxic chemicals. Drake returned to North Carolina State University to pursue a graduate career under the mentorship of Dr. Jeffrey Yoder where he spent his time studying how environmental contaminants impact the innate immune system of fish and humans. Even during the COVID-19 pandemic, Drake remained determined to finish this degree, which would not have happened without the excellent mentors with which he surrounded himself. Looking to the future, Drake currently hopes to start his own research program and, one day, be the Administrator of the United States Environmental Protection Agency.

ACKNOWLEDGMENTS

I would not have made it to the end of this journey if not for so many incredible people. I first must thank Dr. Jeff Yoder who was, is, and will always be a key mentor for my success. He gave me the freedom to pursue the research questions I had, allowing my curiosity to drive this project and his laboratory to uncharted territories. He encouraged me to think bigger, smarter, and harder each day; I could not have had a better graduate mentor. I also have to thank my outstanding committee members, Drs. James Bonner, Heather Patisaul, Katie Sheats, and David Reif. All of them asked excellent questions, challenged me, and gave feedback and advice that I will always hold with me. This committee was a team of rock star scientists that made me feel like a colleague and collaborator rather than a student.

Next, I have to thank my incredible partner, Clinton Willis, for sticking with me through this entire process. He was there when I submitted my application and was accepted into this program. He supported me through all of the highs and lows, making sure that I kept my eyes on the light at the end of a very long tunnel. I love him so much, and I cannot thank him for letting me talk about PFAS, reactive oxygen species, and zebrafish at any given moment. There are not enough words to describe the immense amount of gratitude I hold for this man. Swiper and I are so lucky to have him.

Next, I'd like to thank my parents, William and Kelly Phelps. They brought me into this world and fostered my love for science from a very young age. They were instrumental to my success to this point, and I hope they are proud to see the little boy who used to experiment with putting various things in the freezer grow into a fully-fledged scientist. I am thankful for their sage advice, listening ears, and hot meals.

There is a long list of so many other people that made an impact on me throughout this process – it really does take a village. I'd like to thank former and current members of the Yoder Lab (especially Jacob Driggers, Anika Palekar, and Kara Carlson), Dr. Tamara Tal, Dr. Haleigh Conley, Katie Sapko, Dana Hodorovich, Dr. Jamie DeWitt, Shannon Chiera, the Comparative Biomedical Sciences Graduate Student Association, the students and faculty of Immunology Journal Club, the students of Toxicology Program, the Molecular Biotechnology Training Program, the NC State University PFAS Working Group, the NC State University Center for Environmental and Health Effects of PFAS, the teams at Center for Environmental Health, Clean Cape Fear, and Cape Fear River Watch, and all of my friends who called or texted just to check in or get a research update. The support network I had carried me to the finish line, and I am forever grateful.

I'd like to thank Dr. Karen Erikson and Dr. Steve Vas for their support of my mental and physical health throughout my graduate career and beyond. Lastly, I also would like to thank any musical artist or podcast host who kept me company during long hours alone in the lab.

TABLE OF CONTENTS

LIST OF TABLES

Chapter 1

Chapter 3

LIST OF FIGURES

Chapter 1

Chapter 2

Chapter 3

Appendix A

Appendix B

CHAPTER 1

Per- and polyfluoroalkyl substances alter innate immune function: evidence and data gaps

Drake W. Phelps[1,2,3], Ashley Connors[1], Giuliano Ferrero[1], and Jeffrey A. Yoder[1,2,3,4]

[1]Department of Molecular Biomedical Sciences, College of Veterinary Medicine, North Carolina State University, Raleigh, NC, USA

[2]Comparative Medicine Institute, North Carolina State University, Raleigh, NC, USA

[3] Center for Environmental and Health Effects of PFAS, North Carolina State University, Raleigh, NC, USA

[4]Center for Human Health and the Environment, North Carolina State University, Raleigh, NC, USA

This chapter was written with the intent to be published as a review article, but it was not submitted for publication prior to the defense of this dissertation. DWP wrote the first draft of this chapter. AC, GF, and JAY provided significant contributions regarding structure and content of this chapter.

ABSTRACT

Per- and polyfluoroalkyl substances (PFASs) are a large class of compounds used in a variety of processes and consumer products. Their unique chemical properties make them economically viable and societally convenient while also making them ubiquitous and persistent environmental contaminants. To date, several reviews have been published to synthesize the information regarding the immunotoxic effects of PFASs in the adaptive immune system. However, these reviews often do not acknowledge the contribution of these compounds on innate immunity. Here, I review the existing literature to incorporate the data regarding the effects of PFASs on innate immunity in humans, experimental animals, and wildlife. For many PFASs, their effects on innate immunity are unknown. For those with data in this branch of the immune system, results often conflict among different studies, thus raising more questions than are answered and making conclusions difficult to draw. Despite this, there is data to support that PFASs can activate and suppress the innate immune system in several species. Recommendations are provided for future research foci in order to inform hazard identification, risk assessment, and risk management practices for PFASs in order to protect human and environmental health.

Keywords: per- and polyfluoroalkyl substances, PFAS, innate immunity, human, zebrafish, wildlife

INTRODUCTION

Per- and polyfluoroalkyl substances (PFASs) are a large class of fluorinated compounds that are used in the production of non-stick cookware, food contact materials, water-, oil-, and stain-resistant fabrics and coatings, and aqueous film-forming foams (AFFFs), among other products. To be more specific, PFASs contain at least one carbon atom wherein all hydrogen atoms have been replaced by fluorine atoms and contain a C_nF_{2n+1}-R moiety (Buck et al., 2011). This class of compounds is incredibly diverse, with nearly 5,000 different PFASs registered globally, according to an Organization for Economic Co-operation and Development (OECD) database (OECD, 2018). However, an expansive list from the United States Environmental Protection Agency (USEPA) greatly expands this number to more than 12,000 compounds when other chemical moieties containing a carbon-fluorine bond are considered (USEPA, 2019b). A subset of roughly 1,200 PFASs appear in the United States Toxic Substances Control Act (TSCA) Chemical Inventory, with more than 600 described as commercially active (USEPA, 2019a; Rizzuto, 2020).

PFASs entered large-scale production in the 1950s, and at the time, the most common PFASs intentionally produced were perfluorooctanoic acid (PFOA) and perfluorooctane sulfonic acid (PFOS) (Buck et al. 2011). However, as more studies observed the toxicities exerted by these two legacy PFASs, fluorochemical manufacturers sought, in part due to the PFOA Stewardship Agreement with USEPA, to phase out these compounds with novel replacements possessing more favorable toxicity profiles (USEPA 2006). However, these alternatives were relatively untested before entering the market, and the manufacture of these replacement compounds led to the creation of other PFASs as byproducts (Hopkins et al. 2018). Therefore, even though emissions of long-chain legacy PFASs had decreased, emissions of new, short-chain

replacement PFASs, their byproducts, and their degradants have now increased (Hopkins et al. 2018). Notable members of these new PFASs include a sub-family known as per- and polyfluorinated ether acids (PFEAs), which possess ether linkages in the carbon backbone of the molecule (Hopkins et al. 2018; Cousins et al. 2020). While some studies of how these ether linkages impact persistence, bioaccumulation, and toxicity have been performed, many are ongoing. Structures of the various PFASs discussed in this Chapter can be found in **Figure 1**.

Exposure to PFASs can occur through multiple routes. Most notably, humans are exposed to PFASs through drinking water that is contaminated from industrial sources, use of AFFs at airports and military bases, and runoff from landfill leachate (Hu et al. 2016; Boone et al. 2019; Domingo and Nadal 2019). It has recently been estimated that the drinking water of more than 200 million Americans is contaminated with PFASs (Andrews and Naidenko 2020). Exposure to PFASs also can occur through consumption of contaminated food, inhalation of indoor dust, and dermal exposure with PFAS-treated textiles (Boronow et al. 2018; Chen et al. 2020, Poothong et al. 2020). Fetuses are exposed to PFASs *in utero*, and infants can be exposed to PFASs through breast milk (Blake and Fenton 2020). Given the distinct chemical characteristics of PFASs and their well-documented, widespread exposure, questions have been raised of the hazard and risk that PFASs contribute to human and environmental health. Others have reviewed the toxicity of these compounds in humans, animal models, and wildlife (ATSDR 2021; DeWitt 2015; Fenton et al. 2020; Bangma et al. 2022), which includes elevated cholesterol, thyroid disruption, and cancer. Of particular interest, many have noted the immunotoxicity of these compounds, which has also been reviewed extensively (Chang et al. 2016; DeWitt et al. 2018; NTP 2016). Adverse immune-related outcomes associated with exposure to PFASs include ulcerative colitis, allergic sensitization, and reduced response to vaccination. Indeed, the immune system appears to be a

sensitive target of PFASs, and immunotoxicity has been used to drive risk assessments and statewide regulations across the United States (Cordner et al. 2019; ITRC 2020). While previous reviews were recent and remain relevant, there remains a heightened interest in PFAS-induced immunotoxicity, leading to further research in hazard identification and mechanism of action for these compounds.

In my review of the literature, however, I noted that there is a gap in previous reviews that neglected data indicating that PFASs impact innate immunity. Here, I review the impacts of PFAS exposure on innate immunity in humans, experimental animals, and ecotoxicological models and wildlife. In doing so, I will not only synthesize current data and examine ongoing contradictions, but also reveal where data gaps exist so that future work can focus on filling them. The toxicity of most PFASs remains unknown, and filling these gaps is necessary to understand their hazard and risk to human and environmental health. There are even larger data gaps with regards to these compounds' effects on innate immunity, despite it being well-established that several PFASs are immunotoxic. The scope of this review will be limited to previous reports that investigate innate immunity on several fronts: immunophenotyping of innate immune cell populations, changes in concentrations of cytokines relevant to innate immunity, and functional assays of innate immune cells. The goal of this review is to expand the knowledge base of what is known about PFASs in an oft-overlooked branch of the immune system when it comes to chemical hazard identification and risk assessment.

EVIDENCE OF INNATE IMMUNE MODULATION BY PFASS IN HUMANS

Several studies have sought to understand the impacts of PFAS exposure in the general population as well as populations exposed to high levels of PFAS as a result of large-scale or long-term contamination (summarized in **Table 1**). Most reports have investigated the effects of

PFASs on adaptive immunity in these populations, but few have asked essential questions about their effects on innate immunity. Immunophenotyping has shown that increasing serum levels of PFOA, PFOS, perfluorodecanoic acid (PFDA), perfluorononanoic acid (PFNA), and perfluorohexane sulfonic acid (PFHxS) are correlated with decreases in innate immune cell populations, including the number of monocytes, neutrophils, eosinophils, basophils, and natural killer (NK) cells, though results are not consistent across studies (Lopez-Espinosa et al. 2021, Goodrich et al. 2021). It has been reported that total serum PFASs, when analyzed as a mixture, were linked to increases in the number of basophils in the blood (Oulhote et al. 2017). These studies show that several PFASs are able to impact the levels of innate immune cells in circulation; however, the lack of consensus in this endpoint makes further conclusions difficult.

The impact of PFAS exposure on serum cytokine levels reveal similar contradictory trends. PFOA has been reported to both decrease and increase levels of interferon-γ (IFN-γ) in serum (Bassler et al. 2019; Abraham et al. 2020). These observations point to this compound having the ability to impact this pathway, but the conflicts in the directionality of this endpoint continue to raise questions. Bassler et al. (2019) also noted that PFOA, PFOS, PFHxS, and PFNA downregulate tumor necrosis factor α (TNF-α) and/or interleukin (IL) 8. Given that cytokine levels can decrease or increase in response to PFAS exposure, the response appears to be specific and not linked to a systemic adverse outcome. The conflicts in these observations may be due to differences in exposure levels and duration, interactions of mixtures of PFASs, the timing of when cytokine levels were measured, or genetic differences in one population to another. It is also unknown how recent infections or other environmental conditions may be shaping these epidemiological data. More studies are necessary to elucidate immunological and mechanistic implications from these findings.

In experimental systems, PFASs have been studied to a greater extent because of the flexibility that is offered by human cell lines *in vitro* and primary cells *ex vivo*. Most studies to date have focused on cytokine expression at the transcript and protein level. In whole blood and THP-1 cells (a human monocytic leukemia cell line), PFOA, PFOS, perfluorobutane sulfonic acid (PFBS), perfluorooctane sulfonamide (PFOSA), PFDA, and 8:2 fluorotelomer alcohol (FTOH) downregulated various cytokines, including TNF-α, IL-10, IL-6, IL-8, and IL-4 (Brieger et al. 2011; Corsini et al. 2011; Corsini et al. 2012). However, PFOA also induced TNF-α, IL-6, IL-8, and IL-1β in HMC-1 cells,a human mast cell leukemia cell line (Singh et al. 2012). Although this may point to differences in PFAS susceptibility between monocytic and granulocytic cells, a recent study revealed that the two cell types may share a target as IL-1β also was upregulated in THP-1 cells, with PFOS specifically activating the absent in melanoma 2 (AIM2) inflammasome (Wang et al. 2021); this is an important mechanistic finding which may elucidate some of the pro-inflammatory effects observed after PFAS exposure.

Functional assays using these cellular systems have largely focused on disruption of the nuclear factor κB (NF-κB) activation pathway. As observed for TNFα, results conflict between THP-1 cells and HMC-1 cells: PFOA inhibited NF-κB activation in THP-1 cells but activated this pathway in HMC-1 cells (Corsini et al. 2011; Singh et al. 2012). These findings are intriguing, but there still lacks a singular mechanism that can explain these phenotypes. Corsini et al. (2011; 2012) hypothesized that peroxisome proliferator-activated receptor α (PPARα), a well-known molecular target of PFASs, is responsible; however, their data suggest that this may be a viable candidate for only some PFASs. Other *in vitro and ex vivo* functional investigations in primary human neutrophils have shown that exposure to perflubron, perfluorodecalin (as an ingredient of Fluosol-DA), perfluorotributylamine (PFTBA), PFHxA, GenX, or mixtures of

several PFASs can suppress and activate the production of reactive oxygen species (ROS) (Virmani et al. 1984; Berntsen et al. 2022; See Chapter 3), inhibit phagocytosis (Virmani et al. 1984; Fernandez et al. 2001), and inhibit chemotaxis (Fernandez et al. 2001). NK cell cytolysis was also suppressed by exposure to PFOS (Brieger et al. 2011). Together, these human studies – epidemiological, *in vitro*, and *ex vivo* – illuminate the massive data gaps that remain regarding the effects of PFASs on innate immunity in humans. Contradictory results from epidemiological studies, as well as *in vitro* and *ex vivo* experiments, make it difficult to declare conclusive findings.

EVIDENCE OF INNATE IMMUNE MODULATION BY PFASS IN MAMMALIAN MODELS

Given the impacts of PFAS exposure on innate immunity that have been observed in humans, researchers have sought to replicate these findings in animal models. Most research to date has occurred in mammalian models (summarized in **Table 2**). As described above with human studies, results using mice (*Mus musculus*), rats, (*Rattus norvegicus*) and rabbits (*Oryctolagus cuniculus*) conflict among different laboratories and different PFASs. In these models, exposure to several PFASs, including PFOA, PFOS, PFNA, PFDA, perfluoroundecanoic acid (PFUnDA), PFTBA, perfluorobutanoic acid (PFBA), or perfluoromethoxybutanoic acid (PFMOBA), was associated with increases and decreases in neutrophil, macrophage, and NK cell numbers in blood and tissues (Bodin et al. 2016, Fang et al. 2008, Frawley et al. 2018, Guo et al. 2021, Han et al. 2018a, Han et al. 2018b, Qazi et al. 2009, Qazi et al. 2010, Qazi et al. 2010, Qazi et al. 2012, Virmani et al. 1983, Weatherly et al. 2021, Woodlief et al. 2021, NTP et al. 2019). Even within the same laboratory, it was reported that PFOA can increase or decrease the number of neutrophils and macrophages; however, while decreases were observed in the

blood, increases were observed in the liver (Qazi et al. 2009, Qazi et al. 2010). This may indicate that the immune compartments are differentially affected by PFAS exposure, potentially due to how PFASs themselves distribute *in vivo*. Without further study, however, it is difficult to ascertain whether the increase in the liver is an inflammatory response caused by damage to the liver or a coincidental pro-inflammatory state caused in the immune cells independent of the liver. Regardless, alteration in the immunophenotype remains a sensitive but non-specific endpoint by which PFASs may exert immunotoxicity.

As with human studies, cytokine levels are often studied because they are technically easy to collect and measure from serum and tissues. Recent data have shown that PFOA and PFOS, PFNA, along with three of their novel alternatives, 8:2 FTOH, 6:2 fluorotelomer carboxylic acid (6:2 FTCA) and 6:2 fluorotelomer sulfonic acid (6:2 FTSA), alter expression levels of TNF-α, IL-6, IFN-γ, IL-4, and IL-10 (Qazi et al. 2009, Qazi et al. 2010, Sheng et al. 2017, Han 2 et al. 018a, Han et al. 2018b, Shane et al. 2020, Guo et al. 2021, Kong et al. 2019, Tian et al. 2021, Rockwell et al. 2013, Rockwell et al. 2017). Unsurprisingly, some of these cytokines can be suppressed or increased in response to different PFAS exposures. Comparing these data, though, supports the notion that exposure routes as well as immunological compartments matter in assessing the effects of PFASs. It was observed that after dietary exposure to PFOA or PFOS and challenge with lipopolysaccharide (LPS), TNF-α and IL-6 were increased in bone marrow and peritoneum (Qazi et al. 2009). However, TNF-α was suppressed in the spleen in PFOS-exposed animals but increased in the spleen in PFOA-exposed animals (Qazi et al. 2009). Similarly, a follow-up study from this laboratory reported TNF-α, IFN-γ, and IL-4 reductions in the liver after PFOA or PFOS exposure (Qazi et al. 2010). Increases, however, of TNF-α, IL-1β, and IL-6 were observed in the spleen exposure to PFOS via oral gavage (Dong et

al. 2011). Dermal exposure to PFOA led to an increase in IL-1β in the skin (Shane et al. 2020), albeit this may have resulted from an indirect inflammatory response. Importantly, because these types of studies are conducted *in vivo*, it is difficult to distinguish which cells are producing these cytokines. While cytokines can be produced by innate immune cells, they can also be produced by adaptive immune cells as well as non-immune cells making it likely that multiple cell types are contributing to the observed phenotypes. More work is needed to understand these phenomena, their specificity, and how observed changes in cytokine levels may apply to functional immunotoxic outcomes.

Relatively few functional outcomes have been investigated using these mammalian models. Exposure to PFDA, PFUnDA, or a mixture of several PFASs was linked to reductions in phagocytosis by macrophages (Berntsen et al. 2018, Bodin et al. 2016, Frawley et al. 2018). Alterations in NK cell cytolysis have been observed after PFOA and PFOS exposure (Keil et al. 2008, Dong et al. 2009, Peden-Adams et al. 2008, Zheng et al. 2009), although directionality of this response appears to be dependent on exposure duration, dose and PFAS. No changes in NK cytolysis were observed with exposure to novel, short-chain per- and polyfluorinated ether carboxylic acids, perfluoromethoxyacetic acid (PFMOAA), perfluoromethoxypropanoic acid (PFMOPrA), and PFMOBA (Woodlief et al. 2021). While not entirely functional, studies of signal transduction within the NF-κB pathway have been performed after PFAS exposure, with findings ranging from no effect with PFNA (Fang et al. 2008), activation of the pathway with PFOA, 6:2 FTCA, 6:2 FTSA (Han et al. 2018a, Han et al. 2018b, Sheng et al. 2017, Singh et al. 2012), and suppression of the pathway with PFOA (Shane et al. 2020). Induction of the inflammasome has also been observed in the liver after PFOS exposure (Qin et al. 2021). Gene expression studies after PFAS exposure have also provided some insight, resulting in

upregulation of immune-related genes in the liver after exposure to PFAS mixtures (Lv et al. 2018), upregulation of damage-associated molecular pattern (DAMP) genes in the skin after exposure to PFBA (Weatherly et al. 2021), and downregulation of macrophage activation genes in the liver after perfluoroheptanoic acid (PFHpA), PFOA, or PFDA exposure (McMillan et al. 2004).

EVIDENCE OF INNATE IMMUNE MODULATION BY PFASS IN THE ZEBRAFISH MODEL

One oft-overlooked model that has been used in the experimental investigation of the immunotoxicity of PFASs is zebrafish (*Danio rerio*); to date, studies utilizing this model have gone unreviewed. Zebrafish are an excellent model for toxicology studies due to their small size, external and rapid development, and high fecundity (Planchart et al. 2016). Given that they possess orthologs for 70% of all protein-encoding genes in humans (Howe et al. 2013), zebrafish are an excellent model for human health. Immunologically, zebrafish possess all of the same major immune lineages as mammals, allowing for use as a comparative model (Traver et al. 2003, Yoder and Traver 2020). Their adaptive immune system, however, is not fully functional until ~3 weeks post fertilization, providing an experimental window when vertebrate innate immunity can be studied in a medium- to high-throughput manner with no influence from B and T lymphocytes.

In Chapter 2 of this dissertation, I show how larval zebrafish can be used as a screening tool for identifying compounds that are immunotoxic to the innate immune system. In Chapter 3, I expand on this work to identify PFASs with this phenotype, and I recapitulate these data using a human cell line, indicating there are conserved mechanisms of PFAS-induced immunotoxicity across species. This validates the use of zebrafish for translational immunotoxicity studies,

especially for PFASs. Despite this, zebrafish have been underutilized as a model for study of these compounds' immunotoxicity (summarized in **Table 3**). Most studies in zebrafish to date have focused on cytokine production at the transcript level, reporting that levels of various cytokines, including IL-6, IL-8, IL-10, IL-1β, TNF-α, and IFN have either increased or decreased in response to PFOA, PFOS, 6:2 fluorotelomer sulfonamide alkylbetaine (6:2 FTAB), F-53B, or sodium p-perfluorous nonenoxybenzene sulfonate (OBS) exposure (Liu et al. 2013, Zhang et al. 2014, Shi et al. 2018, Guo et al. 2019, Liu et al. 2021, Huang et al. 2021). Transcriptomic studies after PFOA or PFOS using zebrafish have been performed and showed similar results, along with alterations in pathways related to innate immunity, inflammation, and infection (Martinez et al. 2019, Yu et al. 2021), and these findings were supported by studies of the NF-κB pathway after exposure to PFOA, PFOS, or F-53B (Guo et al. 2019, Zhang et al. 2014, Yang et al. 2020).

Functional assays in zebrafish are limited but nevertheless illuminating. Exposure to PFOA in larval zebrafish reduced neutrophil chemotaxis to a wound site (Pecquiet et al. 2020). PFOS exposure induced granulomatous lesions in the liver (Keiter et al. 2012), indicating likely immune dysregulation. PFOS also has been shown to increase ROS production in adult zebrafish liver through an increase in myeloperoxidase activity, which also was accompanied by increased lysozyme activity (Guo et al. 2019). A novel PFOS replacement, F-53B, also induced ROS production in zebrafish larvae, including nitric oxide (Liu et al. 2021). In contrast, my experiments described in Chapter 3 indicate that PFOS exposure does not alter ROS production in zebrafish larvae at the tested concentrations. These observations continue the trend of contradictions that have been observed in mammalian models. Nevertheless, Chapter 3 reports for the first time that PFHxA and GenX suppress ROS production in larval zebrafish which is then validated using a human neutrophil-like cell line. Taken together, experimental animals

modeling human disease, from rodents to zebrafish, have been useful in understanding the hazard posed to innate immunity by PFASs. More research is needed to resolve the conflicting data from these models and to confirm these models reasonably reflect the impact of PFAS exposure on human immune response. Additional functional assays are also necessary to further elucidate immunotoxic outcomes after exposure to PFASs with little toxicity data.

EVIDENCE OF INNATE IMMUNE MODULATION BY PFASS IN WILDLIFE AND ECOTOXICOLOGICAL MODELS

Finally, the limited amount of data regarding innate immunity in wildlife and ecotoxicological models provides a glimpse into the toxicity induced by PFASs (summarized in **Table 4**). Wildlife not only provide insight into environmental health, but can also serve as sentinels for human health, as they are exposed to similar concentrations of persistent and ubiquitous environmental contaminants. In a population of bottlenose dolphins (*Tursiops truncatus*), increasing serum levels of PFAS were linked to decreases in circulating eosinophils but increases in phagocytosis by granulocytes and monocytes (Fair et al. 2013). Increased lysozyme activity has been observed both in striped bass (*Morone saxatilis*) (Guillette et al. 2020) and white leghorn chickens (*Gallus gallus domesticus*) (Peden-Adams et al. 2009) with increased PFOS serum levels. White-tailed eagles (*Haliaeetus albicilla*) with elevated PFHxS and total PFAS levels also had suppressed ROS production in a leukocyte respiratory burst assay (Hansen et al. 2020). Transcriptomic analyses of wild fish species have shown altered expression of innate immune genes after exposure to PFOS or a mixture of several PFASs (Zhang et al. 2020, Rodríguez-Jorquera et al. 2019), although the directionality of these responses varies between studies and among genes of interest. The lack of data regarding PFAS exposure and

innate immunity in wildlife reveals how much work remains to be done in order to understand the ramifications of PFAS contamination on ecological health.

CONCLUSIONS

To summarize, much remains to be learned about the impacts of PFAS exposure on innate immunity. It can be concluded that as a family, PFASs can suppress and activate innate immune functions, as has been reported for components of the adaptive immune system. However, the observed effects must be dissected further to determine the doses/concentrations, exposure windows, individual PFASs, and PFAS mixtures that contribute to the immunotoxicity of these compounds. While some studies have sought to elucidate universal mechanisms of PFAS toxicity, few have been successful; given that PFASs target multiple organ systems via several different receptors, multiple mechanisms are likely at play. Of course, this makes defining molecular initiating events difficult when working to create adverse outcome pathways. Given the expanding number of PFASs and their structural diversity, there is a need for new high-throughput methods that can assess innate immune function. Moving forward, the field should work to establish functional assays that can be used to infer the hazardous potential of PFASs in the innate immune system in humans, experimental animals, and wildlife. Innate immunity is critical for organismal and population health, and given the scale of PFAS contamination across the globe, it is imperative to work efficiently to answer the essential questions of PFAS-induced toxicities.

TABLES

Table 1. Summary of innate immune modulation by PFASs in humans.

PFAS	CAS-RN	Immunophenotyping	Cytokine alteration	Functional endpoints	Citations
PFOA	335-67-1	↓ neutrophils, ↑ monocytes	↑↓ TNF-α, ↑ IFN-γ, ↑↓ IL-6, ↑↓ IL-8, ↓ IL-10, ↓ IL-4, ↑ IL-1β	↑↓ activation of NF-κB	Lopez-Espinosa et al. 2021, Abraham et al. 2020, Bassler et al. 2019, Corsini et al. 2011, Corsini et al. 2012, Singh et al. 2012

Table 1. (continued)

PFOS	1763-23-1	↓ neutrophils, ↑↓ monocytes	↓ TNF-α, ↓ IL-6, ↓ IL-8, ↓ IL-10, ↓ IL-4, ↑ IL-1β	↓ NK cell cytolysis	Lopez-Espinosa et al. 2021, Goodrich et al. 2021, Bassler et al. 2019, Corsini et al. 2011, Corsini et al. 2012, Singh et al. 2012, Brieger et al. 2011

Table 1. (continued)

PFNA	375-95-1	↓ neutrophils, ↓ eosinophils, ↓ NK cells	↑ IFN-γ, ↓ IL-8	-	Lopez-Espinosa et al. 2021, Goodrich et al. 2021, Bassler et al. 2019
PFDA	335-76-2	↓ monocytes	-	-	Goodrich et al. 2021
PFOSA	754-91-6	-	↓ IL-6, ↓ IL-8, ↓ IL-10, ↓ IL-4	-	Corsini et al. 2011, Corsini et al. 2012
PFHxS	355-46-4	↑ monocytes, ↓ eosinophils	↓ TNF-α	-	Lopez-Espinosa et al. 2021, Bassler et al. 2019

Table 1. (continued)

PFHxA	307-24-4	-	-	↓ ROS production	Chapter 3
PFBS	375-73-5	-	↓ IL-6, ↓ IL-8, ↓ IL-10, ↓ IL-4	-	Corsini et al. 2011, Corsini et al. 2012,
GenX	62037-80-3	-	-	↓ ROS production	Chapter 3
8:2 FTOH	678-39-7	-	↓ IL-6, ↓ IL-8, ↓ IL-10, ↓ IL-4	-	Corsini et al. 2011, Corsini et al. 2012
Perflubron	423-55-2	-	-	↓ chemotaxis, ↓ phagocytosis	Fernandez et al. 2001
Perfluorodecalin	306-94-5	-	-	↓ chemotaxis, ↓ phagocytosis, ↓ ROS production	Virmani et al. 1984
PFTBA	311-89-7	-	-	↓ phagocytosis	Virmani et al. 1983
Mixtures	-	↑ basophils	-	-	Oulhote et al. 2017

Table 2. Summary of innate immune modulation by PFASs in experimental mammals.

PFAS	CAS-RN	Immunophenotyping	Cytokine alteration	Functional endpoints	Citations
PFOA	335-67-1	↑↓ macrophages, ↓ neutrophils, ↑ NK cells, ↑ granulocytes, ↑ myeloid suppressor cells, ↓ myeloid cells	↑↓ TNF-α, ↑↓ IL-6, ↓ IL-4, ↓ IFN-γ, ↑ IL-1β,	↑↓ NK cell cytolysis, ↑↓ activation of NF-κB	Guo et al. 2021, Qazi et al. 2009, Qazi et al. 2010, Qazi et al. 2012, Shane et al. 2020, Guo et al. 2021, Tian et al. 2021, Dong et al. 2011, Keil et al. 2008, Dong et

Table 2. (continued)

					al. 2009, Peden-Adams et al. 2008, Zheng et al. 2009, Han et al. 2018a, Han et al. 2018b, Singh et al. 2012,
PFOS	1763-23-1	↑↓ macrophages, ↓ myeloid cells, ↓ neutrophils	↑↓ TNF-α, ↑↓ IL-6, ↓ IL-4, ↓ IFN-γ, ↑ IL-1β,	↑↓ NK cell cytolysis, ↑ inflammasome activation,	Han 2018a, Han 2019b, Qazi et al. 2009, Qazi et al. 2010, Qazi et al. 2012,

Table 2. (continued)

					NTP 2019, Dong et al. 2011, Keil et al. 2008, Dong et al. 2009, Peden-Adams et al. 2008, Zheng et al. 2009
PFNA	375-95-1	↓ macrophages, ↓ neutrophils, ↓ NK cells, ↑ phagocytes,	↑TNF-α	-	Fang et al. 2008, Rockwell et al. 2013, Rockwell et al. 2017

Table 2. (continued)

PFDA	335-76-2	↓ macrophage, ↓ NK cells	-	↓ phagocytosis	Frawley et al. 2018
PFUnDA	2058-94-8	↓ macrophages	-	↓ phagocytosis	Bodin et al. 2016, Brieger et al. 2011
PFTBA	311-89-7	↓ neutrophils	-	-	Virmani et al. 1983
PFBA	375-22-4	↑ neutrophils, ↑ dendritic cells, ↑ eosinophils, ↑ NK cells	-	-	Weatherly et al. 2021
PFMOBA	863090-89-5	↓ NK cells	-	-	Woodlief et al. 2021
8:2 FTOH	678-39-7	-	↓ TNF-α, ↓ IL-6, ↓ IL-1β	-	Kong et al. 2019

Table 2. (continued)

6:2 FTCA	53826-12-3	-	↑ TNF-α,	↑ activation of NF-κB	Sheng et al. 2017
6:2 FTSA	27619-97-2	-	↑ TNF-α, ↑ IL-1β, ↑ IL-10, ↑ IL-6	↑ activation of NF-κB	Sheng et al. 2017
Mixtures	-	-		↓ phagocytosis	Brieger et al. 2011

Table 3. Summary of innate immune modulation by PFASs in zebrafish.

PFAS	**CAS-RN**	**Cytokine alteration**	**Functional endpoints**	**Citations**
PFOA	335-67-1	↓ IL-1β, ↑↓ IL-4	↓ chemotaxis	Zhang et al. 2014, Pecquiet et al. 2020
PFOS	1763-23-1	↑ IL-8, ↑ IL-6, ↑ IL-1β, ↑ TNF-α,	↑ granulomas, ↑ ROS production, ↑ lysozyme activity	Liu et al. 2013, Guo et al. 2019, Keiter et al. 2012
6:2 FTAB	34455-29-3	↑ IL-8, ↑ IL-1β ↑ TNF-α	-	Shi et al. 2018
F-53B	756426-58-1	↑ IL-1β	↑ ROS production	Liu et al. 2021
OBS	70829-87-7	↑ IL-1β, ↑ IL-8	-	Huang et al. 2021
PFHxA	307-24-4	-	↓ ROS production	Chapter 3
GenX	62037-80-3	-	↓ ROS production	Chapter 3

Table 4. Summary of innate immune modulation by PFASs in wildlife and ecotoxicological models.

PFAS	CAS-RN	Immunophenotyping	Functional endpoints	Citations
PFOS	1763-23-1	-	↑ lysozyme activity (striped bass, chickens)	Guillette et al. 2020, Peden-Adams et al. 2008
PFHxS	355-46-4	-	↓ ROS production (eagles)	Hansen et al. 2020
Mixtures	-	↓ eosinophils (dolphins)	↑ phagocytosis (dolphins), ↓ ROS production (eagles)	Fair et al. 2013, Hansen et al. 2020

FIGURES

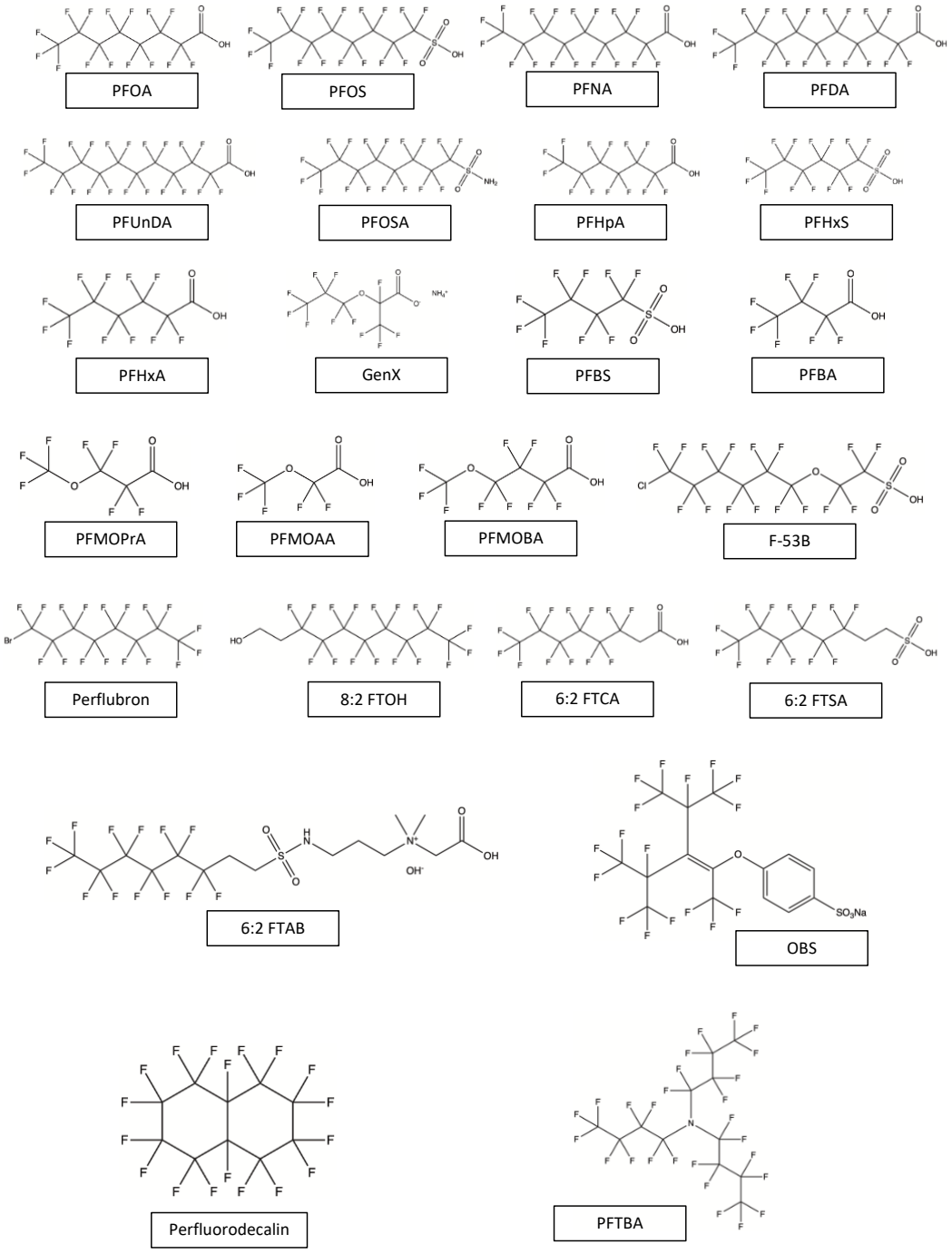

Figure 1. Structures of all PFASs discussed in this Chapter. Structures were made using ChemDraw Professional (v16.0.1.4) and standard International Union of Pure and Applied Chemistry (IUPAC) nomenclature.

REFERENCES

1. Abraham, K, Mielke, H, Fromme, H, Völkel, W, Menzel, J, Peiser, M, Zepp, F, Willich, SN and Weikert, C. 2020. Internal exposure to perfluoroalkyl substances (PFASs) and biological markers in 101 healthy 1-year-old children: associations between levels of perfluorooctanoic acid (PFOA) and vaccine response. Archives of Toxicology. 94(6):2131-2147. doi: 10.1007/s00204-020-02715-4
2. Andrews, DQ and Naidenko, OV. 2020. Population-Wide Exposure to Per- and Polyfluoroalkyl Substances from Drinking Water in the United States. Environ. Sci. Technol. Lett. 7(12):931-936. doi: 10.1021/acs.estlett.0c00713
3. ATSDR. 2021. Toxicological Profile for Perfluoroalkyls. U.S. Department of Health and Human Services.
4. Bangma, J, Guillette, TC, Bommarito, PA, Ng, C, Reiner, JL, Lindstrom, AB and Strynar, MJ. 2022. Understanding the dynamics of physiological changes, protein expression, and PFAS in wildlife. Environment International. 159(107037). doi: 10.1016/j.envint.2021.107037
5. Bassler, J, Ducatman, A, Elliott, M, Wen, S, Wahlang, B, Barnett, J and Cave, MC. 2019. Environmental perfluoroalkyl acid exposures are associated with liver disease characterized by apoptosis and altered serum adipocytokines. Environ Pollut. 247(1055-1063). doi: 10.1016/j.envpol.2019.01.064
6. Berntsen, HF, Bodin, J, Øvrevik, J, Berntsen, CF, Østby, GC, Brinchmann, BC, Ropstad, E and Myhre, O. 2022. A human relevant mixture of persistent organic pollutants induces reactive oxygen species formation in isolated human leucocytes: Involvement of the β2-

adrenergic receptor. Environment International. 158(106900). doi: 10.1016/j.envint.2021.106900

7. Blake, BE and Fenton, SE. 2020. Early life exposure to per- and polyfluoroalkyl substances (PFAS) and latent health outcomes: A review including the placenta as a target tissue and possible driver of peri- and postnatal effects. Toxicology. 443(152565). doi: 10.1016/j.tox.2020.152565
8. Bodin, J, Groeng, EC, Andreassen, M, Dirven, H and Nygaard, UC. 2016. Exposure to perfluoroundecanoic acid (PFUnDA) accelerates insulitis development in a mouse model of type 1 diabetes. Toxicol Rep. 3(664-672. doi: 10.1016/j.toxrep.2016.08.009
9. Boone, JS, Vigo, C, Boone, T, Byrne, C, Ferrario, J, Benson, R, Donohue, J, Simmons, JE, Kolpin, DW, Furlong, ET and Glassmeyer, ST. 2019. Per- and polyfluoroalkyl substances in source and treated drinking waters of the United States. Science of The Total Environment. 653(359-369). doi: 10.1016/j.scitotenv.2018.10.245
10. Boronow, KE, Brody, JG, Schaider, LA, Peaslee, GF, Havas, L and Cohn, BA. 2019. Serum concentrations of PFASs and exposure-related behaviors in African American and non-Hispanic white women. Journal of Exposure Science & Environmental Epidemiology. 29(2):206-217. doi: 10.1038/s41370-018-0109-y
11. Brieger, A, Bienefeld, N, Hasan, R, Goerlich, R and Haase, H. 2011. Impact of perfluorooctanesulfonate and perfluorooctanoic acid on human peripheral leukocytes. Toxicology in Vitro. 25(4):960-968. doi: 10.1016/j.tiv.2011.03.005
12. Buck, RC, Franklin, J, Berger, U, Conder, JM, Cousins, IT, de Voogt, P, Jensen, AA, Kannan, K, Mabury, SA and van Leeuwen, SP. 2011. Perfluoroalkyl and polyfluoroalkyl

substances in the environment: Terminology, classification, and origins. Integrated Environmental Assessment and Management. 7(4):513-541. doi: 10.1002/ieam.258

13. Chang, ET, Adami, H-O, Boffetta, P, Wedner, HJ and Mandel, JS. 2016. A critical review of perfluorooctanoate and perfluorooctanesulfonate exposure and immunological health conditions in humans. Critical Reviews in Toxicology. 46(4):279-331. doi: 10.3109/10408444.2015.1122573
14. Chen, J, Tang, L, Chen, W-Q, Peaslee, GF and Jiang, D. 2020. Flows, Stock, and Emissions of Poly- and Perfluoroalkyl Substances in California Carpet in 2000–2030 under Different Scenarios. Environmental Science & Technology. 54(11):6908-6918. doi: 10.1021/acs.est.9b06956
15. Cordner, A, De La Rosa, VY, Schaider, LA, Rudel, RA, Richter, L and Brown, P. 2019. Guideline levels for PFOA and PFOS in drinking water: the role of scientific uncertainty, risk assessment decisions, and social factors. Journal of Exposure Science & Environmental Epidemiology. 29(2):157-171. doi: 10.1038/s41370-018-0099-9
16. Corsini, E, Avogadro, A, Galbiati, V, dell'Agli, M, Marinovich, M, Galli, CL and Germolec, DR. 2011. In vitro evaluation of the immunotoxic potential of perfluorinated compounds (PFCs). Toxicology and Applied Pharmacology. 250(2):108-116. doi: 10.1016/j.taap.2010.11.004
17. Corsini, E, Sangiovanni, E, Avogadro, A, Galbiati, V, Viviani, B, Marinovich, M, Galli, CL, Dell'Agli, M and Germolec, DR. 2012. In vitro characterization of the immunotoxic potential of several perfluorinated compounds (PFCs). Toxicology and Applied Pharmacology. 258(2):248-255. doi: 10.1016/j.taap.2011.11.004

18. Cousins, IT, DeWitt, JC, Glüge, J, Goldenman, G, Herzke, D, Lohmann, R, Miller, M, Ng, CA, Scheringer, M, Vierke, L and Wang, Z. 2020. Strategies for grouping per- and polyfluoroalkyl substances (PFAS) to protect human and environmental health. Environmental Science: Processes & Impacts. 22(7):1444-1460. doi: 10.1039/D0EM00147C
19. DeWitt. 2015. Toxicological Effects of Perfluoroalkyl and Polyfluoroalkyl Substances. Humana Press.
20. DeWitt, JC, Blossom, SJ and Schaider, LA. 2019. Exposure to per-fluoroalkyl and polyfluoroalkyl substances leads to immunotoxicity: epidemiological and toxicological evidence. Journal of Exposure Science & Environmental Epidemiology. 29(2):148-156. doi: 10.1038/s41370-018-0097-y
21. Domingo, JL and Nadal, M. 2019. Human exposure to per- and polyfluoroalkyl substances (PFAS) through drinking water: A review of the recent scientific literature. Environmental Research. 177(108648). doi: 10.1016/j.envres.2019.108648
22. Dong, GH, Liu, MM, Wang, D, Zheng, L, Liang, ZF and Jin, YH. 2011. Sub-chronic effect of perfluorooctanesulfonate (PFOS) on the balance of type 1 and type 2 cytokine in adult C57BL6 mice. Arch Toxicol. 85(10):1235-44. doi: 10.1007/s00204-011-0661-x
23. Dong, GH, Zhang, YH, Zheng, L, Liu, W, Jin, YH and He, QC. 2009. Chronic effects of perfluorooctanesulfonate exposure on immunotoxicity in adult male C57BL/6 mice. Arch Toxicol. 83(9):805-15. doi: 10.1007/s00204-009-0424-0
24. Fair, PA, Romano, T, Schaefer, AM, Reif, JS, Bossart, GD, Houde, M, Muir, D, Adams, J, Rice, C, Hulsey, TC and Peden-Adams, M. 2013. Associations between perfluoroalkyl compounds and immune and clinical chemistry parameters in highly exposed bottlenose

dolphins (Tursiops truncatus). Environ Toxicol Chem. 32(4):736-46. doi: 10.1002/etc.2122

25. Fang, X, Zhang, L, Feng, Y, Zhao, Y and Dai, J. 2008. Immunotoxic effects of perfluorononanoic acid on BALB/c mice. Toxicol Sci. 105(2):312-21. doi: 10.1093/toxsci/kfn127
26. Fenton, SE, Ducatman, A, Boobis, A, DeWitt, JC, Lau, C, Ng, C, Smith, JS and Roberts, SM. 2021. Per- and Polyfluoroalkyl Substance Toxicity and Human Health Review: Current State of Knowledge and Strategies for Informing Future Research. Environ. Toxicol. Chem. 40(3):606-630. doi: 10.1002/etc.4890
27. Fernandez, R, Sarma, V, Younkin, E, Hirschl, RB, Ward, PA and Younger, JG. 2001. Exposure to perflubron is associated with decreased Syk phosphorylation in human neutrophils. Journal of Applied Physiology. 91(5):1941-1947. doi: 10.1152/jappl.2001.91.5.1941
28. Frawley, RP, Smith, M, Cesta, MF, Hayes-Bouknight, S, Blystone, C, Kissling, GE, Harris, S and Germolec, D. 2018. Immunotoxic and hepatotoxic effects of perfluoro-n-decanoic acid (PFDA) on female Harlan Sprague–Dawley rats and B6C3F1/N mice when administered by oral gavage for 28 days. Journal of Immunotoxicology. 15(1):41-52. doi: 10.1080/1547691X.2018.1445145
29. Goodrich, JM, Calkins, MM, Caban-Martinez, AJ, Stueckle, T, Grant, C, Calafat, AM, Nematollahi, A, Jung, AM, Graber, JM, Jenkins, T, Slitt, AL, Dewald, A, Cook Botelho, J, Beitel, S, Littau, S, Gulotta, J, Wallentine, D, Hughes, J, Popp, C and Burgess, JL. 2021. Per- and polyfluoroalkyl substances, epigenetic age and DNA methylation: a cross-

sectional study of firefighters. Epigenomics. 13(20):1619-1636. doi: 10.2217/epi-2021-0225

30. Guillette, TC, McCord, J, Guillette, M, Polera, ME, Rachels, KT, Morgeson, C, Kotlarz, N, Knappe, DRU, Reading, BJ, Strynar, M and Belcher, SM. 2020. Elevated levels of per- and polyfluoroalkyl substances in Cape Fear River Striped Bass (Morone saxatilis) are associated with biomarkers of altered immune and liver function. Environment International. 136(105358). doi: 10.1016/j.envint.2019.105358
31. Guo, H, Zhang, H, Sheng, N, Wang, J, Chen, J and Dai, J. 2021. Perfluorooctanoic acid (PFOA) exposure induces splenic atrophy via overactivation of macrophages in male mice. Journal of Hazardous Materials. 407(124862). doi: 10.1016/j.jhazmat.2020.124862
32. Guo, J, Wu, P, Cao, J, Luo, Y, Chen, J, Wang, G, Guo, W, Wang, T and He, X. 2019. The PFOS disturbed immunomodulatory functions via nuclear Factor-κB signaling in liver of zebrafish (Danio rerio). Fish & Shellfish Immunology. 91(87-98). doi: 10.1016/j.fsi.2019.05.018
33. Han, R, Hu, M, Zhong, Q, Wan, C, Liu, L, Li, F, Zhang, F and Ding, W. 2018. Perfluorooctane sulphonate induces oxidative hepatic damage via mitochondria-dependent and NF-κB/TNF-α-mediated pathway. Chemosphere. 191(1056-1064). doi: 10.1016/j.chemosphere.2017.08.070
34. Han, R, Zhang, F, Wan, C, Liu, L, Zhong, Q and Ding, W. 2018. Effect of perfluorooctane sulphonate-induced Kupffer cell activation on hepatocyte proliferation through the NF-κB/TNF-α/IL-6-dependent pathway. Chemosphere. 200(283-294). doi: 10.1016/j.chemosphere.2018.02.137

35. Hansen, E, Huber, N, Bustnes, JO, Herzke, D, Bårdsen, B-J, Eulaers, I, Johnsen, TV and Bourgeon, S. 2020. A novel use of the leukocyte coping capacity assay to assess the immunomodulatory effects of organohalogenated contaminants in avian wildlife. Environment International. 142(105861). doi: 10.1016/j.envint.2020.105861

36. Hopkins, ZR, Sun, M, DeWitt, JC and Knappe, DRU. 2018. Recently Detected Drinking Water Contaminants: GenX and Other Per- and Polyfluoroalkyl Ether Acids. Journal AWWA. 110(7):13-28. doi: 10.1002/awwa.1073

37. Howe, K, Clark, MD, Torroja, CF, Torrance, J, Berthelot, C, Muffato, M, Collins, JE, Humphray, S, McLaren, K, Matthews, L, McLaren, S, Sealy, I, Caccamo, M, Churcher, C, Scott, C, Barrett, JC, Koch, R, Rauch, GJ, White, S, Chow, W, Kilian, B, Quintais, LT, Guerra-Assuncao, JA, Zhou, Y, Gu, Y, Yen, J, Vogel, JH, Eyre, T, Redmond, S, Banerjee, R, Chi, J, Fu, B, Langley, E, Maguire, SF, Laird, GK, Lloyd, D, Kenyon, E, Donaldson, S, Sehra, H, Almeida-King, J, Loveland, J, Trevanion, S, Jones, M, Quail, M, Willey, D, Hunt, A, Burton, J, Sims, S, McLay, K, Plumb, B, Davis, J, Clee, C, Oliver, K, Clark, R, Riddle, C, Elliot, D, Threadgold, G, Harden, G, Ware, D, Begum, S, Mortimore, B, Kerry, G, Heath, P, Phillimore, B, Tracey, A, Corby, N, Dunn, M, Johnson, C, Wood, J, Clark, S, Pelan, S, Griffiths, G, Smith, M, Glithero, R, Howden, P, Barker, N, Lloyd, C, Stevens, C, Harley, J, Holt, K, Panagiotidis, G, Lovell, J, Beasley, H, Henderson, C, Gordon, D, Auger, K, Wright, D, Collins, J, Raisen, C, Dyer, L, Leung, K, Robertson, L, Ambridge, K, Leongamornlert, D, McGuire, S, Gilderthorp, R, Griffiths, C, Manthravadi, D, Nichol, S, Barker, G, Whitehead, S, Kay, M, Brown, J, Murnane, C, Gray, E, Humphries, M, Sycamore, N, Barker, D, Saunders, D, Wallis, J, Babbage, A, Hammond, S, Mashreghi-Mohammadi, M, Barr, L, Martin, S, Wray, P,

Ellington, A, Matthews, N, Ellwood, M, Woodmansey, R, Clark, G, Cooper, J, Tromans, A, Grafham, D, Skuce, C, Pandian, R, Andrews, R, Harrison, E, Kimberley, A, Garnett, J, Fosker, N, Hall, R, Garner, P, Kelly, D, Bird, C, Palmer, S, Gehring, I, Berger, A, Dooley, CM, Ersan-Urun, Z, Eser, C, Geiger, H, Geisler, M, Karotki, L, Kirn, A, Konantz, J, Konantz, M, Oberlander, M, Rudolph-Geiger, S, Teucke, M, Lanz, C, Raddatz, G, Osoegawa, K, Zhu, B, Rapp, A, Widaa, S, Langford, C, Yang, F, Schuster, SC, Carter, NP, Harrow, J, Ning, Z, Herrero, J, Searle, SM, Enright, A, Geisler, R, Plasterk, RH, Lee, C, Westerfield, M, de Jong, PJ, Zon, LI, Postlethwait, JH, Nusslein-Volhard, C, Hubbard, TJ, Roest Crollius, H, Rogers, J and Stemple, DL. 2013. The zebrafish reference genome sequence and its relationship to the human genome. Nature. 496(7446):498-503. doi: 10.1038/nature12111

38. Hu, XC, Andrews, DQ, Lindstrom, AB, Bruton, TA, Schaider, LA, Grandjean, P, Lohmann, R, Carignan, CC, Blum, A, Balan, SA, Higgins, CP and Sunderland, EM. 2016. Detection of Poly- and Perfluoroalkyl Substances (PFASs) in U.S. Drinking Water Linked to Industrial Sites, Military Fire Training Areas, and Wastewater Treatment Plants. Environ Sci Technol Lett. 3(10):344-350. doi: 10.1021/acs.estlett.6b00260
39. Huang, J, Wang, Q, Liu, S, Zhang, M, Liu, Y, Sun, L, Wu, Y and Tu, W. 2021. Crosstalk between histological alterations, oxidative stress and immune aberrations of the emerging PFOS alternative OBS in developing zebrafish. Science of The Total Environment. 774(145443). doi: 10.1016/j.scitotenv.2021.145443
40. ITRC. 2020. Basis for PFOA and PFOS Values Tables. https://pfas-1.itrcweb.org/fact-sheets/

41. Keil, DE, Mehlmann, T, Butterworth, L and Peden-Adams, MM. 2008. Gestational Exposure to Perfluorooctane Sulfonate Suppresses Immune Function in B6C3F1 Mice. Toxicological Sciences. 103(1):77-85. doi: 10.1093/toxsci/kfn015

42. Keiter, S, Baumann, L, Färber, H, Holbech, H, Skutlarek, D, Engwall, M and Braunbeck, T. 2012. Long-term effects of a binary mixture of perfluorooctane sulfonate (PFOS) and bisphenol A (BPA) in zebrafish (Danio rerio). Aquatic Toxicology. 118-119(116-129). doi: 10.1016/j.aquatox.2012.04.003

43. Kong, B, Wang, X, He, B, Wei, L, Zhu, J, Jin, Y and Fu, Z. 2019. 8:2 fluorotelomer alcohol inhibited proliferation and disturbed the expression of pro-inflammatory cytokines and antigen-presenting genes in murine macrophages. Chemosphere. 219(1052-1060). doi: 10.1016/j.chemosphere.2018.12.091

44. Liu, C, Wang, Q, Liang, K, Liu, J, Zhou, B, Zhang, X, Liu, H, Giesy, JP and Yu, H. 2013. Effects of tris(1,3-dichloro-2-propyl) phosphate and triphenyl phosphate on receptor-associated mRNA expression in zebrafish embryos/larvae. Aquatic Toxicology. 128-129(147-157). doi: 10.1016/j.aquatox.2012.12.010

45. Liu, S, Lai, H, Wang, Q, Martínez, R, Zhang, M, Liu, Y, Huang, J, Deng, M and Tu, W. 2021. Immunotoxicity of F53B, an alternative to PFOS, on zebrafish (Danio rerio) at different early life stages. Sci Total Environ. 790(148165). doi: 10.1016/j.scitotenv.2021.148165

46. Lopez-Espinosa, M-J, Carrizosa, C, Luster, MI, Margolick, JB, Costa, O, Leonardi, GS and Fletcher, T. 2021. Perfluoroalkyl substances and immune cell counts in adults from the Mid-Ohio Valley (USA). Environment International. 156(106599). doi: 10.1016/j.envint.2021.106599

47. Lv, Z, Wu, W, Ge, S, Jia, R, Lin, T, Yuan, Y, Kuang, H, Yang, B, Wu, L, Wei, J and Zhang, D. 2018. Naringin protects against perfluorooctane sulfonate-induced liver injury by modulating NRF2 and NF-κB in mice. Int Immunopharmacol. 65(140-147). doi: 10.1016/j.intimp.2018.09.019
48. Martínez, R, Navarro-Martín, L, Luccarelli, C, Codina, AE, Raldúa, D, Barata, C, Tauler, R and Piña, B. 2019. Unravelling the mechanisms of PFOS toxicity by combining morphological and transcriptomic analyses in zebrafish embryos. Science of The Total Environment. 674(462-471). doi: 10.1016/j.scitotenv.2019.04.200
49. McMillian, M, Nie, AY, Parker, JB, Leone, A, Kemmerer, M, Bryant, S, Herlich, J, Yieh, L, Bittner, A, Liu, X, Wan, J and Johnson, MD. 2004. Inverse gene expression patterns for macrophage activating hepatotoxicants and peroxisome proliferators in rat liver. Biochem Pharmacol. 67(11):2141-65. doi: 10.1016/j.bcp.2004.01.029
50. NTP. 2016. Monograph on Immunotoxicity Associated with Exposure to Perfluorooctanoic acid (PFOA) and perfluorooctane sulfonate (PFOS). National Toxicology Program.
51. NTP. 2019. Toxicity Report 96 - NTP Technical Report on the Toxicity Studies of Perfluoroalkyl Sulfonates (Perfluorobutane Sulfonic Acid, Perfluorohexane Sulfonate Potassium Salt, and Perfluorooctane Sulfonic Acid) Administered by Gavage to Sprague Dawley (Hsd:Sprague Dawley SD) Rats.
52. OECD. 2018. Environment Directorate Joint Meeting of the Chemicals Committee and the Working Party on Chemicals, Pesticides and Biotechnology. Toward a New Comprehensive Global Database of Per- and Polyfluoroalkyl Substances (PFASs):

Summary Report On Updating The OECD 2007 List Of Per- and Polyfluoroalkyl Substances (PFASs). Organisation for Economic Co-operation and Development.

53. Oulhote, Y, Shamim, Z, Kielsen, K, Weihe, P, Grandjean, P, Ryder, LP and Heilmann, C. 2017. Children's white blood cell counts in relation to developmental exposures to methylmercury and persistent organic pollutants. Reprod Toxicol. 68(207-214. doi: 10.1016/j.reprotox.2016.08.001
54. Pecquet, AM, Maier, A, Kasper, S, Sumanas, S and Yadav, J. 2020. Exposure to perfluorooctanoic acid (PFOA) decreases neutrophil migration response to injury in zebrafish embryos. BMC Research Notes. 13(1):408. doi: 10.1186/s13104-020-05255-3
55. Peden-Adams, MM, Keller, JM, EuDaly, JG, Berger, J, Gilkeson, GS and Keil, DE. 2008. Suppression of Humoral Immunity in Mice following Exposure to Perfluorooctane Sulfonate. Toxicological Sciences. 104(1):144-154. doi: 10.1093/toxsci/kfn059
56. Peden-Adams, MM, Stuckey, JE, Gaworecki, KM, Berger-Ritchie, J, Bryant, K, Jodice, PG, Scott, TR, Ferrario, JB, Guan, B, Vigo, C, Boone, JS, McGuinn, WD, DeWitt, JC and Keil, DE. 2009. Developmental toxicity in white leghorn chickens following in ovo exposure to perfluorooctane sulfonate (PFOS). Reprod Toxicol. 27(3-4):307-318. doi: 10.1016/j.reprotox.2008.10.009
57. Planchart, A, Mattingly, CJ, Allen, D, Ceger, P, Casey, W, Hinton, D, Kanungo, J, Kullman, SW, Tal, T, Bondesson, M, Burgess, SM, Sullivan, C, Kim, C, Behl, M, Padilla, S, Reif, DM, Tanguay, RL and Hamm, J. 2016. Advancing toxicology research using in vivo high throughput toxicology with small fish models. Altex. 33(4):435-452. doi: 10.14573/altex.1601281

58. Poothong, S, Papadopoulou, E, Padilla-Sánchez, JA, Thomsen, C and Haug, LS. 2020. Multiple pathways of human exposure to poly- and perfluoroalkyl substances (PFASs): From external exposure to human blood. Environment International. 134(105244. doi: 10.1016/j.envint.2019.105244

59. Qazi, MR, Abedi, MR, Nelson, BD, DePierre, JW and Abedi-Valugerdi, M. 2010. Dietary exposure to perfluorooctanoate or perfluorooctane sulfonate induces hypertrophy in centrilobular hepatocytes and alters the hepatic immune status in mice. International Immunopharmacology. 10(11):1420-1427. doi: 10.1016/j.intimp.2010.08.009

60. Qazi, MR, Bogdanska, J, Butenhoff, JL, Nelson, BD, DePierre, JW and Abedi-Valugerdi, M. 2009. High-dose, short-term exposure of mice to perfluorooctanesulfonate (PFOS) or perfluorooctanoate (PFOA) affects the number of circulating neutrophils differently, but enhances the inflammatory responses of macrophages to lipopolysaccharide (LPS) in a similar fashion. Toxicology. 262(3):207-14. doi: 10.1016/j.tox.2009.06.010

61. Qazi, MR, Dean Nelson, B, DePierre, JW and Abedi-Valugerdi, M. 2012. High-dose dietary exposure of mice to perfluorooctanoate or perfluorooctane sulfonate exerts toxic effects on myeloid and B-lymphoid cells in the bone marrow and these effects are partially dependent on reduced food consumption. Food and Chemical Toxicology. 50(9):2955-2963. doi: 10.1016/j.fct.2012.06.023

62. Qazi, MR, Nelson, BD, Depierre, JW and Abedi-Valugerdi, M. 2010. 28-Day dietary exposure of mice to a low total dose (7 mg/kg) of perfluorooctanesulfonate (PFOS) alters neither the cellular compositions of the thymus and spleen nor humoral immune responses: does the route of administration play a pivotal role in PFOS-induced immunotoxicity? Toxicology. 267(1-3):132-9. doi: 10.1016/j.tox.2009.10.035

63. Qin, Y, Gu, T, Ling, J, Luo, J, Zhao, J, Hu, B, Hua, L, Wan, C and Jiang, S. PFOS facilitates liver inflammation and steatosis: An involvement of NLRP3 inflammasome-mediated hepatocyte pyroptosis. Journal of Applied Toxicology. doi: 10.1002/jat.4258

64. Rizzuto, P. 2020. Honeywell, Chemours Among PFAS Makers on EPA Chemicals List (2). Bloomberg Law. https://news.bloombergenvironment.com/environment-and-energy/honeywell-chemours-among-pfas-makers-on-epa-chemicals-list

65. Rockwell, CE, Turley, AE, Cheng, X, Fields, PE and Klaassen, CD. 2013. Acute Immunotoxic Effects of Perfluorononanoic Acid (PFNA) in C57BL/6 Mice. Clin Exp Pharmacol. doi: 10.4172/2161-1459.S4-002

66. Rockwell, CE, Turley, AE, Cheng, X, Fields, PE and Klaassen, CD. 2017. Persistent alterations in immune cell populations and function from a single dose of perfluorononanoic acid (PFNA) in C57Bl/6 mice. Food Chem Toxicol. 100(24-33). doi: 10.1016/j.fct.2016.12.004

67. Rodríguez-Jorquera, IA, Colli-Dula, RC, Kroll, K, Jayasinghe, BS, Parachu Marco, MV, Silva-Sanchez, C, Toor, GS and Denslow, ND. 2019. Blood Transcriptomics Analysis of Fish Exposed to Perfluoro Alkyls Substances: Assessment of a Non-Lethal Sampling Technique for Advancing Aquatic Toxicology Research. Environmental Science & Technology. 53(3):1441-1452. doi: 10.1021/acs.est.8b03603

68. Shane, HL, Baur, R, Lukomska, E, Weatherly, L and Anderson, SE. 2020. Immunotoxicity and allergenic potential induced by topical application of perfluorooctanoic acid (PFOA) in a murine model. Food and Chemical Toxicology. 136(111114). doi: 10.1016/j.fct.2020.111114

69. Sheng, N, Zhou, X, Zheng, F, Pan, Y, Guo, X, Guo, Y, Sun, Y and Dai, J. 2017. Comparative hepatotoxicity of 6:2 fluorotelomer carboxylic acid and 6:2 fluorotelomer sulfonic acid, two fluorinated alternatives to long-chain perfluoroalkyl acids, on adult male mice. Archives of Toxicology. 91(8):2909-2919. doi: 10.1007/s00204-016-1917-2
70. Shi, G, Xie, Y, Guo, Y and Dai, J. 2018. 6:2 fluorotelomer sulfonamide alkylbetaine (6:2 FTAB), a novel perfluorooctane sulfonate alternative, induced developmental toxicity in zebrafish embryos. Aquatic Toxicology. 195(24-32). doi: 10.1016/j.aquatox.2017.12.002
71. Singh, TS, Lee, S, Kim, HH, Choi, JK and Kim, SH. 2012. Perfluorooctanoic acid induces mast cell-mediated allergic inflammation by the release of histamine and inflammatory mediators. Toxicol Lett. 210(1):64-70. doi: 10.1016/j.toxlet.2012.01.014
72. Tian, J, Hong, Y, Li, Z, Yang, Z, Lei, B, Liu, J and Cai, Z. 2021. Immunometabolism-modulation and immunotoxicity evaluation of perfluorooctanoic acid in macrophage. Ecotoxicology and Environmental Safety. 215(112128. doi: 10.1016/j.ecoenv.2021.112128
73. Traver, D, Herbomel, P, Patton, EE, Murphey, RD, Yoder, JA, Litman, GW, Catic, A, Amemiya, CT, Zon, LI and Trede, NS. 2003. The zebrafish as a model organism to study development of the immune system. Adv Immunol. 81(253-330).
74. Traver, D and Yoder, JA. 2020. Chapter 19 - Immunology. Academic Press.
75. USEPA. 2006. Fact Sheet: 2010/2015 PFOA Stewardship Program. http://www.epa.gov/opptintr/pfoa/pubs/stewardship/
76. USEPA. 2019. EPA's Per- and Polyfluoroalkyl Substances (PFAS) Action Plan. https://www.epa.gov/sites/production/files/2019-02/documents/pfas_action_plan_021319_508compliant_1.pdf

77. USEPA. 2020. PFAS Master List of PFAS Substances. https://comptox.epa.gov/dashboard/chemical-lists/PFASMASTER

78. Virmani, R, Fink, LM, Gunter, K and English, D. 1984. Effect of perfluorochemical blood substitutes on human neutrophil function. Transfusion. 24(4):343-7. doi: 10.1046/j.1537-2995.1984.24484275579.x

79. Virmani, R, Warren, D, Rees, R, Fink, LM and English, D. 1983. Effects of perfluorochemical on phagocytic function of leukocytes. Transfusion. 23(6):512-515. doi: 10.1046/j.1537-2995.1983.23684074274.x

80. Wang, L-Q, Liu, T, Yang, S, Sun, L, Zhao, Z-Y, Li, L-Y, She, Y-C, Zheng, Y-Y, Ye, X-Y, Bao, Q, Dong, G-H, Li, C-W and Cui, J. 2021. Perfluoroalkyl substance pollutants activate the innate immune system through the AIM2 inflammasome. Nature Communications. 12(1):2915. doi: 10.1038/s41467-021-23201-0

81. Weatherly, LM, Shane, HL, Lukomska, E, Baur, R and Anderson, SE. 2021. Systemic toxicity induced by topical application of heptafluorobutyric acid (PFBA) in a murine model. Food and Chemical Toxicology. 156(112528). doi: 10.1016/j.fct.2021.112528

82. Woodlief, T, Vance, S, Hu, Q and DeWitt, J. 2021. Immunotoxicity of Per- and Polyfluoroalkyl Substances: Insights into Short-Chain PFAS Exposure. Toxics. 9(5):100.

83. Yang, H, Lai, H, Huang, J, Sun, L, Mennigen, JA, Wang, Q, Liu, Y, Jin, Y and Tu, W. 2020. Polystyrene microplastics decrease F–53B bioaccumulation but induce inflammatory stress in larval zebrafish. Chemosphere. 255(127040). doi: 10.1016/j.chemosphere.2020.127040

84. Yu, J, Cheng, W, Jia, M, Chen, L, Gu, C, Ren, H-q and Wu, B. 2022. Toxicity of perfluorooctanoic acid on zebrafish early embryonic development determined by single-

cell RNA sequencing. Journal of Hazardous Materials. 427(127888). doi: 10.1016/j.jhazmat.2021.127888

85. Zhang, H, Fang, W, Wang, D, Gao, N, Ding, Y and Chen, C. 2014. The role of interleukin family in perfluorooctanoic acid (PFOA)-induced immunotoxicity. Journal of Hazardous Materials. 280(552-560). doi: 10.1016/j.jhazmat.2014.08.043
86. Zhang, L, Sun, W, Chen, H, Zhang, Z and Cai, W. 2020. Transcriptomic Changes in Liver of Juvenile Cynoglossus semilaevis following Perfluorooctane Sulfonate Exposure. Environ Toxicol Chem. 39(3):556-564. doi: 10.1002/etc.4633
87. Zheng, L, Dong, G-H, Jin, Y-H and He, Q-C. 2009. Immunotoxic changes associated with a 7-day oral exposure to perfluorooctanesulfonate (PFOS) in adult male C57BL/6 mice. Archives of Toxicology. 83(7):679-689. doi: 10.1007/s00204-008-0361-3

CHAPTER 2

In vivo assessment of respiratory burst inhibition by xenobiotic exposure using larval zebrafish

Drake W. Phelps[1,2], Ashley A. Fletcher[1], Ivan Rodriguez-Nunez[1], Michele R. Balik-Meisner[3], Debra T. Tokarz[1,4,] David M. Reif[3,4,5], Dori R. Germolec[6], and Jeffrey A. Yoder[1,2,4]

[1]Department of Molecular Biomedical Sciences, College of Veterinary Medicine, North Carolina State University, Raleigh, NC, USA

[2]Comparative Medicine Institute, North Carolina State University, Raleigh, NC, USA

[3]Department of Biological Sciences, North Carolina State University, Raleigh, NC, USA

[4]Center for Human Health and the Environment, North Carolina State University, Raleigh, NC, USA

[5]Bioinformatics Research Center, North Carolina State University, Raleigh, NC, USA

[6]National Toxicology Program, National Institute of Environmental Health Sciences, Research Triangle Park, NC, USA

Corresponding author: Jeffrey Yoder, Department of Molecular Biomedical Sciences, College of Veterinary Medicine, NC State University, 1060 William Moore Drive, Raleigh, NC 27607, USA. Tel: +1 919 515 7406; jayoder@ncsu.edu

The authors report no conflict of interest. The authors alone are responsible for the content of this manuscript.

This chapter was published in Journal of Immunotoxicology in May 2020. The full citation can be found below. DWP performed flow cytometry experiments and prepared figures. AAF, IRN, and DAT performed developmental toxicity and respiratory burst experiments. MRBM and DRM aided in statistical analyses of results. DRG aided in chemical selection and study design. The first draft of the manuscript was written by DWP. All authors commented on previous versions of the manuscript, and read and approved the final manuscript. JAY secured funding for this study. JAY supervised the completion of the project.

Drake W. Phelps, Ashley A. Fletcher, Ivan Rodriguez-Nunez, Michele R. Balik-Meisner, Debra A. Tokarz, David M. Reif, Dori R. Germolec & Jeffrey A. Yoder (2020) *In vivo* assessment of respiratory burst inhibition by xenobiotic exposure using larval zebrafish, Journal of Immunotoxicology, 17:1, 94-104, DOI: 10.1080/1547691X.2020.1748772

ABSTRACT

Currently, assessment of the potential immunotoxicity of a given agent involves a tiered approach for hazard identification and mechanistic studies, including observational studies, evaluation of immune function, and measurement of susceptibility to infectious and neoplastic diseases. These studies generally use costly low-throughput mammalian models. Zebrafish, however, offer an excellent alternative due to their rapid development, ease of maintenance, and homology to mammalian immune system function and development. Larval zebrafish also are a convenient model to study the innate immune system with no interference from the adaptive immune system. In this study, a respiratory burst assay (RBA) was utilized to measure reactive oxygen species (ROS) production after developmental xenobiotic exposure. Embryos were exposed to non-teratogenic doses of chemicals and at 96 h post-fertilization, the ability to produce ROS was measured. Using the RBA, 12 compounds with varying immune-suppressive properties were screened. Seven compounds neither suppressed nor enhanced the respiratory burst; five reproducibly suppressed global ROS production, but with varying potencies: benzo[a]pyrene, 17β-estradiol, lead acetate, methoxychlor, and phenanthrene. These five compounds have all previously been reported as immunosuppressive in mammalian innate immunity assays. To evaluate whether the suppression of ROS by these compounds was a result of decreased immune cell numbers, flow cytometry with transgenic zebrafish larvae was used to count the numbers of neutrophils and macrophages after chemical exposure. With this assay, benzo[a]pyrene was found to be the only chemical that induced a change in the number of immune cells by increasing macrophage but not neutrophil numbers. Taken together, this work demonstrates the utility of zebrafish larvae as a vertebrate model for identifying compounds that impact innate immune function at non-teratogenic levels and validates measuring ROS

production and phagocyte numbers as metrics for monitoring how xenobiotic exposure alters the innate immune system.

Keywords: chemical screen; high throughput; phagocyte; reactive oxygen species (ROS); polycyclic aromatic hydrocarbons (PAH); endocrine disrupting compounds (EDC); lead

INTRODUCTION

Exposure to xenobiotics that alter immune function may confer susceptibility to infectious or neoplastic disease. With tens of thousands of chemicals in production globally, frameworks are needed in order to assess them for immunotoxic potential. Current practices for immunotoxicity testing consist of a low-throughput tiered approach in rodent models (Germolec et al. 2017). While Tier I involves screens to assess basic immunologic function after exposure to xenobiotics, Tier II follows in order to provide a meaningful depth of those effects by using multiple immunologic assays for apical endpoints (Germolec et al. 2017). In fact, the United States Environmental Protection Agency (USEPA) Toxic Substances Control Act Health Effects Guidelines for evaluating immunotoxicity are intended only for use in rodent models, and they do not require functional assessment of myeloid cells in the innate immune system (USEPA 1998). Given this, throughput is limited, and studies may often be limited by the lack of resources needed to maintain mammalian systems. While in vitro methods exist for high-throughput assessment, reliability is variable and focuses heavily on the adaptive immune system (Gehen et al. 2014; Germolec et al. 2017), leaving a gap in knowledge regarding the innate immune system. All these points considered, there is a necessity for high-throughput animal models for innate immunotoxicity testing and hazard identification. To fill this gap, we propose the use of zebrafish (Danio rerio) as a potential animal model.

The zebrafish model has risen in popularity in recent years for laboratory use, especially with regards to toxicity studies. Zebrafish are highly fecund, with a single female producing hundreds of embryos in a single clutch that are fertilized externally (Lawrence 2016). These transparent embryos develop rapidly, allowing researchers to track development from the single-cell stage through organogenesis and into their larval state (Kimmel et al. 1995). The small size

of the zebrafish embryo provides another advantage to the model, adding to its throughput capability; embryos can be placed into 96- or 384-well plates, for testing multiple chemicals and/or multiple doses on the same plate (Lantz-McPeak et al. 2015; Poureetezadi et al. 2016). By 72 h post-fertilization (hpf), the liver of the embryonic zebrafish has developed (Wang et al. 2017) and has the ability to biotransform xenobiotics (Saad et al. 2016). This may be especially important for identification of chemicals that must be bioactivated to exert toxicity, an aspect which may be overlooked in high-throughput in vitro assays. Perhaps the most important aspect of the zebrafish model is their homology to humans; the zebrafish genome encodes orthologs to 70% of all human protein-encoding genes (Howe et al. 2013), including immunoglobulin and T-cell receptor genes that undergo RAG-mediated V(D)J recombination, Toll-like receptors, and numerous cytokines, making them an excellent model for human immunological health.

Although zebrafish are an exceptional model for toxicity studies, they have been widely neglected as a model for immunotoxicity (Planchart et al. 2016; Espenschied et al. 2018). As teleost fish, they possess both an innate immune system and an adaptive immune system capable of defending the host from pathogens, and all major immune cell lineages and pathways in zebrafish are conserved in mammalian models (reviewed in Stachura and Traver 2016; Traver and Yoder 2020). Within 24 hpf, the zebrafish has a beating heart (Kimmel et al. 1995), which aids in the circulation of immune cells in the blood. At this same time, macrophages have developed and are able to phagocytose microbes and apoptotic bodies (Herbomel et al. 1999; Willett et al. 1999; Stachura and Traver 2016). By 48 hpf, neutrophils are present within the embryo and possess the ability to migrate to sites of wounding (Willett et al. 1999; Lieschke et al. 2001; Stachura and Traver 2016) and of infection to clear pathogens (Yang et al. 2012). Lymphocytes - which comprise the adaptive immune system – are not identifiable until three

weeks post-fertilization (Willett et al. 1999; Stachura and Traver 2016) and antibody production is not fully functional until ≈ 4 wk post-fertilization (Lam et al. 2004). Thus, embryonic and larval zebrafish provide a vertebrate experimental system in which the innate immune system can be studied in vivo with no "interference" from the adaptive immune system.

Because the zebrafish lacks adaptive immunity during early development, they must rely on the innate immune system for defense against pathogens for survival during early development. One of the most useful tools in this process is the respiratory burst - the rapid production of reactive oxygen species (ROS) in response to immune stimulation. Zebrafish encode homologs to the mammalian nicotinamide adenine dinucleotide phosphate hydrogen (NADPH) oxidase (Weaver et al. 2016) and inducible nitric oxide synthase (Vojtech et al. 2009; Huang et al. 2014) enzymes involved in the respiratory burst. Once pathogens are phagocytosed, the NADPH oxidase complex assembles from several different proteins (reviewed by Flannagan et al. 2009). This complex then oxidizes NADPH to produce NADP+, H+, and superoxide (reviewed by Bogdan et al. 2000). Superoxide can be further acted upon to create hydrogen peroxide, hydroxyl radicals, or hypochlorous acid. These highly reactive compounds target several essential microbial molecules (proteins, lipids, and nucleic acids), disrupting their function and inducing microbial death (reviewed by Flannagan et al. 2009).

In this study, larval zebrafish were utilized to determine if exposure to 12 different xenobiotics of known/suspected immunomodulatory potential were able to modulate the production of ROS in vivo after stimulation with phorbol 12-myristate 13-acetate (PMA). For compounds shown to suppress larval ROS production, follow-up experiments were performed to determine if chemical exposure altered phagocyte number. Of the 12 compounds tested, five suppressed ROS production and one altered phagocyte number. Not only does this study

recapitulate findings from mammalian studies, it also demonstrates the utility of the zebrafish as a model for high-throughput hazard identification of immunotoxic compounds.

MATERIALS AND METHODS

Zebrafish embryos

Adult zebrafish were maintained in a recirculating aquarium facility (Aquatic Habitats, Apopka, FL) at 28 °C with a 14 h light/10 h dark cycle and fed a commercial grade zebrafish diet. Wild-type zebrafish were purchased from LiveAquaria (www.LiveAquaria.com) and Doctors Foster and Smith (www.drsfostersmith.com). Transgenic zebrafish lines *Tg(mpx:GFP)* (Renshaw et al. 2006) and *Tg(mfap4:tdTomato-caax)* (Walton et al. 2015) were kind gifts from Stephen Renshaw (University of Sheffield) and David Tobin (Duke University), respectively. Zebrafish embryos were obtained by natural spawning. At 2 hpf, embryos were treated with 0.06% sodium hypochlorite (bleach [v/v]) in 10% Hanks Balanced Salt Solution (HBSS) in ultrapure water using two 5 min washes to eliminate extra-ovum microbes. The embryos were then maintained in 100 mm Petri dishes in 10% HBSS at 28 °C until use. Zebrafish husbandry and experiments involving live animals were approved by the North Carolina State University Institutional Animal Care and Use Committee.

Compounds

A total of 12 chemicals were selected for study (Figure 1) based on their immunomodulatory properties in mammalian models. Chemicals (20 mM) stocks diluted in dimethyl sulfoxide (DMSO) were provided by Batelle (Columbus, OH) and MRI Global (Kansas City, MO). Chemicals stocks were serially diluted at 1:3.125 in DMSO (Sigma, St. Louis, MO) eight times, yielding nine total working stock concentrations. These working stocks were then diluted at 1:250 in 10% HBSS for the zebrafish embryo treatments. Exposures of the embryos to

these concentrations (80.0, 25.6, 8.19, and 2.62 μM and 839, 268, 85.9, 27.5, and 8.80 nM, respectively) were evaluated in a range-finding developmental toxicity assay to determine the highest non-teratogenic concentration (*aka* no-observed-effect level (NOEL)) for use in the respiratory burst and flow cytometry assays.

Developmental toxicity assay

At 6 hpf, zebrafish embryos were placed in 24-well plates at a density of three embryos/well in 10% HBSS with chemical dilution (see above). Two wells (six embryos total) were used for each chemical dilution. Two 90% media changes were performed to achieve 99% HBSS/chemical renewal at 24, 48, and 72 hpf. At 96 hpf, embryos were observed under a light microscope and scored as dead, abnormal, or normal. For each chemical, the highest concentration exposure with all normal embryos was considered the NOEL and used as the starting (highest) concentration for subsequent respiratory burst assays (RBA).

Chemical exposure of zebrafish embryos for RBA

Embryos were exposed to HBSS/chemical solution from 6 hpf until the RBA was run at 96 hpf. Embryos were maintained in two 24-well plates at three embryos/well with three dilutions of 1:9.767 from the starting concentration determined in the developmental toxicity assay, using four concentrations in total. A total of 24 embryos/chemical concentration were treated and 48 embryos were treated with 0.4% DMSO as a negative control. HBSS/chemical solutions were replaced daily (99% exchange - see above).

RBA

The RBA here was a modified version of a previously-published assay (Hermann et al. 2004; Goody et al. 2013). At 96 hpf, embryos were washed to remove compounds and re-plated into black 96-well plates with clear bottoms (#3603; Corning Inc., Corning, NY) in 100 μl

of 10% HBSS (one embryo/well). In contrast to the original methods, 10% HBSS was used in place of egg water. For each chemical concentration, 16 embryos were plated in two columns of the plate; for DMSO-treated (vehicle control) embryos, 32 embryos were plated. As a positive control, 1 µl of 1 mM bisindolylmaleimide I (Bis I, a protein kinase C inhibitor; EMD Millipore, Burlington, MA), was added to 16 of the DMSO-treated embryo wells for a final concentration of 10 µM. The plate was then incubated in the dark at 28 °C for 30 min before 100 µl of 10% HBSS containing 2′,7′-dichlorofluorescin-diacetate (H_2DCFDA; Thermo Fisher Scientific, Waltham, MA) at a final concentration of 500 ng/ml was added to each well. PMA (Sigma; final concentration of 200 ng/ml) was added to stimulate ROS production; DMSO (final concentration of 0.2% [v/v]), was employed as a vehicle control. H_2DCFDA was prepared fresh for each experiment rather than making aliquots as detailed in the originally published methods. The fluorescence from each well was then read on a Fluoroskan Ascent FL plate reader (Thermo Fisher) at 28 °C using excitation and emission filters set at 485 and 530 nm, respectively. Fluorescence was measured every 2.5 min over the course of 150 min. Data presented in this study represent the maximum fluorescence detected for each well over the 150min period.

Flow cytometry

For the experiments counting neutrophils and macrophages via flow cytometry, 60 *Tg(mpx:GFP)* or *Tg(mfap4:tdTomato-caax)* embryos were exposed as previously described to each of the five compounds that were positive for ROS suppression. Due to the high number of embryos needed for flow cytometry (31–60 embryos/treatment group), only the highest dose at which ROS suppression occurred was evaluated for each chemical. Larvae that died or had physical malformations were excluded. To measure baseline autofluorescence, unexposed wild-type non-fluorescent embryos were included in all experiments.

In order to dissociate larvae into a single-cell suspension, an adapted version of a previously published protocol was used (Manoli and Driever 2012). To include an anesthesia step, at 96 hpf, larvae were anesthetized using MS-222 (Syndel, Ferndale, WA) at a final concentration of 100 mg/l and then collected into 15-ml conical tubes. Excess media was removed, and larvae were re-suspended in 1 ml freshly prepared deyolking buffer (856 ml molecular biology-grade water, 9 µl 2.0 M KCl, 100 µl 5.0 M NaCl, and 25 µl 0.5 M sodium bicarbonate). Larvae were then pipetted up and down to thoroughly mix and de-yolk. The larvae were then centrifuged at 400x g for 1 min, the resulting supernatant was removed, and the larvae re-suspended in 1 ml of fluorescence-activated cell sorting (FACS) buffer (phosphate-buffered saline containing 5% fetal bovine serum (Corning, Manassas, VA) and 100 mg MS-222/l), instead of FACSmax buffer as in the original protocol. A 40 µm cell strainer was placed atop a 50 ml conical tube and rinsed with 250 µl of FACS buffer. Larvae were then transferred to the strainer and homogenized with the rubber plunger of a 1 ml syringe. The strainer was then rinsed again into the conical tube with FACS buffer. The tube was then centrifuged (400x g, 1 min) and placed on ice until further analysis.

Flow cytometry experiments were performed in the Flow Cytometry and Cell Sorting facility at the North Carolina State University College of Veterinary Medicine. Due to laser configurations, *Tg(mpx:GFP)* samples were analyzed on a Becton Dickinson LSRII (Franklin Lakes, NJ) while the *Tg(mfap4:tdTomato-caax)* samples were analyzed on a Beckman Coulter MoFlo XDP (Brea, CA). Cells were gated based on forward-scatter and side-scatter to gate for cellular events, excluding debris, and then gated for singlet events to exclude any large cellular debris or groups of cells that were not in single-cell suspension. A final gate was drawn in the singlet population to quantify GFP^+ or $tdTomato^+$ cells (see Supplemental Figure 1 for gating

strategy). Data is shown as a percentage of GFP^+ or $tdTomato^+$ cells from all singlet events. These data were analyzed using Prism software v.7.0e (GraphPad, La Jolla, CA, www.graphpad.com).

Statistical analyses

Statistical analyses of zebrafish RBA and flow cytometry experiments were performed using a one-way analysis of variance (ANOVA) to compare the means of results for all doses/chemicals. If there was a significant effect observed for an experiment with the one-way ANOVA ($p < 0.05$), a Dunnett's *post-hoc* test was performed to compare each dose in that experiment to the 0.4% DMSO control (Dunnett 1955). Zebrafish RBA experiments where Bis I control did not significantly reduce ROS (when compared to 0.4% DMSO controls) were excluded from analyses.

RESULTS

Developmental toxicity

The initial goal of this project was to investigate if exposure to nonteratogenic levels of twelve structurally diverse chemicals (**Figure 1**) impacted ROS production in zebrafish embryos. To identify exposure levels at which embryos were viable and lacked identifiable morphological malformations, an initial range-finding study to determine a NOEL for developmental toxicity was performed. Embryos were exposed to various doses (8.80 nM to 80.0 μM) of each chemical, beginning at 6 hpf. Daily media changes were performed until 96 hpf upon which gross morphological assessment was performed via dissecting light microscope (**Figure 2(A)**). Among the xenobiotics, the NOEL for developmental toxicity varied (**Figure 2(B)**). Of the 12 tested compounds, five (azathioprine, dexamethasone, dichloroacetic acid, lead acetate, and trichloroethylene) had no adverse effects in the developmental toxicity assay. For these

compounds in this assay, the NOEL was determined to be 80 μM. The remaining seven agents had varying potencies ranging from 27.5 nM to 8.19 μM (**Figure 2(B)**). The most potent xenobiotic identified in this assay was hydroquinone.

Five of 12 xenobiotics tested suppressed the respiratory burst in zebrafish embryos

To identify compounds with potential immunosuppressive ability, an RBA using whole zebrafish embryos was employed. Embryos were exposed to multiple dilutions of non-teratogenic doses of the test xenobiotics using the dosing scheme outlined in **Figure 2(A)** and subjected to the RBA at 96 hpf. After stimulation with PMA to induce ROS production, five of the 12 test agents reproducibly suppressed ROS production in the RBA: 17β-estradiol, benzo[a]pyrene (BaP), lead acetate, methoxychlor, and phenanthrene (**Figure 3**). For each compound, a lowest-observed-effect level (LOEL) was determined to be the lowest concentration at which an effect was observed in two biological replicates (**Figure 4**). These five compounds had a wide range of potencies as determined by their LOEL, ranging from 27.5 nM to 80 μM. The other seven agents did not affect ROS production in this assay. No compounds were identified that enhanced ROS production.

One of five immunosuppressive xenobiotics altered phagocyte numbers

Whether the five compounds identified as immunotoxic at non-teratogenic concentrations could alter embryo levels of neutrophils/macrophages *in vivo* and thus, in turn, lead to the observed suppression of ROS production, was evaluated. Transgenic zebrafish embryos with fluorescent neutrophils [*Tg(mpx:GFP)*] (Renshaw et al. 2006) or macrophages [*Tg(mfap4:tdTomato-caax)*] (Walton et al. 2015) were exposed as above (**Figure 2(A)**) to the test compounds at the highest dose where ROS suppression was detected (**Figures 3** and **4**). At 96 hpf, larvae were homogenized to single cell suspensions and numbers of fluorescently labeled

neutrophils and macrophages were counted via flow cytometry (Supplemental Figure 1). None of the compounds tested significantly altered the percentages of neutrophils present in larvae (**Figure 5(A)**). However, exposure to 8.19 μM benzo[a]pyrene induced a slight, but significant, increase in the percentage of macrophages present *in vivo* (**Figure 5(B)**).

DISCUSSION

In this study, 12 chemicals with varying levels of reported immunosuppressive properties in mammals were evaluated to investigate the potential utility of the zebrafish embryo as a viable model for screening xenobiotics for immunotoxicity. Based on studies in laboratory rodents, the compounds targeted differing immune processes with the idea of assessing the utility of the zebrafish model as a screen for a spectrum of immunotoxicities, rather than a specific effect. Due to their high fecundity and rapid development, larval zebrafish offer a unique model for high-throughput toxicology studies that would be difficult or expensive in rodent models. Larval zebrafish can also be employed in 96- or 384-well plate formats similar to *in vitro* systems (Lantz-McPeak et al. 2015; Poureetezadi et al. 2016), and by 72 hpf they have a functional liver capable of biotransformation that would otherwise be overlooked in a cell culture system (Saad et al. 2016; Wang et al. 2017).

Because adaptive immunity is not functional until later in development (Willett et al. 1999; Traver and Yoder 2020), the present study measured ROS production as a readout of innate immunity in larval zebrafish. Methods for measuring ROS *in vivo* using zebrafish embryos and larvae existed prior to this study, and they can be employed in a high-throughput manner (Hermann et al. 2004; Astin et al. 2017). One common method involves the use of H_2DCFDA, which offers a sensitive cost-effective way to measure ROS production. Once cellular esterases cleave the diacetate moiety of the molecule, it is trapped within the cell

(Rosenkranz et al. 1992). When H_2DCF is oxidized to DCF via interactions with ROS, the molecule fluoresces, an event that can be detected via microplate reader. This method, along with other ROS detection methods, has been used frequently in mammalian *in vitro* systems (Dahlgren and Karlsson 1999). In these systems, PMA is often used to induce ROS; PMA bypasses the cellular membrane and activates protein kinase C, leading to the phosphorylation and stimulation of the previously-noted NADPH oxidase complex (Karlsson et al. 2000). PMA successfully induces ROS production *in vivo* using whole zebrafish embryos and larvae, as well as *ex vivo* using kidney cells isolated from adult zebrafish (Hermann et al. 2004).

In the present study, the advantages of the zebrafish model were used in conjunction with the PMA-induced respiratory burst and H_2DCFDA as a model for innate immune function in an assay that has been previously established (Hermann et al. 2004). This study demonstrated that five compounds that target innate immune function in mammalian systems suppress the respiratory burst in larval zebrafish. As expected, chemicals that target the adaptive immune function did not suppress the respiratory burst in zebrafish larvae which lacked functional adaptive immunity. Overall, the 12 compounds could be classified into four distinct groups based on their biological activity: (1) compounds with no observable developmental or immunotoxicity, (2) compounds with developmental but no observable immunotoxicity, (3) compounds with no observable developmental but observable immunotoxicity, and (4) compounds with both observable developmental and immunotoxicity.

Compounds with no observable developmental toxicity or immunotoxicity

The present study identified four compounds that induced no developmental toxicity and no suppression of respiratory burst, e.g. azathioprine, dexamethasone, trichloroethylene, and dichloroacetic acid. All these compounds suppress or are implicated in suppression of the

adaptive immune response (e.g. T-cell function). At 96 hpf, zebrafish larvae used in these assays do not possess functional T-cells, and as T-cell function was not a target of these assays, suppression of the respiratory burst was not anticipated.

Azathioprine is a common anti-inflammatory pharmaceutical in autoimmune disorders and organ transplantation that has been shown to inhibit T-cell activation (Patel et al. 2006). While evidence exists to indicate that azathioprine can down-regulate genes associated with the respiratory burst in liver and macrophage cell lines (Moeslinger et al. 2006; Magkoufopoulou et al. 2012), the present study did not observe a functional suppression of the respiratory burst in the zebrafish larvae.

Dexamethasone (DEX) is a glucocorticoid pharmaceutical used as an anti-inflammatory and anti-cancer therapeutic (Löwenberg et al. 2007; Burwick and Sharma 2019). Though DEX has been shown to have immunosuppressive properties in larval zebrafish – as determined by impaired wound healing and increased rates of infections (Sharif et al. 2015; Voelz et al. 2015), the current study did not observe a suppression of the respiratory burst. This outcome is in line with data in human neutrophils wherein DEX inhibited bactericidal activity and neutrophil extracellular trap (NET) formation, but did not inhibit ROS production (Wan et al. 2017). DEX has been shown to have direct action on T-cells, leading to immunosuppression (Löwenberg et al. 2007), which may indicate that T-cell signaling is required for DEX-induced immunosuppression in innate immune populations. A pharmacodynamic study of DEX in adult humans supports this hypothesis, i.e. DEX treatment resulted in reduced ROS production by neutrophils and mononuclear cells (Dandona et al. 1999). Given that larval zebrafish do not possess functional T-cells, testing this hypothesis was beyond the scope of this study. In contrast, it was reported that DEX exposure increased ROS levels in a human osteoblast cell line (Liu

et al. 2018), as well as in human M2 macrophages; the latter finding was unusual in that M2 macrophages are generally regarded as an anti-inflammatory (Kraaij et al. 2011).

Epidemiological studies have indicated that the solvent trichloroethylene (TCE) impacts on host adaptive immunity, resulting in autoimmunity and in T-cell suppression that is not mediated through innate immunity (Cichocki et al. 2016). Indeed, the Integrated Risk Information System (IRIS) Toxicological Report on TCE details numerous studies wherein T-cells were susceptible to dysregulation by TCE exposure (USEPA 2011). However, no observations were made based on impacts upon myeloid cell populations.

Dichloroacetic acid, as a metabolite of TCE (Lash et al. 2014), may also impact on adaptive immunity. Previous studies have shown that genes related to the respiratory burst were down-regulated in the livers of mice chronically-exposed to dichloroacetic acid; similar changes were noted in a murine T cell lymphoma model (Kumar et al. 2012; Wehmas et al. 2017). Given that these findings were not identified in innate immune cells, this may indicate that dichloroacetic acid might down-regulate these genes in other tissues. Further studies should evaluate whether the above-identified genes are also down-regulated in innate immune cells and whether this could contribute to functional reductions in ROS production by immune cells.

Compounds with developmental but no observable immunotoxicity

In this study, three compounds were identified as developmentally toxic but did not alter ROS production in the zebrafish RBA, e.g. acenaphthenequinone, hydroquinone, and tributyltin oxide. In the developmental toxicity assay here, NOEL values for these compounds were similar to those previously reported (Knecht et al. 2013; Truong et al. 2014; Quevedo et al. 2019; USEPA 2019). Although changes in ROS production in the zebrafish RBA were not observed here, hydroquinone has been shown to modulate ROS production in cell-based assays (Lee

et al. 2007). Results from a prior study examining the impact of hydroquinone on macrophage function revealed that exposing a murine macrophage cell line to 25, 50, or 100 μM hydroquinone resulted in increased ROS production. However, this result was confounded by a simultaneous observation that LPS-induced ROS production was inhibited by 25 and 50 μM hydroquinone. Such data exemplify that the experimental context of exposure greatly influences the perceived activation or inhibition of ROS production (Lee et al. 2007).

Tributyltin oxide has been reported to impact the adaptive immune system, having been linked to suppression of natural killer cells and cytotoxic T-lymphocytes in exposed rats (Smialowicz et al. 1989). However, Kergosien and Rice (1998) found that a single low dose (but not higher doses) of tributyltin oxide resulted in enhanced macrophage secretory function and the respiratory burst in mice six days after intraperitoneal injection. Because the burst in a macrophage can take up to 24 h to detect (Sponseller et al. 2016), the zebrafish RBA may not be sensitive enough to detect a macrophage respiratory burst after only 2.5 h of PMA treatment (instead primarily detecting neutrophil respiratory bursts). This interpretation is supported by the flow cytometry data in this study wherein it was observed that there were roughly 10-fold more neutrophils at 96 hpf as compared to macrophages (see **Figure 5**).

A review of the literature could not identify any published studies revealing immunotoxic properties of acenaphthenequinone. The current study did not observe any induced modulations in ROS production in the zebrafish RBA. Nevertheless, further studies are still quite necessary to characterize its hazardous potential.

Compounds not developmentally toxic but immunotoxic

In this study, only one compound was not developmentally toxic but immunotoxic, i.e. lead (II) acetate trihydrate. Although the highest concentration evaluated here (80 μM) showed

no signs of causing developmental toxicity, a previous report indicated that higher levels (≥200 μM) did cause such toxicity in zebrafish embryos (Roy et al. 2014). In the zebrafish RBA, lead acetate (II) trihydrate only suppressed ROS production at the highest dose tested, indicating that it was not a potent respiratory burst inhibitor. While this capability has previously not been fully explored, there is evidence to support the findings here; other studies have reported that lead acetate exposure resulted in decreased levels of proteins related to the respiratory burst in the brains of exposed mice (Liu et al. 2013). Mishra et al. (2006) showed that, along with effects on the adaptive immune system, lead acetate exposure of a mouse macrophage cell line reduced nitric oxide production. In the context of effects on phagocyte numbers, Xu et al. (2018) reported that lead nitrate increased neutrophil numbers in exposed zebrafish larvae; no such change in neutrophil number was observed here. This difference in outcome may be due to the fact that Xu et al. (2018) focused on lead nitrate instead of lead acetate. Studies comparing the impact of lead acetate to lead nitrate, as well as those assessing both reactive oxygen and reactive nitrogen species, may be worth exploring in the future.

Compounds both developmentally toxic and immunotoxic

In this study, four compounds were identified that exhibited both developmental toxicity and immunotoxicity: BaP, 17β-estradiol, methoxychlor, and phenanthrene. Developmental toxicity of these compounds has been investigated previously, and the current findings are similar to those findings – except for that of phenanthrene (Truong et al. 2014; Fang et al. 2015; USEPA 2019). Phenanthrene had variable results in previous studies; here, it was identified it as a potent developmental toxicant. The reasons for these inter-laboratory variances in outcomes might be due to differences in dosing scheme, genetics of the zebrafish strains being used (Balik-Meisner et al. 2018), or even composition of microbiota in the aquaculture facilities

(Turner 2018). Such sources of potential variability between laboratories should be acknowledged until standards are agreed upon within the field.

The present study identified two polycyclic aromatic hydrocarbons, i.e. BaP and phenanthrene, that suppressed ROS production *in vivo*. The immunotoxicity of BaP has been widely studied to date; the data in this study adds to that wealth of knowledge. In the zebrafish RBA, BaP was shown to be a potent inhibitor. Interestingly, it was also observed that BaP caused an unexpectedly slight, but significant, increased number of macrophages *in vivo*. Previous studies have identified numerous genes related to the respiratory burst that are down-regulated by BaP exposure (Kann et al. 2005; Mathijs et al. 2009; Scott et al. 2011; Lizarraga et al. 2012; Fang et al. 2015); these support the current findings in the zebrafish embryos. Aside from this impact on gene expression, BaP has also been shown to inhibit ROS production in phagocytes (Zaccaria and McClure 2013) and inhibit monocytic differentiation into macrophages (van Grevenynghe et al. 2003).

In contrast to BaP, the effects of phenanthrene on the immune system have gone under-studied in mammalian models. One study noted no significant changes in the antibody responses of immunized mice exposed to phenanthrene (Silkworth et al. 1995). Conversely, phenanthrene has been studied in two freshwater fish species, revealing immunotoxic outcomes. Loughery et al. (2018) reported that phenanthrene down-regulated immune pathways after a subchronic developmental exposure in fathead minnow. Haque et al. (2018) noted that phenanthrene reduced immunoglobulin levels, lysozyme activity, and white blood cell count in olive flounders. In the present study, phenanthrene suppressed the respiratory burst of the zebrafish embryos. To our knowledge, this is the first study to report this outcome. The only other study related to this

effect was that of Chen et al. (2016) who reported that certain phenanthrene derivatives inhibited reactive nitrogen species production in a murine macrophage cell line.

As the current work in the zebrafish supports the general conclusion that phenanthrene could suppresses the immune system of freshwater fish, future studies should work to better establish the immunomodulatory potential of phenanthrene in mammalian models. Given that both phenanthrene and BaP are polycyclic aromatic hydrocarbons (PAH) identified by the USEPA as "priority pollutants" (Andersson and Achten 2015), and given their environmental ubiquity, future work should more fully characterize the immunotoxicity of various PAH to understand their common/disparate mechanisms of action(s) in order to reduce exposure risks and prevent adverse outcomes.

The present study also revealed that 17β-estradiol, an estrogen steroid hormone, was a potent inhibitor of the zebrafish RBA. This outcome is in line with reports that exposure of adult male rats to 17β-estradiol resulted in a down-regulation of genes related to the respiratory burst (Razmara et al. 2005; Shih et al. 2006). Others have reviewed the roles of estrogens in inflammation, noting that pregnancy levels of 17β-estradiol are linked to decreased ROS production, potentially through decreased expression of NADPH oxidase (Straub 2007). Though the present study did not observe changes in embryo neutrophil numbers, Xu et al. (2018) reported that exposure of zebrafish larvae to a lower dose of 17β-estradiol (18 nM) significantly increased the numbers of neutrophils. This difference in observations may be a result of differences in the doses employed, differences in transgene promoters used to label the neutrophils, and/or genetic backgrounds of the transgenic larvae. It is widely accepted that 17β-estradiol is an immunomodulator of the innate and adaptive immune systems, even as an

endogenous hormone (Kovats 2015; Moulton 2018); the present work with the zebrafish RBA validates these findings.

Previous studies have shown that methoxychlor is able to inhibit antibody production in rodent models (Chapin et al. 1997; Hayashi et al. 2013), indicating potential toxicity to the adaptive immune system. However, in the zebrafish RBA, methoxychlor inhibited the respiratory burst, indicating this agent also impacts innate immunity. To our knowledge, this study is the first to show that methoxychlor suppresses the respiratory burst. The current observations are supported by a previous study that showed that exposing a mouse macrophage cell line to methoxychlor reduced interferon (IFN)-β signaling after lipopolysaccharide challenge (Ohnishi et al. 2008).

Given that this study identified two known endocrine-disrupting compounds, i.e. 17β-estradiol and methoxychlor, as potent inhibitors of the respiratory burst, future studies should address mechanisms by which endocrine-disrupting compounds inhibit innate immune function, either dependent or independent of their endocrine disruption. Endocrine disrupting compounds are highly proliferative and prevalent in the environment and have been of increasing concern for decades (Acerini and Hughes 2006). This study further confirms that endocrine disruption plays a role in immune suppression.

In conclusion, the current study employed the larval zebrafish RBA as a model to identify compounds that alter the respiratory burst *in vivo*. From among 12 diverse compounds, five were identified with a potential to suppress innate immunity without inhibiting hematopoiesis. As these agents were known/predicted to be immunotoxic in mammalian models, this supports the validity of the larval zebrafish RBA as a screening tool that could be used with other high throughput and/or *in vitro* and *in silico* methods as part of a defined approach to assess potential

immunotoxicity. Of the five, BaP unexpectedly led to increased macrophage numbers *in vivo*, thereby warranting follow-up mechanistic studies.

SUMMARY

A goal of this study was to determine if results from the zebrafish RBA might be comparable to those from mammalian models. It does not elude us that comparing rodent and cell culture models to zebrafish embryos is not straightforward; the differences among models, species, and experimental designs are readily acknowledged. Nevertheless, it is proposed here that the zebrafish RBA could be a reproducible high-throughput *in vivo* tool for screening and prioritizing potentially immunotoxic compounds prior to evaluations in more costly rodent studies. The zebrafish embryo model can also be used to evaluate the impact of chemical exposure on other innate immune functions, such as *in vivo* chemotaxis and phagocytosis by macrophages and neutrophils. Though beyond the scope of this study, it will be of interest to determine if inhibition of the respiratory burst is a true indicator of *in situ* immune suppression and increased host susceptibility to infectious diseases by these agents. Given that this assay focused on myeloid cell function, it helps fill a gap in the current paradigm under the Toxic Substances Control Act wherein currently only lymphocytes are being investigated for immunotoxic effects from test agents. It is anticipated that this assay can be used for hazard identification and risk evaluation processes and to better inform decision makers in the regulation of toxic chemicals with innate immunotoxic potential.

ACKNOWLEDGEMENTS

The authors thank Stephen Renshaw (University of Sheffield) and David Tobin (Duke University) for the transgenic zebrafish lines. Thanks, are also extended to Javid Mohammed (NC State University) for the assistance in the flow cytometry experiments, and to John Rawls

(Duke University) for helpful discussions. The authors thank Nisha Sipes (NIEHS) for a thoughtful and comprehensive review of this manuscript.

FIGURES

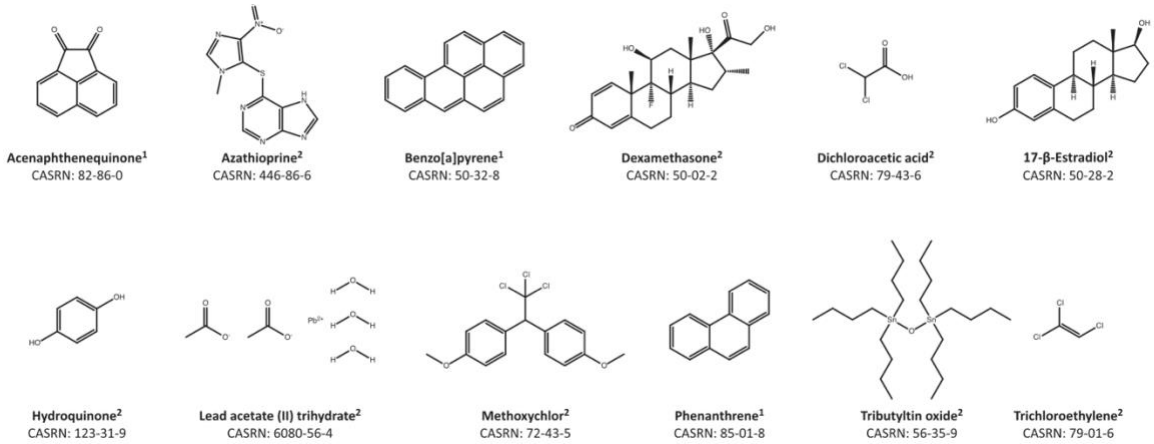

Figure 1. Chemicals for zebrafish exposures. Names and structures of chemicals used for zebrafish exposures. Chemicals were provided by (1) Battelle or (2) MRI Global. Chemical structures were generated with ChemDraw Professional (v16.0.1.4) using International Union of Pure and Applied Chemistry (IUPAC) nomenclature.

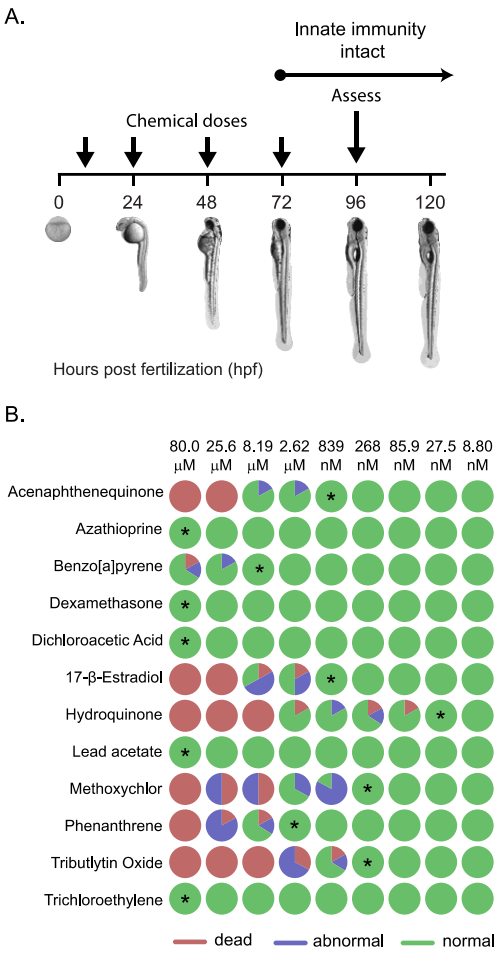

Figure 2. **Developmental toxicity of 12 structurally different xenobiotics.** (A) Experimental design. Zebrafish embryos were exposed to several concentrations of xenobiotics from 6–96 hpf and monitored for gross malformation and death. (B) Summary graphic of all twelve chemicals tested at all concentrations. Six embryos were exposed to each condition. Pie charts indicate the percentage of embryos that, by 96 hpf, were dead (red), appeared malformed (abnormal, blue), or appeared normal (green). The highest concentrations for each chemical at which no adverse effects were observed (no-observed-effect level or NOEL) are indicated by asterisks and employed as the highest doses for respiratory burst experiments in **Figure 3**.

Figure 3. **ROS production in whole zebrafish larvae.** Zebrafish embryos were exposed to several concentrations of xenobiotics from 6–96 hpf. At 96 hpf, larvae were plated into a 96 well plate, and ROS production was measured via H_2DCFDA after stimulation with PMA. Maximum fluorescence of each well was used for all analyses; results of two replicate experiments are reported. (A) Acenaphthenequinone, (B) azathioprine, (C) benzo[a]pyrene, (D) dexamethasone, (E) dichloroacetic acid, (F) 17-β-estradiol, (G) hydroquinone, (H) lead (II) acetate trihydrate, (I) methoxychlor, (J) phenanthrene, (K) tributyltin oxide, and (L) trichloroethylene. Bis I (10 μM; selective protein kinase C inhibitor) was used as a positive control. Significance ($p<0.05$) was determined by a one-way ANOVA with Dunnett's post-hoc test for pairwise comparisons to the DMSO control. Red data points denote significance for tested chemicals.

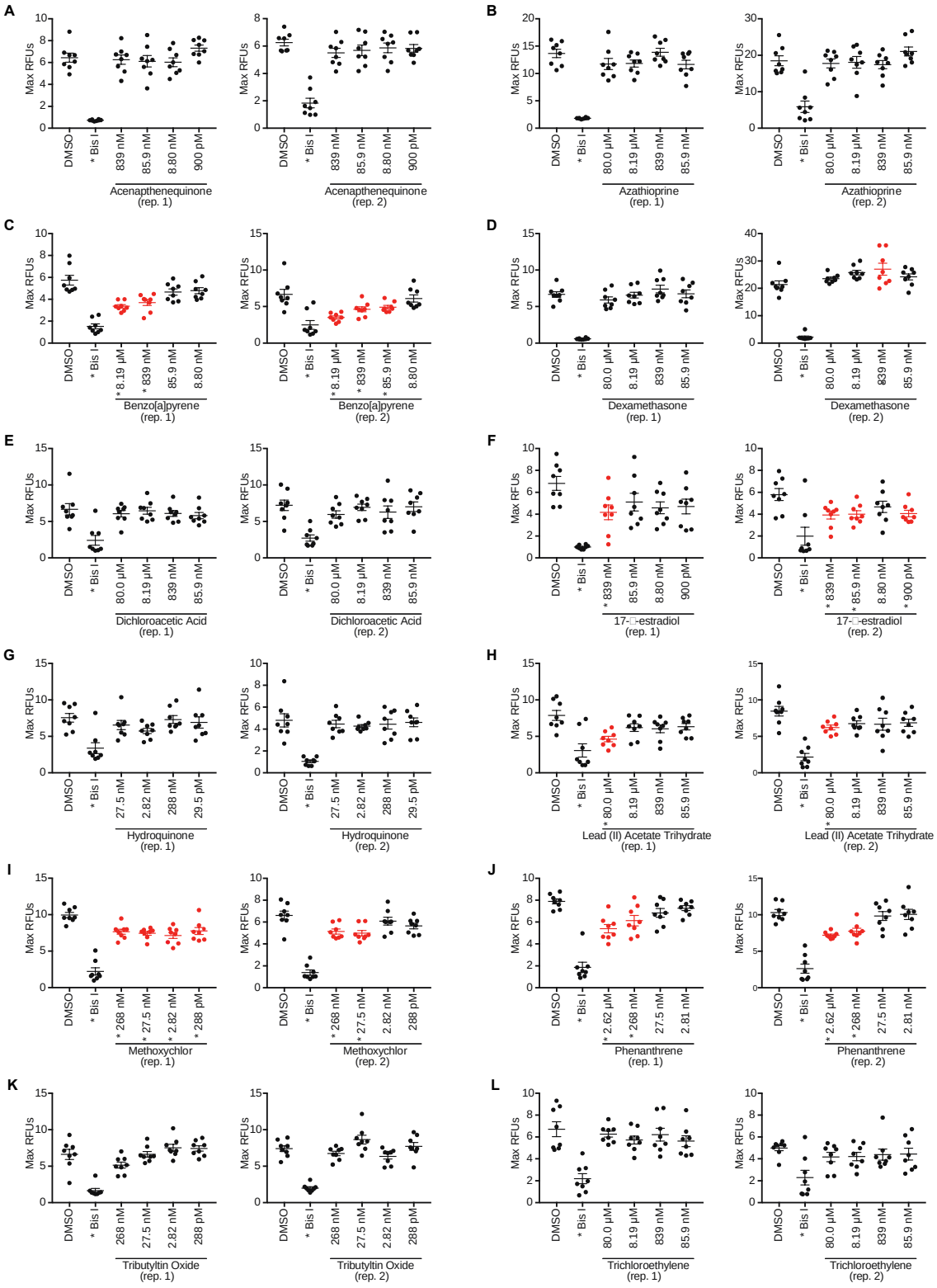
A
Max RFUs
DMSO
* Bis I
839 nM
85.9 nM
8.80 nM
900 pM
Acenapthenequinone (rep. 1)
Acenapthenequinone (rep. 2)
B
80.0 µM
8.19 µM
839 nM
85.9 nM
Azathioprine (rep. 1)
Azathioprine (rep. 2)
C
* 8.19 µM
* 839 nM
85.9 nM
8.80 nM
Benzo[a]pyrene (rep. 1)
Benzo[a]pyrene (rep. 2)
D
Dexamethasone (rep. 1)
Dexamethasone (rep. 2)
E
Dichloroacetic Acid (rep. 1)
Dichloroacetic Acid (rep. 2)
F
* 839 nM
85.9 nM
8.80 nM
900 pM
17-□-estradiol (rep. 1)
17-□-estradiol (rep. 2)
G
27.5 nM
2.82 nM
288 nM
29.5 pM
Hydroquinone (rep. 1)
Hydroquinone (rep. 2)
H
* 80.0 µM
8.19 µM
839 nM
85.9 nM
Lead (II) Acetate Trihydrate (rep. 1)
Lead (II) Acetate Trihydrate (rep. 2)
I
* 268 nM
* 27.5 nM
* 2.82 nM
* 288 pM
Methoxychlor (rep. 1)
Methoxychlor (rep. 2)
J
* 2.62 µM
* 268 nM
27.5 nM
2.81 nM
Phenanthrene (rep. 1)
Phenanthrene (rep. 2)
K
268 nM
27.5 nM
2.82 nM
288 pM
Tributyltin Oxide (rep. 1)
Tributyltin Oxide (rep. 2)
L
Trichloroethylene (rep. 1)
Trichloroethylene (rep. 2)

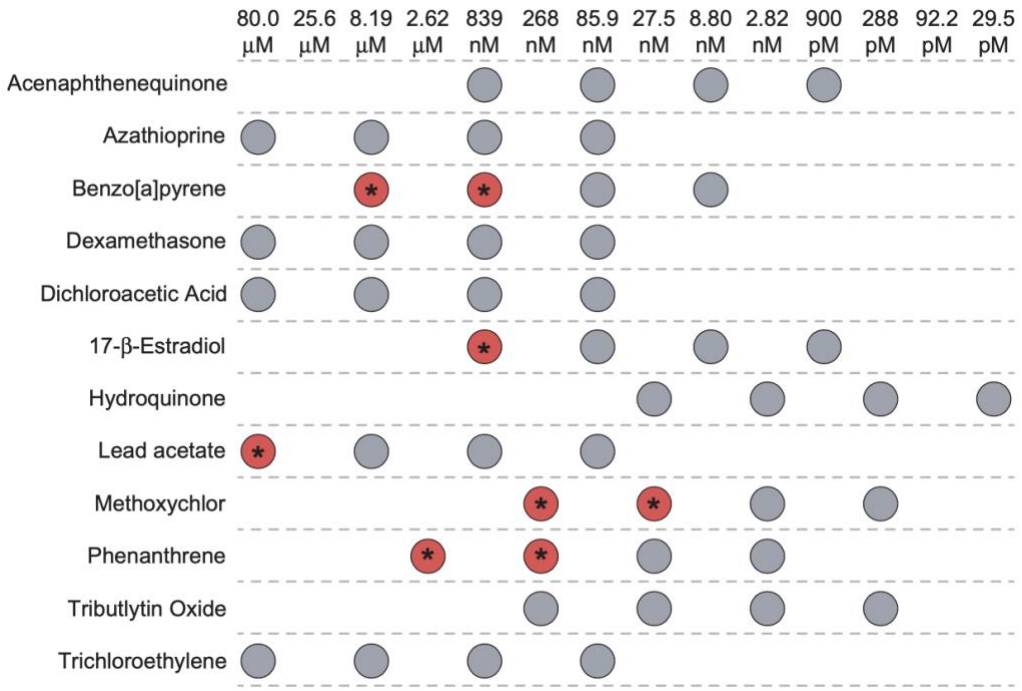

Figure 4. Summary of zebrafish larval RBA results. Data provided in **Figure 3** are summarized to highlight the range of chemical doses employed in, and doses that suppressed the zebrafish RBA. Each circle indicates the dose (above) used for each chemical (left) in the RBA assay. Combinations that led to significant reproducible suppression of the zebrafish RBA are indicated by red circles with asterisks.

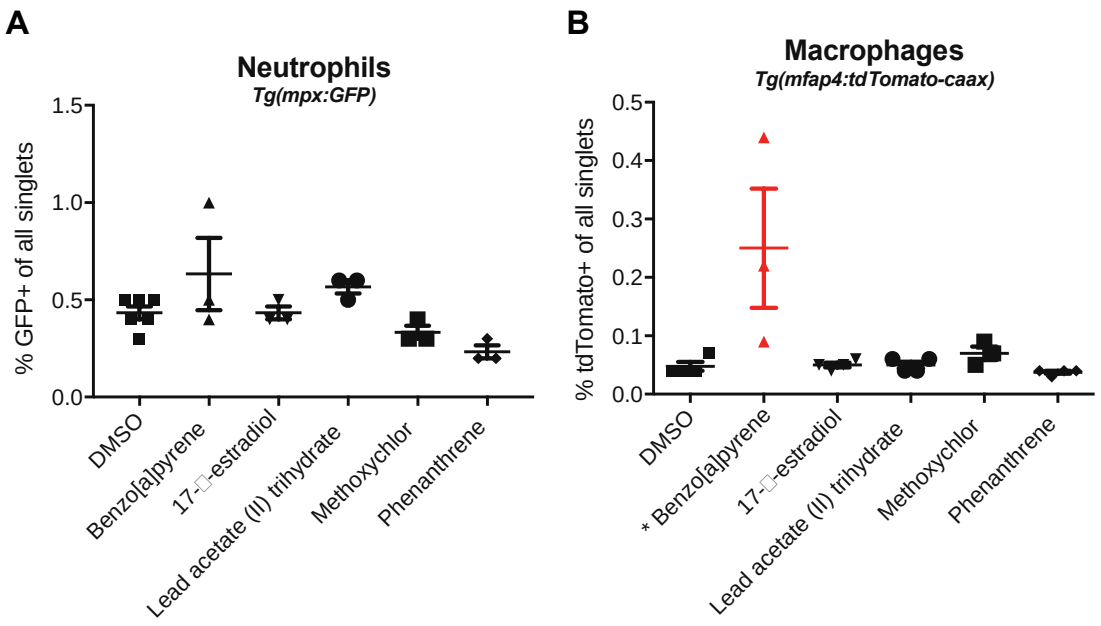

Figure 5. Benzo[a]pyrene alters macrophage number, but not neutrophil number, in whole zebrafish larvae. *Tg(mpx:GFP)* or *Tg(mfap4:tdTomato-caax)* transgenic zebrafish embryos were exposed to highest dose of one of the five compounds that suppressed ROS production in the RBA (8.19 µM benzo[a]pyrene, 839 nM 17-β-estradiol, 80 µM lead (II) acetate trihydrate, 268 nM methoxychlor, and 2.62 mM phenanthrene), or exposed to DMSO from ~6–96 hpf. At 96 hpf, larvae were mechanically homogenized into a single cell suspension and the numbers of GFP^+ and $tdTomato^+$ cells were quantified via flow cytometry. Wild-type unexposed larvae were included in all experiments in order to measure baseline autofluorescence. Data are presented as percentage of (A) GFP^+ neutrophils or (B) $tdTomato^+$ macrophages observed in individual experiments and include at least three biological replicates per compound. Significance ($p < 0.05$) was determined by one-way ANOVA with a Dunnett's post-hoc test for pairwise compare-sons to the DMSO control. Flow cytometry gating methods are outlined in **Supplemental Figure S1**.

SUPPLEMENTAL INFORMATION

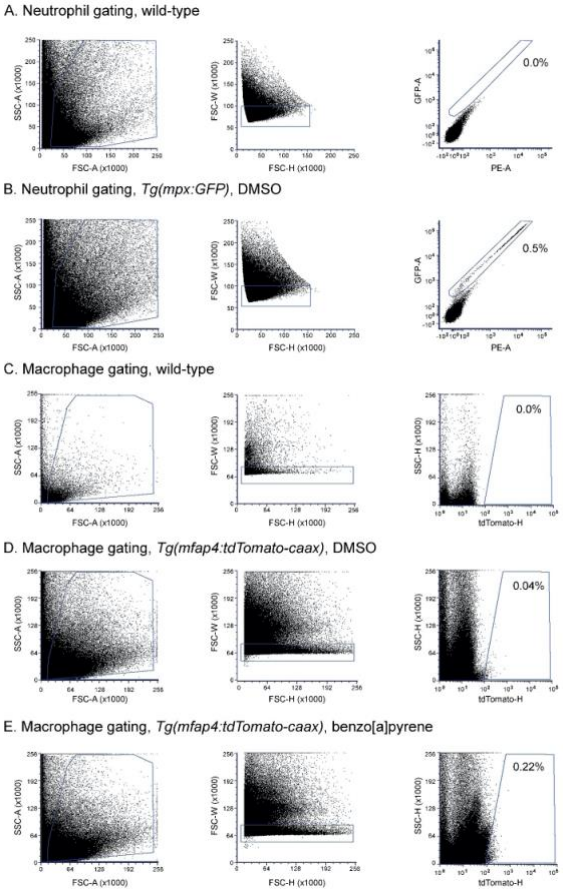

Supplemental Figure S1. Representative dot plots showing the gating strategy used in all flow cytometry experiments with transgenic *Tg(mpx:GFP)* or *Tg(mfap4:tdTomato-caax)* zebrafish. Cells were initially gated on forward- and side-scatter to exclude acellular debris (left), and then gated to exclude multicellular groups (middle). The final gate quantifies GFP^+ or $tdTomato^+$ cells (right). (A) Cells from wild-type (non-transgenic) larvae analyzed in Tg(mpx:GFP) experiments. (B) Cells from *Tg(mpx:GFP)* larvae treated with DMSO. (C) Cells from wild-type (non-transgenic) larvae analyzed in *Tg(mfap4:tdTomato-caax)* experiments. (D) Cells from *Tg(mfap4:tdTomato-caax)* larvae treated with DMSO. (E) Cells from *Tg(mfap4:tdTomato-caax)* larvae treated with 8.19 μM benzo[a]pyrene.

REFERENCES

1. Acerini C, Hughes I. 2006. Endocrine-disrupting chemicals: A new and emerging public health problem? Arch Dis Childhood. 91(8):633–641.
2. Andersson J, Achten C. 2015. Time to say goodbye to the 16 EPA PAHs? Toward an up-to-date use of PACs for environmental purposes. Polycyclic Aromat Compd. 35(2-4):330–354
3. Astin J, Keerthisinghe P, Du L, Sanderson L, Crosier K, Crosier P, Hall C. 2017. Innate immune cells and bacterial infection in zebrafish. Meth Cell Biol. 138:31–60.
4. Balik-Meisner M, Truong L, Scholl E, La Du J, Tanguay R, Reif D. 2018. Elucidating gene-by-environment interactions associated with differential susceptibility to chemical exposure. Environ Health Perspect. 126(6):067010.
5. Bogdan C, Röllinghoff M, Diefenbach A. 2000. Reactive oxygen and reactive nitrogen intermediates in innate and specific Immunity. Curr Opin Immunol. 12(1):64–76.
6. Burwick N, Sharma S. 2019. Glucocorticoids in multiple myeloma: Past, present, and future. Ann Hematol. 98(1):19–28.
7. Chapin R, Harris M, Davis B, Ward S, Wilson R, Mauney M, Lockhart A, Smialowicz R, Moser V, Burka L, et al. 1997. The effects of perinatal/juvenile methoxychlor exposure on adult rat nervous, immune, and reproductive system function. Fundam Appl Toxicol. 40(1):138–157.
8. Chen L, Shen X, Hu B, Lin Y, Igbe I, Zhang C, Zhang G, Yuan X, Wang F. 2016. Nitric oxide production inhibition and mechanism of phenanthrene analogs in LPS-stimulated RAW264.7 macrophages. Bioorg Med Chem Lett. 26(10):2521–2525.

9. Cichocki J, Guyton K, Guha N, Chiu W, Rusyn I, Lash L. 2016. Target organ metabolism, toxicity, and mechanisms of trichloroethylene and perchloroethylene: Key similarities, differences, and data gaps. J Pharmacol Exp Ther. 359(1):110–123.
10. Dahlgren C, Karlsson A. 1999. Respiratory burst in human neutrophils. J Immunol Meth. 232(1-2):3–14.
11. Dandona P, Mohanty P, Hamouda W, Aljada A, Kumbkarni Y, Garg R. 1999. Effect of dexamethasone on reactive oxygen species generation by leukocytes and plasma IL-10 concentrations: A pharmacodynamic study. Clin Pharmacol Ther. 66(1):58–65.
12. Dunnett C. 1955. A multiple comparison procedure for comparing several treatments with a control. J Am Stat Assoc. 50(272):1096–1121
13. Espenschied S, Tighe R, Gowdy K. 2018. Flow cytometry for the immunotoxicologist. Meth Mol Biol. 1803:183–197.
14. Fang X, Corrales J, Thornton C, Clerk T, Scheffler B, Willett K. 2015. Transcriptomic changes in zebrafish embryos and larvae following B[a]P exposure. Toxicol Sci. 146(2):395–411.
15. Flannagan R, Cosío G, Grinstein S. 2009. Anti-microbial mechanisms of phagocytes and bacterial evasion strategies. Nat Rev Microbiol. 7(5):355–366.
16. Gehen S, Blacker A, Boverhof D, Hanley T, Hastings C, Ladics G, Lu H, O'Neal F. 2014. Retrospective evaluation of the impact of functional immunotoxicity testing on pesticide hazard identification and risk assessment. Crit Rev Toxicol. 44(5):407–419
17. Germolec D, Luebke R, Rooney A, Shipkowski K, Vandebriel R, van Loveren H. 2017. Immunotoxicology: A brief history, current status and strategies for future immunotoxicity assessment. Curr Opin Toxicol. 5:55–59.

18. Goody M, Peterman E, Sullivan C, Kim C. 2013. Quantification of the respiratory burst response as an indicator of innate immune health in zebrafish. J Visualized Exp. 79:e50667.
19. Haque M, Eom H, Rhee J. 2018. Waterborne phenanthrene modulates immune, biochemical, and anti-oxidant parameters in the bloods of juvenile olive flounder. Toxicol Environ Health Sci. 10(3):194–202.
20. Hayashi K, Fukuyama T, Ohnuma A, Tajima Y, Kashimoto Y, Yoshida T, Kosaka T. 201 3. Immunotoxicity of the organochlorine pesticide methoxychlor in female ICR, BALB/c, and C3H/He mice. J Immunotoxicol. 10(2):119–124
21. Herbomel P, Thisse B, Thisse C. 1999. Ontogeny and behavior of early macrophages in the zebrafish embryo. Development. 126:3735–3745.
22. Hermann A, Millard P, Blake S, Kim C. 2004. Development of a respiratory burst assay using zebrafish kidneys and embryos. J Immunol Meth. 292(1-2):119–129.
23. Howe K, Clark M, Torroja C, Torrance J, Berthelot C, Muffato M, Collins J, Humphray S, McLaren K, Matthews L, et al. 2013. The zebrafish reference genome sequence and its relationship to the human genome. Nature. 496(7446):498–503.
24. Huang S, Feng C, Hung H, Chakraborty C, Chen C, Chen W, Jean Y, Wang H, Sung C, S un Y, et al. 2014. A novel zebrafish model to provide mechanistic insights into the inflammatory events in carrageenan-induced abdominal edema. PloS One. 9(8):e104414.
25. Kann S, Huang M, Estes C, Reichard J, Sartor M, Xia Y, Puga A. 2005. Arsenite-induced aryl hydrocarbon receptor nuclear translocation results in additive induction of Phase I genes and synergistic induction of Phase II genes. Mol Pharmacol. 68(2):336–346.

26. Karlsson A, Nixon J, McPhail L. 2000. Phorbol Myristate acetate induces neutrophil NADPH-oxidase activity by two separate signal transduction pathways: Dependent or independent of phosphatidylinositol 3-kinase. J Leukoc Biol. 67(3):396–404.
27. Kergosien D, Rice C. 1998. Macrophage secretory function is enhanced by low doses of tributyltin oxide (TBTO), but not tributyltin chloride (TBTCl). Arch Environ Contam Toxicol. 34(3):223–228.
28. Kimmel C, Ballard W, Kimmel S, Ullmann B, Schilling T. 1995. Stages of embryonic development of the zebrafish. Dev Dyn. 203(3):253–310.
29. Knecht A, Goodale B, Truong L, Simonich M, Swanson A, Matzke M, Anderson K, Wat ers K, Tanguay R. 2013. Comparative developmental toxicity of environmentally-relevant oxygenated PAHs. Toxicol Appl Pharmacol. 271(2):266–275.
30. Kovats S. 2015. Estrogen receptors regulate innate immune cells and signaling pathways. Cell. Immunol. 294(2):63–69.
31. Kraaij M, van der Kooij S, Reinders M, Koekkoek K, Rabelink T, van Kooten C, Gelderman K. 2011. Dexamethasone increases ROS production and T-cell suppressive capacity by anti-inflammatory macrophages. Mol Immunol. 49(3):549–557.
32. Kumar A, Kant S, Singh S. 2012. Novel molecular mechanisms of anti-tumor action of dichloroacetate against T-cell lymphoma: Implication of altered glucose metabolism, pH homeostasis and cell survival regulation. Chem Biol Interact. 199(1):29–37.
33. Lam S, Chua H, Gong Z, Lam T, Sin Y. 2004. Development and maturation of immune system in zebrafish, *Danio rerio*: A Gene expression profiling, *in situ* hybridization and immuno-logical study. Develop Comp Immunol. 28(1):9–28.

34. Lantz-McPeak S, Guo X, Cuevas E, Dumas M, Newport G, Ali S, Paule M, Kanungo J. 2015. Developmental toxicity assay using high content screening of zebrafish embryos. J Appl Toxicol. 35(3):261–272.

35. Lash L, Chiu W, Guyton K, Rusyn I. 2014. Trichloroethylene biotransformation and its role in mutagenicity, carcinogenicity and target organ toxicity. Mutat Res. 762:22–36.

36. Lawrence C. 2016. New frontiers for zebrafish management. Meth Cell Biol. 135:483–508.

37. Lee J, Kim J, Lee Y, Shin W, Chun T, Rhee M, Cho J. 2007. Hydroquinone, a reactive metabolite of benzene, reduces macrophage-mediated immune responses. Mol Cells. 23:198–206.

38. Lieschke G, Oates A, Crowhurst M, Ward A, Layton J. 2001. Morphologic and functional characterization of granulocytes and macrophages in embryonic and adult zebrafish. Blood. 98(10):3087–3096.

39. Liu C, Zheng G, Cheng C, Sun J. 2013. Quercetin protects mouse brain against lead-induced neurotoxicity. J Agric Food Chem. 61(31):7630–7635.

40. Liu W, Zhao Z, Na Y, Meng C, Wang J, Bai R. 2018. Dexamethasone-induced production of reactive oxygen species promotes apoptosis via endoplasmic reticulum stress and autophagy in MC3T3-E1 Cells. Intl J Mol Med. 41:2028–2036.

41. Lizarraga D, Gaj S, Brauers KJ, Timmermans L, Kleinjans JC, van Delft J. 2012. B[a]P-induced changes in microRNA-mRNA networks. Chem Res Toxicol. 25(4):838–849.

42. Loughery J, Kidd K, Mercer A, Martyniuk C. 2018. Part B: Morphometric and transcriptomic responses to sub-chronic exposure to the polycyclic aromatic hydrocarbon phenanthrene in the fathead minnow (*Pimephales promelas*). Aquat Toxicol. 199:77–89.
43. Löwenberg M, Verhaar A, van den Brink G, Hommes D. 2007. Glucocorticoid signaling: A non-genomic mechanism for T-cell immunosuppression. Trends Mol Med. 13(4):158–163.
44. Magkoufopoulou C, Claessen S, Tsamou M, Jennen D, Kleinjans J, van Delft J. 2012. A trans-criptomics-based *in vitro* assay for predicting chemical genotoxicity *in vivo*. Carcinogenesis. 33(7):1421–1429.
45. Manoli M, Driever W. 2012. Fluorescence-activated cell sorting (FACS) of fluorescentlytagged cells from zebrafish larvae for RNA isolation. Cold Spring Harb Protoc. 2012(8):pdb.prot069633.
46. Mathijs K, Brauers K, Jennen D, Boorsma A, van Herwijnen M, Gottschalk R, Kleinjans J, van Delft J. 2009. Discrimination for genotoxic and non-genotoxic carcinogens by gene expression profiling in primary mouse hepatocytes improves with exposure time. Toxicol Sci. 112(2):374–384.
47. Mishra K, Chauhan U, Naik S. 2006. Effect of lead exposure on serum immunoglobulins and reactive nitrogen and oxygen intermediate. Hum Exp Toxicol. 25(11):661–665.
48. Moeslinger T, Friedl R, Spieckermann P. 2006. Inhibition of inducible nitric oxide synthesis by azathioprine in a macrophage cell line. Life Sci. 79(4):374–381.
49. Moulton V. 2018. Sex hormones in acquired immunity and autoimmune disease. Front Immunol. 9:2279.

50. Ohnishi T, Yoshida T, Igarashi A, Muroi M, Tanamoto K. 2008. Effects of possible endocrine disruptors on MyD88-independent TLR4 signaling. FEMS Immunol Med Microbiol. 52(2):293–295.

51. Patel A, Swerlick R, McCall C. 2006. Azathioprine in dermatology: The past, the present, and the future. J Am Acad Dermatol. 55(3):369–389.

52. Planchart A, Mattingly C, Allen D, Ceger P, Casey W, Hinton D, Kanungo J, Kullman S, Tal T, Bondesson M, et al. 2016. Advancing toxicology research using high-throughput toxicology with small fish models. ALTEX. 33:435–452.

53. Poureetezadi S, Cheng C, Chambers J, Drummond B, Wingert R. 2016. Prostaglandin signaling regulates nephron segment patterning of renal progenitors during zebrafish kidney development. eLife. 5:e17551.

54. Quevedo C, Behl M, Ryan K, Paules R, Alday A, Muriana A, Alzualde A. 2019. Detectio n and prioritization of developmentally neurotoxic and/or neurotoxic compounds using zebrafish. Toxicol. Sci. 168(1):225–240.

55. Razmara A, Krause D, Duckles S. 2005. Testosterone augments endotoxin-mediated cerebrovascular inflammation in male rats. Am J Physiol. 289(5):H1843–1850.

56. Renshaw S, Loynes C, Trushell D, Elworthy S, Ingham P, Whyte M. 2006. A transgenic zebrafish model of neutrophilic inflammation. Blood. 108(13):3976–3978.

57. Rosenkranz A, Schmaldienst S, Stuhlmeier K, Chen W, Knapp W, Zlabinger G. 1992. A micro-plate assay for the detection of oxidative products using 2',7. dichlorofluorescin-diacetate. J Immunol Meth. 156(1):39–45.

58. Roy N, DeWolf S, Schutt A, Wright A, Steele L. 2014. Neural alterations from lead exposure in zebrafish. Neurotoxicol Teratol. 46:40–48.

59. Saad M, Cavanaugh K, Verbueken E, Pype C, Casteleyn C, van Ginneken C, van Cruchten S. 2016. Xenobiotic metabolism in the zebrafish: A review of the spatiotemporal distribution, modulation and activity of cytochrome P_{450} families 1 to 3. J Toxicol Sci. 41(1):1–11.

60. Scott D, Devonshire A, Adeleye Y, Schutte M, Rodrigues M, Wilkes T, Sacco M, Gribal do L, Fabbri M, Coecke S, et al. 2011. Inter- and intra-laboratory study to determine the reproducibility of toxicogenomics datasets. Toxicology. 290(1):50–58.

61. Sharif F, Steenbergen P, Metz J, Champagne D. 2015. Long-lasting effects of dexamethasone on immune cells and wound healing in the zebrafish. Wound Rep and Reg. 23(6):855–865.

62. Shih H, Lin C, Lee T, Lee W, Hsu C. 2006. 17β-Estradiol inhibits subarachnoid hemorrhage-induced inducible nitric oxide synthase gene expression by interfering with the NF-κB trans-activation. Stroke. 37(12):3025–3031.

63. Silkworth J, Lipinskas T, Stoner C. 1995. Immunosuppressive potential of several polycyclic aromatic hydrocarbons (PAHs) found at a Superfund site: New model used to evaluate additive interactions between benzo[a]pyrene and TCDD. Toxicology. 105(2-3):375–386.

64. Smialowicz R, Riddle M, Rogers R, Luebke R, Copeland C. 1989. Immunotoxicity of tributyltin oxide in rats exposed as adults or pre-weanlings. Toxicology. 57(1):97–111.

65. Sponseller B, Clark S, Gilbertie J, Wong D, Hepworth K, Wiechert S, Chandramani P, Sp on-Seller B, Alcott C, Bellaire B, et al. 2016. Macrophage effector responses of horses are influenced by expression of CD154. Vet Immunol Immunopathol. 180:40–44.

66. Stachura D, Traver D. 2016. Cellular dissection of zebrafish hematopoiesis. Meth Cell Biol. 133:11–53.

67. Straub R. 2007. The complex role of estrogens in inflammation. Endocrine Rev. 28(5):521–574.

68. Traver D, Yoder J. 2020. Immunology.
In: Cartner S, Eisen J, Farmer S, Guillemin K, Kent M, Sanders G, editors. The Zebrafish in biomedical research. New York: Academic Press; p. 191–216.

69. Truong L, Reif D, St Mary L, Geier M, Truong H, Tanguay R. 2014. Multi-dimensional *in vivo* hazard assessment using zebrafish. Toxicol Sci. 137(1):212–233.

70. Turner P. 2018. The role of the gut microbiota on animal model reproducibility. Animal Model Exp Med. 1(2):109–115.

71. [USEPA] United States Environmental Protection Agency 1998. Health effects test guidelines OPPTS 870.7800 Immunotoxicity. [accessed 2019 June 17]. https://www.epa.gov/test-guide-lines-pesticides-and-toxic-substances/series-870-health-effects-test-guidelines

72. USEPA. 2011. Toxicological review of trichloroethylene. [accessed 2019 June 17]. https://cfpub.epa.gov/ncea/iris2/chemicalLanding.cfm?-substance_nmbr=199

73. USEPA. 2019. ToxCast *& Tox21 Summary Files from invitroDBv3.2*. Exploring ToxCast Data: Downloadable Data. 2019. [accessed 2019 June17]. https://www.epa.gov/chemical-research/toxicity-forecaster-toxcasttm-data

74. van Grevenynghe J, Rion S, Le Ferrec E, Le
Vee M, Amiot L, Fauchet R, Fardel O. 2003. Poly-cyclic aromatic hydrocarbons inhibit differentiation of human monocytes into macrophages. J Immunol. 170(5):2374–2381.

75. Voelz K, Gratacap R, Wheeler R. 2015. A zebrafish larval model reveals early tissue-specific innate immune responses to *Mucor circinelloides*. Dis Models Mech. 8(11):1375–1388.

76. Vojtech L, Sanders G, Conway C, Ostland V, Hansen J. 2009. Host immune response and acute disease in a zebrafish model of *Francisella* pathogenesis. Infect Immun. 77(2):914–925.

77. Walton E, Cronan M, Beerman R, Tobin D. 2015. The macrophage-specific promoter Mfap4 allows live, long-term analysis of macrophage behavior during mycobacterial infection in zebrafish. PloS One. 10(10):e0138949.

78. Wang S, Miller S, Ober E, Sadler K. 2017. Making it new again: Insight into liver development, regeneration, and disease from zebrafish research. Curr Topics Develop Biol. 124:161–195.

79. Wan T, Zhao Y, Fan F, Hu R, Jin X. 2017. Dexamethasone inhibits *S. aureus*-induced neutrophil extracellular pathogen-killing mechanism, possibly through toll-like receptor regulation. Front Immunol. 8:60.

80. Weaver C, Leung Y, Suter D. 2016. Expression dynamics of NADPH oxidases during early zebrafish development. J Comp Neurol. 524(10):2130–2141.

81. Wehmas L, DeAngelo A, Hester S, Chorley B, Carswell G, Olson G, George M, Carter J, Eldridge S, Fisher A, et al. 2017. Metabolic disruption early in life is associated with latent carcinogenic activity of dichloroacetic acid in mice. Toxicol Sci. 159(2):354–365.

82. Willett C, Cortes A, Zuasti A, Zapata A. 1999. Early hematopoiesis and developing lymphoid organs in the zebrafish. Dev Dyn. 214(4):323–336.

83. Xu H, Zhang X, Li H, Li C, Huo X, Hou L, Gong Z. 2018. Immune response induced by major environmental pollutants through altering neutrophils in zebrafish larvae. Aquat Toxicol. 201:99–108.
84. Yang C, Cambier C, Davis J, Hall C, Crosier P, Ramakrishnan L. 2012. Neutrophils exert protection in the early tuberculous granuloma by oxidative killing of mycobacteria phagocytosed from infected macrophages. Cell Host Microbe. 12(3):301–312.
85. Zaccaria K, McClure P. 2013. Using immunotoxicity information to improve cancer risk assessment for polycyclic aromatic hydrocarbon mixtures. Int J Toxicol. 32(4):236–250.

CHAPTER 3

GenX, an emerging perfluoroalkyl substance (PFAS), suppresses human neutrophil function

Drake W. Phelps[1,2,3], Anika I. Palekar[1], Haleigh E. Conley[2,4], Jacob H. Driggers[1], Keith E. Linder[5,6], Seth W. Kullman[3,6,7,8], David M. Reif[3,6,7,8], M. Katie Sheats[4], Jamie C. DeWitt[3,6,9], and Jeffrey A. Yoder[1,2,3,6,8]

[1] Department of Molecular Biomedical Sciences, College of Veterinary Medicine, North Carolina State University, Raleigh, NC, USA

[2] Comparative Medicine Institute, North Carolina State University, Raleigh, NC, USA

[3] Center for Environmental and Health Effects of PFAS, North Carolina State University, Raleigh, NC, USA

[4] Department of Clinical Sciences, College of Veterinary Medicine, North Carolina State University, Raleigh, NC, USA

[5] Department of Population Health and Pathobiology, College of Veterinary Medicine, North Carolina State University, Raleigh, NC, USA

[6] Center for Human Health and the Environment, North Carolina State University, Raleigh, NC, USA

[7] Department of Biological Sciences, College of Sciences, North Carolina State University, Raleigh, NC, USA

[8] Toxicology Program, North Carolina State University, Raleigh, NC, USA

[9]Department of Pharmacology and Toxicology, Brody School of Medicine, East Carolina University, Greenville, NC, USA

Corresponding author: Jeffrey Yoder, Department of Molecular Biomedical Sciences, College of Veterinary Medicine, NC State University, 1060 William Moore Drive, Raleigh, NC 27607, USA. Tel: +1 919 515 7406; jayoder@ncsu.edu

Conflicts of Interest

DWP was paid as a scientific advisor by the Center for Environmental Health (Oakland, CA, USA) to aid in writing a petition under the Toxic Substances Control Act to the United States Environmental Protection Agency, regarding testing of certain PFASs. JCD serves/has served as a plaintiff's expert witness for several court cases involving PFAS manufacturers. All other authors declare no competing interests relevant to the content of this article.

This chapter was submitted for publication in March 2022. At the time of submission of this dissertation, it has not yet been published. DWP and JAY contributed to study conception. DWP, MKS, SWK, JCD and JAY contributed to study design. Material preparation and data collection were performed by DWP, AIP, JHD, HEC, KEL, and MKS. Data analyses were performed by DWP, and DMR aided in statistical analysis. The first draft of the manuscript was written by DWP. All authors commented on previous versions of the manuscript, and read and approved the final manuscript. SWK, JCD, and JAY secured funding for this study. JAY supervised the completion of the project.

ABSTRACT

Per- and polyfluoroalkyl substances (PFASs) are used in a multitude of processes and products, including nonstick coatings, food wrappers, and fire-fighting foams. These chemicals are environmentally persistent, ubiquitous and can be detected in the serum of 98% of Americans. Despite evidence that PFASs alter adaptive immunity, few studies have investigated their effects on innate immunity. We investigated the impact of nine environmentally relevant PFASs on one component of the innate immune response, respiratory burst. We observed that exposure to perfluorohexanoic acid (PFHxA) and ammonium perfluoro(2-methyl-3-oxahexanoate) (GenX) suppresses the respiratory burst in zebrafish larvae and a human neutrophil-like cell line, and that GenX also suppresses the respiratory burst in primary human neutrophils. This report is the first to demonstrate that these PFASs suppress neutrophil function and validates the utility of employing zebrafish larvae and a human cell line as screening tools to identify chemicals that may suppress human immune function.

Keywords: innate immunity; neutrophils; per- and polyfluoroalkyl substances; PFAS; reactive oxygen species; zebrafish

INTRODUCTION

Per- and polyfluoroalkyl substances (PFASs) are a diverse group of anthropogenic chemicals that contain linked chains of carbon and fluorine. As a class, these compounds are used to produce non-stick cookware, hydrophobic and oleophobic fabrics and coatings, fire-fighting foams, food wrappers, and more (Evich et al. 2022). The convenience provided by the unique chemistry of these compounds is now overshadowed by their persistence and ubiquity in the environment (Wang et al. 2017; Ahrens et al. 2009) and the fact that many PFASs studied to date bioaccumulate in biota (Conder et al. 2008; Ng and Hungerbühler 2014). Human exposure to these compounds is commonplace due to their presence in surface and drinking water and it is estimated that PFASs contaminate the drinking water of 200 million Americans and are detectable in the serum of 98% of Americans (Hu et al. 2016; Calafat et al. 2007; Andrews and Naidenko 2020; CDC 2020). Concerningly, PFASs are associated with a myriad of adverse health outcomes in humans, experimental animals, and wildlife (Fenton et al. 2021; ATSDR 2021).

PFASs have been linked to several immunotoxic outcomes in humans including: ulcerative colitis (Steenland et al. 2013), allergic sensitization (Averina et al. 2019; Buser and Scinicariello 2016), decreased response to vaccines (Grandjean et al. 2017a; Grandjean et al. 2017b), and increased susceptibility to infectious disease (Goudarzi et al. 2017; Dalsager et al. 2016; Ait Bamai et al. 2020). This body of evidence has led the National Toxicology Program (NTP) to conclude that two PFASs, perfluorooctanoic acid (PFOA) and perfluorooctane sulfonic acid (PFOS), are “presumed to be immune hazards to humans” (NTP 2016). It has been well established that these PFASs are immunotoxic in humans and experimental animal models (DeWitt et al. 2019); however, to date, most studies have focused on the impact of these and a

small number of other PFASs on adaptive immunity (e.g., antibody production, B cells, T cells). The effects of PFASs on innate myeloid cells (e.g., neutrophils, macrophages) have gone understudied with only a few studies investigating if PFASs modulate innate immune function (Brieger et al. 2011; Berntsen et al. 2018; Liang et al. 2022). Even with this large data gap, manufacturing of PFASs continues, and the number of PFASs is growing – the Organization for Economic Cooperation and Development (OECD) Database listing nearly 5,000 unique PFASs (OECD 2018) and the United States Environmental Protection Agency (USEPA) listing more than 12,000 PFASs (USEPA 2020) Toxicological studies have been conducted on a relatively small number of these PFASs, and there remains a scarcity of studies regarding their effects on innate immune function. Filling this gap is critical to understand the breadth of immunological ramifications of exposure to PFASs.

Recently, we reported that larval zebrafish can be used as a screening tool to identify compounds that suppress one component of innate immune function, the respiratory burst (Phelps et al. 2020). The respiratory burst is a critical function of neutrophils and macrophages involving the rapid production of reactive oxygen species (ROS), which have microbicidal properties and act as second messengers in signal transduction, further amplifying immune responses (Herb and Schramm 2021; Dupré-Crochet et al. 2013). Defects in the respiratory burst have been linked to increased susceptibility to infection (Neehus et al. 2021). In this study, we sought to expand on our earlier work by screening nine environmentally relevant PFASs for their ability to suppress the respiratory burst in larval zebrafish. Additionally, we also adapted our *in vivo* methods for use in the human neutrophil-like HL-60 cell line (Gallagher et al. 1979) to measure the respiratory burst *in vitro* to better model human responses after exposure to PFASs. HL-60 cells are a human promyeloblast cell line that can be differentiated to a neutrophil-like

phenotype which can perform the respiratory burst, phagocytosis, chemotaxis, and release neutrophil extracellular traps (NETs), making them an excellent model for human neutrophil function (Blanter et al. 2021). To validate our *in vitro* results, we also exposed isolated primary human neutrophils to PFASs *ex vivo* and assessed respiratory burst. With our *in vivo*, *in vitro*, and *ex vivo* respiratory burst assays, our data demonstrate for the first time that a short-chain perfluoroether carboxylic acid – GenX – suppressed the neutrophil respiratory burst.

RESULTS

PFOS-K, PFNA, PFHxS, and Nafion byproduct 2 induced developmental toxicity in zebrafish larvae

The initial goal of this study was to expand on our earlier work (Phelps et al. 2020) by testing the immunosuppressive properties of nine different PFASs (PFOA, PFOS-K, PFNA, PFHxA, PFHxS, PFBS, GenX, Nafion byproduct 2, and PFMOAA-Na; structures and chemical names are provided in **Fig. 1** and **Supplementary Table S1**) in zebrafish larvae using the exposure schematic in **Fig. 2**. To identify non-teratogenic concentrations of these compounds, we performed range-finding studies to assess developmental toxicity by measuring for three separate endpoints: the percentage of normal, viable larvae in each experiment (**Fig. 3**), body length, and eye size (**Supplementary Figs. S1-S2**). In this screen, we identified PFOS-K, PFNA, PFHxS, and Nafion byproduct 2 as developmentally toxic. Only PFOS-K and Nafion byproduct 2 induced toxicity in all three endpoints. To derive potency for each endpoint, AC_{50} values were calculated with a two-parameter logistic regression (**Supplementary Fig. S3**). Across all three endpoints, PFOS-K was the most potent PFAS. In contrast, even though Nafion byproduct 2 was a positive hit in all three endpoints, it was the least potent PFAS for these endpoints. PFNA, which was positive only for decreasing body length, was the second-most potent, followed by

PFHxS. Subsequent respiratory burst studies of these four compounds using zebrafish larvae excluded concentrations where developmental toxicity was observed.

PFHxA and GenX suppressed the respiratory burst *in vivo*

Using the non-teratogenic concentrations established in range-finding studies, we asked which of the nine PFASs in this study were able to suppress the respiratory burst in zebrafish larvae. At 96 hr post fertilization (hpf), PFAS-exposed larvae were treated with phorbol 12-myristate 13-acetate (PMA) to induce ROS production, which was measured using the fluorescent probe H_2DCFDA. The maximum fluorescence of H_2DCFDA as well as the total fluorescence for the entire testing period (area under the curve, AUC) were measured. Out of the nine PFASs that were tested, two suppressed the respiratory burst with statistical significance: PFHxA, and GenX. Both compounds suppressed ROS production as measured by the maximum and AUC endpoints (**Fig. 4** and **Supplementary Fig. S4**). As with the developmental toxicity positive hits, AC_{50} values were derived for both compounds for both endpoints measuring immunotoxicity (**Supplementary Fig. S5**). While they were similar in potency, PFHxA was slightly more potent than GenX in this assay. We also observed that 8.20 µM PFBS was a positive hit in this screen; however, given the non-monotonicity (i.e., lack of uniformly decreasing response with concentration) of this response, we did not pursue this compound further.

PFOA, PFOS, PFNA, PFHxS, and Nafion byproduct 2 react with PrestoBlue

To build upon our previous *in vivo* work with zebrafish larvae, we utilized an *in vitro* model of the respiratory burst using the neutrophil-like nHL-60 human cell line. Initial studies began with range-finding cytotoxicity assays using PrestoBlue to assess viability of nHL-60 cells after exposure to individual PFASs. We did not observe cytotoxicity for any of the PFASs that

were tested up to 80 µM. Unexpectedly, however, we did observe that long-chain PFASs interacted directly with PrestoBlue, causing an increase in fluorescence (**Fig. 5, Supplementary Note S1,** and **Supplementary Fig. S6**). Because we could not confirm the viability of cells at these PFAS concentrations, they were excluded from subsequent experiments.

PFOA, PFHxA, and GenX suppressed the respiratory burst *in vitro* after 96 hr of exposure

Using the concentrations of PFASs identified as non-cytotoxic in range-finding studies, we next assessed the immunotoxicity of these compounds *in vitro*. HL-60 cells were differentiated to a nHL-60 phenotype and maintained in 1.3% DMSO for 96 hr PFAS exposures (**Supplementary Note 2** and **Supplementary Figs. S7-S8**). Cells were then stimulated with PMA to induce ROS production, and DHR was used to measure ROS production. Of the nine PFASs that were tested, three inhibited the respiratory burst in this model: PFOA, PFHxA, and GenX (**Fig. 6**). PFOA, however, was only a positive hit for the maximum fluorescence and not the AUC for all fluorescence, unlike PFHxA and GenX (**Fig. 6** and **Supplementary Fig. S9**). AC_{50} values were also derived for these endpoints where PFOA was the most potent, followed by PFHxA and then GenX (**Supplementary Fig. S10**). We also observed that 0.46 µM PFNA was a positive hit in this screen. As with the *in vivo* assay above, due to the non-monotonicity of this response, we did not pursue this further.

PFHxA and GenX suppressed the respiratory burst *in vitro* after 24 hr of exposure

For the three PFASs that suppressed the respiratory burst in nHL-60 cells after a 96 hr exposure, we asked if a shorter exposure was sufficient to replicate the suppressive phenotype. nHL-60 cells were exposed to PFOA, PFHxA, or GenX for 24 hr, and the respiratory burst was measured. We observed that after a 24 hr exposure, PFHxA and GenX suppressed the respiratory burst (**Fig. 7** and **Supplementary Fig. S11**). AC_{50} values for this endpoint contrasted from the

AC_{50} values at 96 hr as GenX was more potent at 24 hr than at 96 hr; GenX was also more potent than PFHxA at this timepoint (**Supplementary Fig. S12**).

GenX suppressed the respiratory burst *ex vivo*

Finally, to test whether our positive hits were representative of human exposure, we isolated primary human neutrophils from six different donors and exposed them *ex vivo* to PFHxA, GenX, or PFBS. PFBS was included to evaluate the specificity of this assay since it was not bioactive in our previous assays. Using a flow cytometry-based approach, none of the compounds were cytotoxic, as measured by PI staining (**Supplementary Figs. S13-S14**). After 24 hours of exposure, only GenX showed significant suppression of the respiratory burst, and no effect of sex was observed with this compound (**Fig. 8** and **Supplmentary Fig. S15**). In calculating AC_{50} values for this assay, we observed that GenX was slightly less potent in the *ex vivo* assay than the *in vitro* assay (**Supplementary Fig. S16**), which may be due to variability between donors.

DISCUSSION

In this study, we investigated the immunosuppressive properties of nine different PFASs known to be in drinking water and human serum (**Supplementary Note S3**) (Kotlarz et al. 2020; Yao et al. 2020; Sun et al. 2016). We began by expanding upon our previous work employing zebrafish larvae to assess if specific chemical exposures suppressed the respiratory burst in larval zebrafish (Phelps et al. 2020). Our initial range-finding studies identified four developmentally toxic PFASs: PFOS-K, PFNA, PFHxS, and Nafion byproduct 2, all of which are long-chain PFASs. PFOS-K, PFNA, and PFHxS have been reported as developmental toxicants in larval zebrafish and other models (Gaballah et al. 2020; Mylroie et al. 2021; Zheng et al. 2011; Williams et al. 2021; Williams et al. 2017). However, to our knowledge, we are the first to report

that Nafion byproduct 2 is toxic in larval zebrafish. To date, only two studies have investigated toxicity for this compound in experimental models (Lang et al. 2020; Conley et al. 2022), including Conley et al. (2022) who concluded that Nafion byproduct 2 is developmentally toxic in rats. These data are particularly concerning given that Nafion byproduct 2 has been detected in surface water, drinking water, and wildlife and human serum for those living downstream of fluorochemical manufacturers (Kotlarz et al. 2020; Yao et al. 2020; McCord et al. 2019; Guillette et al. 2020). Interestingly, however, Gaballah et al. (2020) did not identify Nafion byproduct 1 (CAS 29311-67-9) as developmentally toxic in larval zebrafish despite structural similarity to Nafion byproduct 2. With our assessment of the respiratory burst after exposure to these compounds *in vivo*, we identified two PFASs that suppress the respiratory burst in zebrafish larvae: PFHxA and GenX (**Fig. 4**), with PFHxA being slightly more potent than GenX (**Supplementary Fig. S5**). To our knowledge, this is the first demonstration that either of these PFASs suppress the respiratory burst in any species.

We then sought to recapitulate these findings using a human neutrophil-like cell line. Using nHL-60 cells, we began with range-finding cytotoxicity testing to mirror *in vivo* approaches. Our initial cytotoxicity experiments revealed that none of the PFASs were cytotoxic (up to 80 μM; **Fig. 5**), which is consistent with previous reports in the literature, albeit those reports examined other cell types (Williams et al. 2021; Williams et al. 2017; Bangma et al. 2020; Behr et al. 2018; Behr et al. 2020; Jabeen et al. 2020; Rosenmai et al. 2020). Employing *in vitro* respiratory burst assays with nHL-60 cells, we determined that, as observed *in vivo*, a 96 hr exposure to PFHxA or GenX suppressed the respiratory burst. In addition, PFOA also suppressed the respiratory burst *in vitro* (**Fig. 6**). PFOA was identified as the most potent in this assay followed by PFHxA and then GenX (**Supplementary Fig. S10**). When comparing the

positive hits shared between models, both PFHxA and GenX were more potent *in vivo* than *in vitro*. One possible explanation for this observation is the species differences between zebrafish and humans, as it has been reported that neutrophils vary in several aspects among different species (Fingerhut et al. 2020). Despite their genetic similarity (Howe et al. 2013), zebrafish may simply be more sensitive to the immunotoxic effects of PFASs when compared to humans. This discrepancy between the models may also be driven by the larval zebrafish being an *in vivo* model with multiple cell types capable of producing ROS and immune-mediators (e.g., cytokines) that can induce ROS production, while nHL-60 cells are of a single cell lineage. The complexity of PFAS-induced immunotoxicity may also be complicated by absorption, distribution, metabolism, and elimination (ADME) of the compound *in vivo*, whereas test compounds are not subject to the same ADME considerations *in vitro*.

We next asked if a shorter (24 hr) exposure to these PFASs would reproduce the observed suppression after 96-hr exposures (**Fig. 7**). Although PFOA did not suppress the respiratory burst after a 24 hr exposure, this duration of exposure to both PFHxA and GenX resulted in immunosuppression. In fact, a 24 hr GenX exposure was more potent than a 24 hr PFHxA exposure and, interestingly, more potent than a 96 hr GenX exposure (**Supplementary Fig. S12**). With regards to PFOA, it may indicate that longer exposures are needed to induce the suppressive phenotype. Interpreting the suppression induced by PFHxA is simpler to understand; exposure for four days (96 hr) resulted in an AC_{50} that was roughly three times more potent than a one day exposure (24 hr). Conversely, the suppressive phenotype caused by GenX *in vitro* is intriguing, as its potency decreased over time. This may suggest cells have compensatory mechanisms to recover from GenX exposure or uptake kinetics of GenX change over time in this model.

As primary human neutrophils can be maintained in culture for a few days (Brach et al. 1992), we asked if a 24 hr exposure to PFHxA, GenX, or PFBS would suppress the respiratory burst in primary human neutrophils (**Fig. 8)**. Of these, only GenX suppressed the respiratory burst *ex vivo* with statistical significance, while PFHxA trended toward statistical significance (p-value of 0.1029 for AUC fluorescence of all donors). Statistical significance was detected for individual donors when exposed to PFHxA, but not when results were pooled. This may indicate variability in susceptibility to the immunotoxic effects of PFHxA in the general population and that more statistical power is needed. It is also worth noting that the serum concentrations of PFASs in our human donors are unknown, which may have affected results. Regardless, we identified PFOA, PFHxA, and GenX as immunotoxic in at least one of our innate immune assays. Previous studies have also reported suppression of the T cell-dependent antibody response, an adaptive immune endpoint, in mice after exposure to PFOA or GenX (Shane et al. 2020; Yang et al. 2002; DeWitt et al. 2008; Rushing et al. 2017). While there are currently no reports of PFHxA's influence on the T cell-dependent antibody response, PFHxA and one of its precursors have been linked to other immunotoxic outcomes in rodents (Rice et al. 2020).

Finally, we used ToxPi (Marvel et al. 2018; Reif et al. 2010) as a way to integrate our data using an unbiased weight-of-evidence framework to compare our results for these nine PFASs and prioritize them for further testing., GenX and PFHxA were the most bioactive in our assays, despite their lack of developmental toxicity, and they clustered separately from all other tested PFASs (**Supplementary Fig. S17**). PFNA, PFHxS, and Nafion byproduct 2 cluster closely together based on developmental toxicity; given the lack of publicly available toxicity data for Nafion byproduct 2, this may provide a starting point for future research to assess mechanisms of its hazardous properties. These data also reveal that developmental toxicity was not predictive of

immunotoxicity for the nine PFASs in this report. We suggest prioritization of PFHxA and GenX for further immunotoxicity studies. As more immunotoxic endpoints are investigated in these models and others, we encourage others to utilize ToxPi for summarizing results and prioritizing next steps for hazard identification and risk assessment.

While our findings are conclusive, further research is needed on several fronts. There is a need to understand the structural and mechanistic implications of the developmental toxicity induced by PFOS, PFNA, PFHxS, and Nafion byproduct 2. In the *in vivo* zebrafish respiratory burst assay, more studies are needed to assess the sensitivity of this assay. Although the genetic diversity of outbred wild-type zebrafish can mimic the diversity of a human population (Balik-Meisner et al. 2018a; Balik-Meisner 2018b), it may reduce the sensitivity and reproducibility of this assay in the absence of large numbers of replicates. It must also be emphasized that, even though multiple PFASs were not positive hits in our respiratory burst screens, this does not mean that these chemicals are not immunotoxic. Further study is especially needed on emerging PFASs with unknown toxicity profiles. While many mechanisms have been proposed for PFAS-induced immunotoxicity (Liang et al. 2022; Neagu et al. 2021), it remains unclear how the data presented here fit into the proposed frameworks - the molecular mechanisms by which these PFASs suppress the respiratory burst remain unknown. In addition, studies designed to evaluate the immunotoxicity of these compounds across several validated endpoints are needed. The respiratory burst is but one aspect of innate immunity, which ultimately is linked to susceptibility to infectious disease. There are few studies in experimental models that have investigated the impact of PFAS exposure on host resistance or susceptibility to pathogens (Guruge et al. 2009; Brown et al. 2021) and these results are supported by human epidemiologic data (Goudarzi et al.

2017); there is a critical need for development and implementation of high-throughput infection assays that can be used to assess whether PFASs confer susceptibility to infectious disease.

With this report, we are the first to demonstrate that PFOA, PFHxA, and GenX inhibit the respiratory burst. We are also the first to show that GenX suppresses innate immune function in three different models from two different species. This work complements the testing paradigm laid out by Verdon et al. (2021) wherein they describe utilizing nHL-60 cells to prioritize chemicals prior to testing in primary neutrophils and *in vivo* models. With these findings, we have further cemented that the respiratory burst can be inhibited by xenobiotics. However, investigation of innate immune function is still lacking from the Health Effects Test Guidelines for Immunotoxicity from USEPA, which rely on a tiered approach in low-throughput rodent models (USEPA 1998). Development of new approach methodologies and new testing guidelines are necessary to implement high-throughput testing strategies and reduce animal testing for immunotoxicity, while also working to incorporate endpoints for both innate and adaptive immunity to protect human and environmental health.

MATERIALS AND METHODS

Chemicals

Full names, chemical structures, and CAS numbers of test compounds can be found in **Fig. 1** and **Supplementary Table S1**. Unless otherwise noted stock solutions were created at a concentration of 80 mM and exposure solutions were prepared at a 250X concentration (**Supplementary Note S4**).

Human Subjects

Primary human neutrophils were isolated from peripheral blood of healthy adult volunteers in accordance with protocols approved by NCSU Institutional Review Board (#616).

Samples were collected from both male (n=3) and female (n=3) donors aged 20–45 years (**Supplementary Note S5**).

Vertebrate animals

Adult zebrafish were maintained in a recirculating aquarium facility at 28 °C with a 14 hr light/10 hr dark cycle, and embryos were obtained by natural spawning (Westerfield et al. 2007). Embryos were maintained in 100 mm Petri dishes in 10% Hank's saline (Westerfield et al. 2007) at 28 °C until use (**Supplementary Note S6)**.

***In vivo* exposures of zebrafish larvae to PFASs and developmental toxicity assays**

Zebrafish embryos were exposed to individual PFASs as described (Phelps et al. 2020) with slight modifications. In this study, 6 hpf embryos were sorted into 6-well plates containing 5 mL of 10% Hank's saline at a density of ten embryos per well. After sorting, 20 µL of the 250X exposure solution were added to each well for a 1X final chemical concentration. Plates were gently swirled to disperse the chemical, wrapped in parafilm, and placed in a 28 °C incubator on a 14 hr light/10 hr dark cycle. Prior to daily media changes, the plates were inspected for abnormal or dead embryos/larvae, which were removed from the wells. The plates then received a 99% media change by performing two consecutive 90% media changes. The test compound was replenished after each media change. Range-finding studies for developmental toxicity in the larval zebrafish were performed by gross examination and quantitative measurements (**Supplementary Note S7**). Embryos/larvae were inspected daily for death and malformations, and their eye area and body length measured at 96 hpf.

***In vivo* respiratory burst assays for zebrafish larvae**

The respiratory burst assay used here was modified from our previously published assayhttps://paperpile.com/c/QdjDgy/aeGRi (Phelps et al. 2020). In brief, PFAS-exposed larvae

were washed using three consecutive 80% media changes. Larvae were then plated individually into black, clear-bottom 96-well plates and stimulated with 10% Hank's saline containing 2',7'-dichlorofluorescin-diacetate (H_2DCFDA; Thermo Fisher Scientific, Waltham, MA, USA; catalog number D399) and phorbol 12-myristate 13-acetate (PMA; Sigma, St. Louis, MO, USA; catalog number P8139). In contrast to our previous study, the concentrations of H_2DCFDA and PMA were increased to 1 µg/mL and 400 ng/mL, respectively, to increase the sensitivity of the assay. Wells containing larvae that received no H_2DCFDA were included, as well as wells containing larvae that received no PMA; these larvae received DMSO as a vehicle control for both of these reagents. As a positive control for inhibition of the respiratory burst, larvae treated with bisindolylmaleimide I (Bis I; EMD Millipore, Burlington, MA, USA; catalog number 203290) at a final concentration of 10 µM for ~10 min prior to plating were also included. Bis I was not washed out prior to plating. Experiments in which the fluorescent signal from the Bis I-treated cells was not significantly reduced when compared to the vehicle control were excluded from analysis. As a quality control check for each assay, experiments were excluded in which the fluorescent signal from the Bis I-treated larvae was not significantly reduced when compared to the vehicle control.

Fluorescence was measured as described (Phelps et al. 2020). Data presented represent the maximum fluorescence from each well over the entire testing period. In addition to this, the area under the curve (AUC) was also measured to measure all fluorescence over the entire testing period. AUC was calculated using the DescTools package (v. 0.99.44) in R using the AUC function which used a spline to calculate the AUC as close as possible to the curve (Signorell 2021). Data for both endpoints were normalized to the vehicle control by dividing

each data point by the mean of the vehicle control and multiplying by 100 to convert it to a percentage.

***In vitro* exposures of human nHL-60 neutrophil-like cells to PFASs**

HL-60 cells (ATCC CCL-240) were differentiated to neutrophil-like phenotype and referred to as nHL-60 cells (**Supplementary Note S8**). nHL-60 cells were centrifuged at 0.4 x g for 10 min, and the supernatant was discarded. Cells were resuspended in 1.0 mL of media and counted using a Cellometer Vision (Nexcelom Biosciences, Lawrence, MA, USA) using trypan blue exclusion to determine the concentration and viability of the cells. Cells were then diluted to a concentration of 0.1 x 10^6 cells/mL in fresh media supplemented with DMSO (final concentration of 1.3%). DMSO was required to maintain the neutrophil-like phenotype (**Supplementary Notes S2 and S9** and **Supplementary Figs. S7 and S8**). Cells were aliquoted into microcentrifuge tubes for dosing where 1.0 mL of cells was dosed with 4.0 µL of a 250X PFAS exposure solution. Exposed cells were plated into a black, clear-bottom 96-well plate with 100 µL per well. Plates were incubated at 37 °C and 5% CO_2 for 24 or 96 hr prior to subsequent assays.

***In vitro* cell viability assays for nHL-60 neutrophil-like cells**

Range-finding studies for HL-60 cell viability were performed using PrestoBlue (ThermoFisher, Waltham, MA, USA; cat no. A13261), according to the manufacturer's protocol. At the time of each assay, 11 µL of PrestoBlue was added to each of the 96 wells containing 100 µL of cells (see above). To measure the background fluorescence of PrestoBlue, wells containing media with no cells were included. After adding PrestoBlue to the wells, the plates were shaken on an orbital shaker at ~100 rpm for ~10 seconds to uniformly mix the reagent. The plate was then incubated at 37 °C and 5% CO_2 for 30 min. After incubation, plates were analyzed on a

Fluoroskan Ascent FL with an excitation wavelength at 544 nm and an emission wavelength at 590. As a positive control, cells were induced to undergo apoptosis by treatment with 10 µM CAMP (King et al. 2002). Experiments in which the fluorescent signal from the CAMP-treated cells was not significantly reduced when compared to the vehicle control were excluded. Background fluorescence was calculated as the mean fluorescence of wells containing PrestoBlue with no cells. This value was subtracted from all other wells in the data set. Data were then normalized to the background-subtracted vehicle control by dividing each data point by the mean of the vehicle control and multiplying by 100 to convert it to a percentage.

***In vitro* respiratory burst assays for HL-60 neutrophil-like cells**

In vitro respiratory burst assays were performed by adapting the *in vivo* methods described above in combination with previously reported methods for primary neutrophils (Martin et al. 2017; Westerman et al. 2018). Dihydrorhodamine-123 (DHR; Sigma cat. no. D1054) stocks were prepared at a final concentration of 28.87 mM in DMSO and stored at -20 °C. At 24 or 96 hr post PFAS exposure, cells were stimulated with cell culture media containing PMA and DHR at final concentrations of 400 ng/mL and 10 µM, respectively. In contrast to the *in vivo* assay, the cells were not washed prior to stimulation. Wells with no cells were included to measure background fluorescence of DHR. Wells containing cells that received no DHR were included, as well as wells containing cells that received no PMA; these cells received DMSO as a vehicle control for both of these reagents. As a positive control, cells treated with Bis I at a final concentration of 10 µM for ~10 min prior to stimulation were also included. Experiments in which the fluorescent signal from the Bis I-treated cells was not significantly reduced when compared to the vehicle control were excluded from analysis. Fluorescence was measured as described above for the *in vivo* assays, and maximum fluorescence and AUC were calculated.

Background fluorescence was calculated as the mean fluorescence of the wells with DHR and no cells. This value was subtracted from all other wells in the data set. Data for both maximum and AUC fluorescence were then normalized to the background-subtracted vehicle control by dividing each data point by the mean of the vehicle control and multiplying by 100 to convert it to a percentage.

***Ex vivo* exposures of primary human neutrophils to PFASs**

Isolated neutrophils were centrifuged at 1200 rpm for 10 min, and the supernatant was discarded. Cells were then resuspended in 1.0 mL of media and diluted to a concentration of 0.1 x 10^6 cells/mL in fresh media. Cells were aliquoted into microcentrifuge tubes and exposed to PFASs as described above for the *in vitro* exposures. Cells were plated into a black 96-well plate with 100 µL per well and incubated at 37 °C and 5% CO_2 for 24 hr prior to subsequent assays.

***Ex vivo* cell viability assays for primary human neutrophils**

At 24 hr post PFAS exposure, 1.0 mL of neutrophils from each treatment group was transferred to a microcentrifuge tube and stained with propidium iodide (PI; final concentration of 2.0 µM). Cells were incubated for ~15 min at room temperature prior to analysis by flow cytometry. As a positive control for cell death, a group of neutrophils were heat-killed by incubating at 55 °C for 30 min prior to staining. Flow cytometry experiments were performed in the Flow Cytometry and Cell Sorting facility at the North Carolina State University College of Veterinary Medicine using a Becton Dickinson LSRII (Franklin Lakes, NJ, USA). Cells were gated based on forward-scatter and side-scatter to gate for cellular events, excluding debris, and then gated for singlet events to exclude any large cellular debris or groups of cells that were not in single-cell suspension. A final gate was drawn in the singlet population to quantify PI^+ cells.

For each sample, 10,000 singlet events were recorded. Data were analyzed using FCS Express 6 (De Novo Software, Pasadena, CA, USA).

Ex vivo respiratory burst assays for human primary neutrophils

Respiratory burst assays with primary neutrophils were performed using previously described methods (Martin et al. 2017; Westerman et al. 2018). In brief, at 24 hr post PFAS exposure, cells were stimulated with cell culture media containing PMA and DHR at final concentrations of 50 ng/mL and 10 µM, respectively. Wells with no cells were included to measure background fluorescence of DHR. Wells containing cells that received no DHR were included, as well as wells containing cells that received no PMA; these cells received DMSO as a vehicle control for both of these reagents. As a positive control, cells treated with Bis I at a final concentration of 10 µM for ~10 min prior to stimulation were also included. Experiments in which the fluorescent signal from the Bis I-treated cells was not significantly reduced when compared to the vehicle control were excluded from analysis. Fluorescence was measured as described above to calculate normalized maximum fluorescence and AUC.

Statistical analysis

All data presented represent at least three independent, combined biological replicates. Statistical analyses for developmental toxicity, cytotoxicity, and immunotoxicity assays were performed as previously described (Phelps et al. 2020). Briefly, one-way analysis of variance tests (ANOVAs) were performed in GraphPad Prism (v7.0e, GraphPad Software, La Jolla, CA). When statistical significance ($p < 0.05$) was observed for the ANOVA, a Dunnett's post-hoc test was performed for pairwise comparisons between each treatment and the vehicle control. For *ex vivo* experiments with primary neutrophils, data were stratified by sex and treatment group for

each PFAS. Two-way ANOVAs were performed in GraphPad Prism to determine if there were effects of sex and/or treatment. If there was an effect of sex, a Dunnett's post-hoc test was performed within both sexes for pairwise comparisons between treatment groups and the vehicle control. If there was not an effect of sex, a Sidak's post-hoc test was performed for pairwise comparisons of treatment groups and the vehicle control regardless of sex. For endpoints where statistical significance was observed at the highest concentration tested, AC_{50} values were calculated using the drc package in R (Ritz et al. 2015). This was done using a two-parameter logistic regression where the maximum was fixed at 100% and the minimum was fixed at the mean of the highest concentration for each dataset.

ACKNOWLEDGEMENTS

The authors thank Ashley M. Connors and Giuliano Fererro (NC State University) for critical review of the manuscript, volunteer donors for their time and blood for *ex vivo* studies, and the NC State University Center for Human Health and the Environment (CHHE) - Comparative Pathology Core for assistance with cytology experiments. Research reported in this publication was supported by the National Institute of Environmental Health Sciences (NIEHS) of the United States National Institutes of Health (NIH) (P42-ES031009 to D.M.R., S.W.K., J.C.D. and J.A.Y.) and the NC State University CHHE (P30-ES025128 to M.K.S. and J.A.Y.). D.W.P. was supported by a NIH Biotechnology Traineeship (T32-GM008776). The content is solely the responsibility of the authors and does not necessarily represent the official views of the NIH.

DATA AVAILABILITY

Raw data from zebrafish developmental toxicity assays, cell viability assays, respiratory burst assays, and ToxPi analysis are freely available through the Dryad database at doi: https://doi.org/10.5061/dryad.qjq2bvqj4.

FIGURES

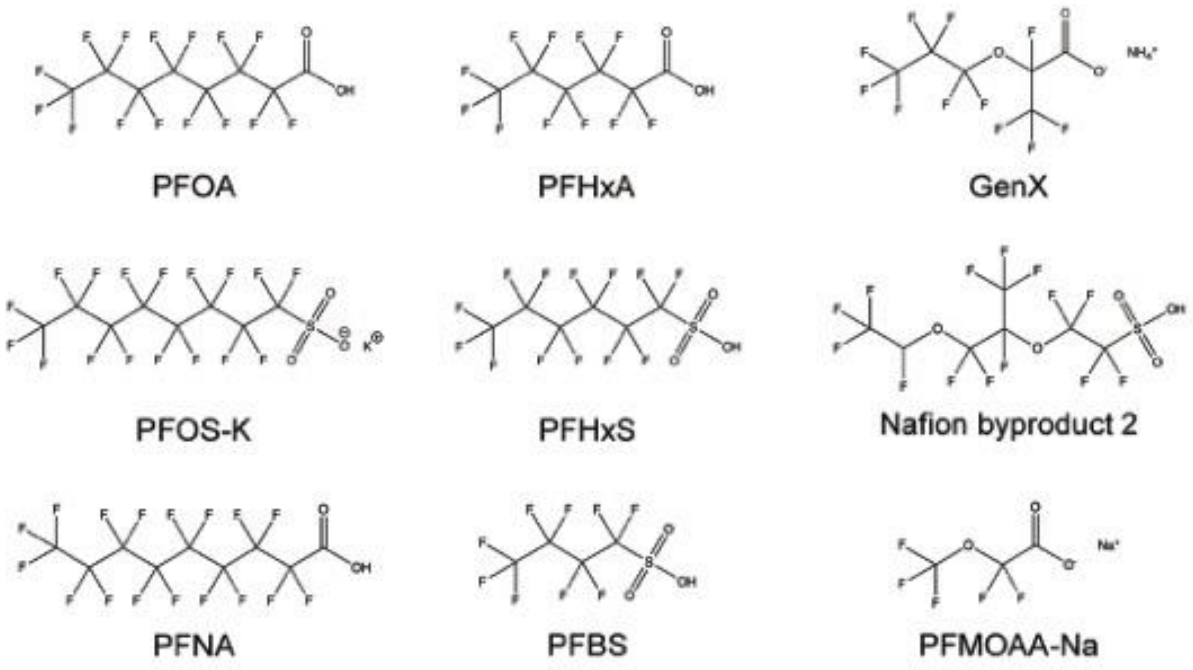

Figure 1. PFASs used in this study. Names and structures of the PFASs used in this study. Vendors and CAS-RN numbers are provided in Supplementary Table S1. Chemical structures were generated with ChemDraw Professional (v16.0.1.4) using International Union of Pure and Applied Chemistry (IUPAC) nomenclature.

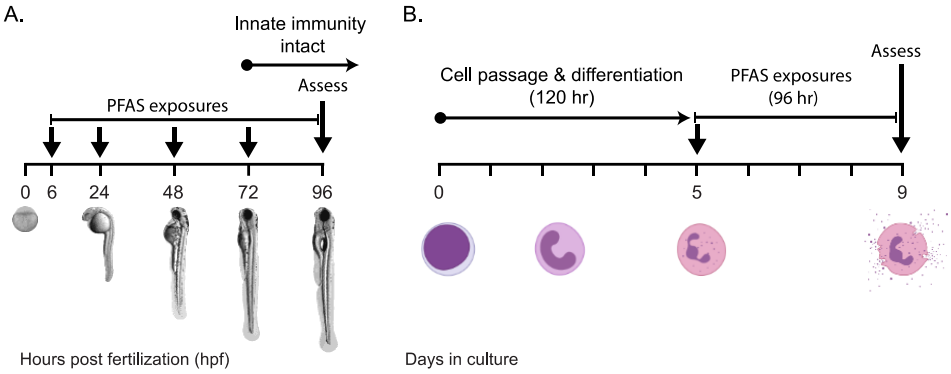

Figure 2. *In vivo* and *in vitro* screens. (a) Zebrafish embryos were exposed to several concentrations of different PFASs from ~6 hpf to 96 hpf. At 96 hpf, larvae were assessed for developmental toxicity or respiratory burst. (b) HL-60 cells were differentiated to a neutrophil-like phenotype (nHL-60) via DMSO treatment for 5 days. At 5 days, cells were dosed with PFASs and plated into a 96-well plate. At 96 hours post plating, cells were assessed for cytotoxicity or respiratory burst. This strategy was also employed for a 24 hr PFAS exposure. Panel A is adapted from 28. Neutrophil images in panel B were acquired from BioRender.

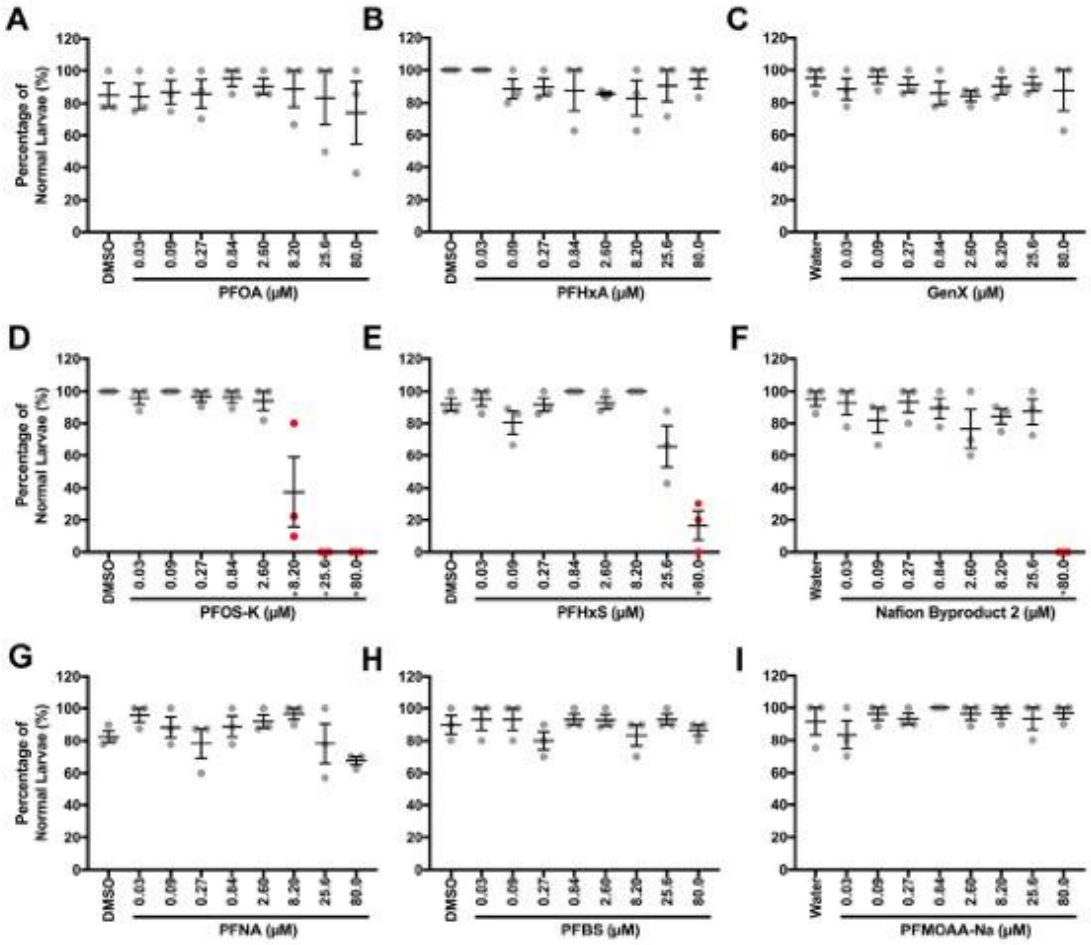

Figure 3. Developmental toxicity in zebrafish larvae varies among nine structurally different PFASs. Images of zebrafish larvae (96 hpf) were taken via brightfield microscopy. Developmental malformations (e.g. spinal curvature, pericardial edema) and death were classified in a binary manner. Individual symbols represent individual clutches of zebrafish larvae with 5-10 imaged larvae in each treatment group. Data shown are from three, combined, independent biological replicates. Statistical significance (*, $p<0.05$) was determined by a one-way ANOVA with Dunnett's post-hoc test for pairwise comparisons to the vehicle control. Body length and eye size measurements are provided in **Supplementary Figures S1 and S2**.

Figure 4. PFHxA and GenX suppressed the respiratory burst *in vivo.* Zebrafish larvae were exposed to (a) PFOA, (b) PFHxA, (c) GenX, (d) PFOS-K, (e) PFHxS, (f) Nafion byproduct 2, (g) PFNA, (h) PFBS or (i) PFMOAA-Na for 96 hr. Larvae were then washed and distributed into a 96 well-plate. Larvae were then treated with PMA, to induce ROS production, and H_2DCFDA to measure ROS produced. Fluorescence of H_2DCFDA was measured for 2.5 hours on a fluorescent plate reader set to 28.5°C. Larvae receiving no PMA and no H_2DCFDA were included as controls. Larvae treated with Bis I, a protein kinase C inhibitor, were included as a positive control for inhibition of the respiratory burst. Data shown are from at least three, combined, independent biological replicates with 4-16 larvae in each treatment group. Data represent the maximum amount of fluorescence over the entire testing period, with each symbol representing an individual larvae. Statistical significance (*, $p<0.05$) was determined by a one-way ANOVA with Dunnett's post-hoc test for pairwise comparisons to the vehicle control. AUC measurements can be seen in **Supplementary Figure S4**. Concentration responses are provided in **Supplementary Figure S5**.

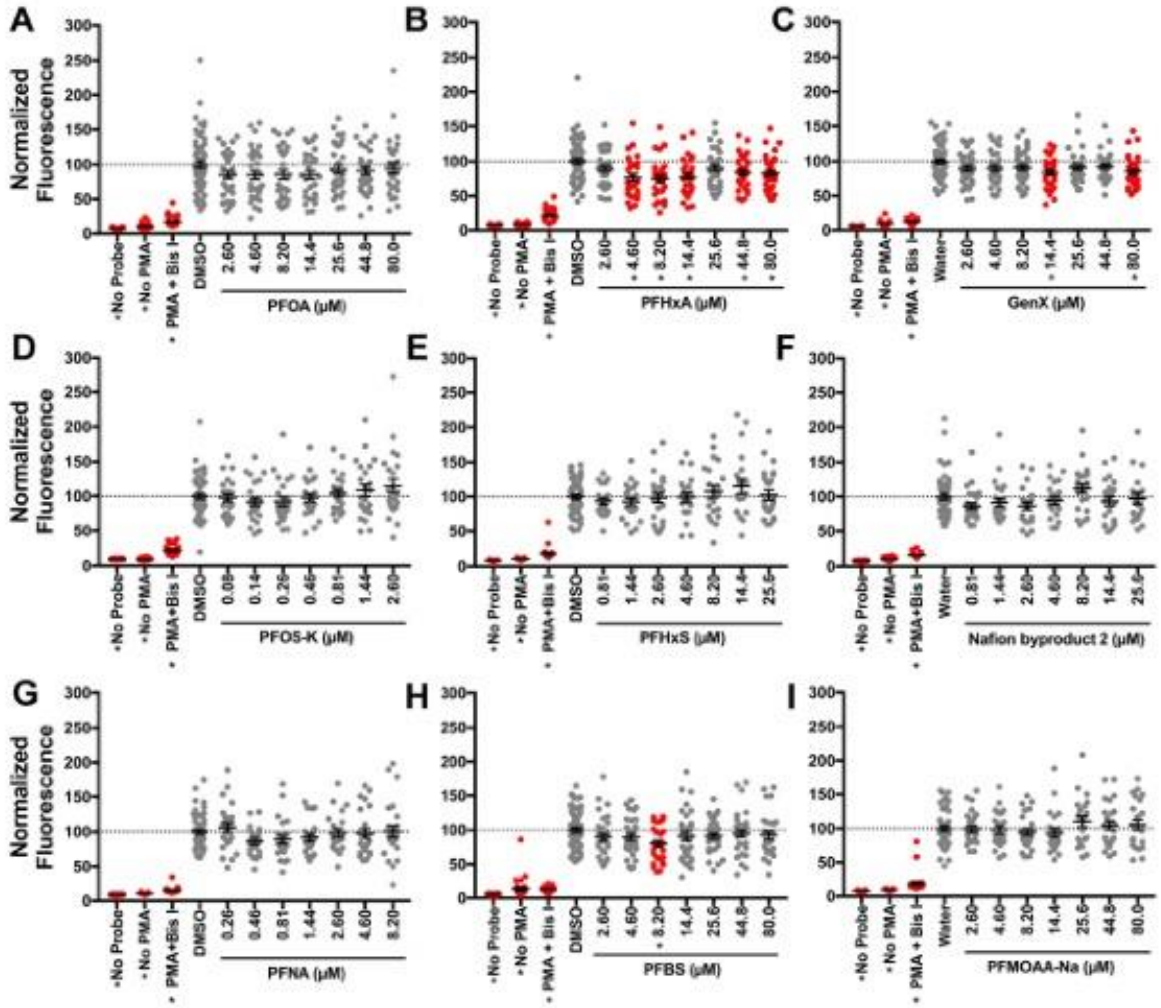
A
B
C
D
E
F
G
H
I
Normalized Fluorescence
300
250
200
150
100
50
0
-No Probe
-No PMA
+ PMA + Bis I
DMSO
Water
2.60
4.60
8.20
14.4
25.6
44.8
80.0
0.08
0.14
0.26
0.46
0.81
1.44
0.26
0.40
PFOA (μM)
PFHxA (μM)
GenX (μM)
PFOS-K (μM)
PFHxS (μM)
Nafion byproduct 2 (μM)
PFNA (μM)
PFBS (μM)
PFMOAA-Na (μM)

Figure 5. Long-chain PFASs, but not short-chain PFASs, induced increased fluorescence of PrestoBlue. After differentiation to nHL-60, cells were exposed to vehicle control or (a) PFOA, (b) PFHxA, (c) GenX, (d) PFOS-K, (e) PFHxS, (f) Nafion byproduct 2, (g) PFNA, (h) PFBS or (i) PFMOAA-Na for 96 hr. Cells were then plated into a 96 well plate with PrestoBlue and incubated at 37 °C for 30 min. Plates were then analyzed via a fluorescent plate reader. Data shown are from three, combined, independent biological replicates, except for PFHxA, which had four biological replicates. Each biological replicate included 7-8 technical replicates per treatment group. Individual symbols represent individual wells of a 96-well plate. Statistical significance (*, $p<0.05$) was determined by a one-way ANOVA with Dunnett's post-hoc test for pairwise comparisons to the vehicle control. In following up on this phenotype, we observed that PFOA directly interacts with PrestoBlue (See **Supplementary Figure S6**). Concentrations of PFASs where increased fluorescence was observed were not included in subsequent experiments.

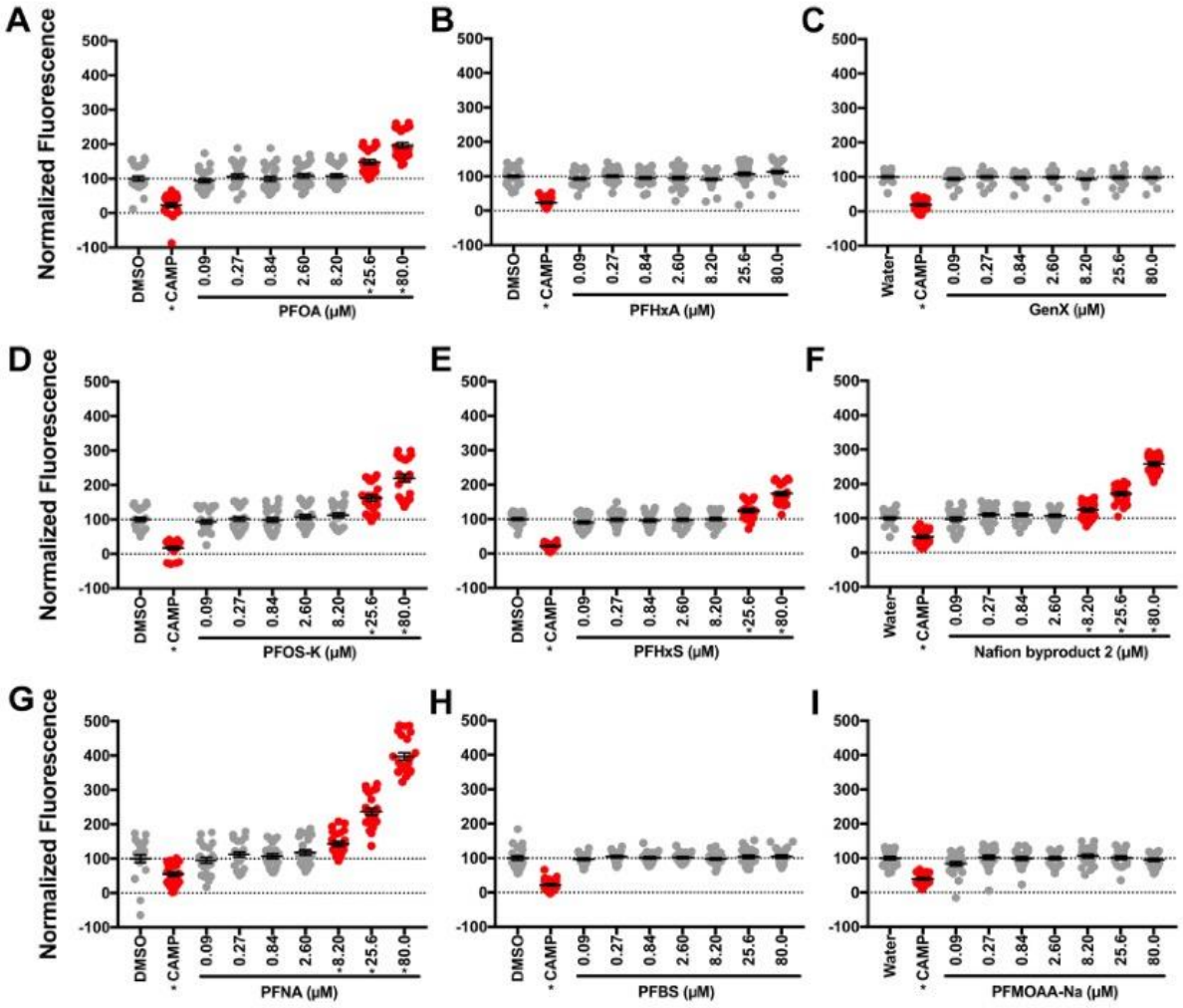
A
B
C
D
E
F
G
H
I
Normalized Fluorescence
500
400
300
200
100
0
-100
DMSO
+ CAMP
Water
0.09
0.27
0.84
2.60
8.20
25.6
80.0
PFOA (µM)
PFHxA (µM)
GenX (µM)
PFOS-K (µM)
PFHxS (µM)
Nafion byproduct 2 (µM)
PFNA (µM)
PFBS (µM)
PFMOAA-Na (µM)

Figure 6. *In vitro* respiratory burst at 96 hours. After differentiation to nHL-60, cells were exposed to vehicle control or (a) PFOA, (b) PFHxA, (c) GenX, (d) PFOS-K, (e) PFHxS, (f) Nafion byproduct 2, (g) PFNA, (h) PFBS or (i) PFMOAA-Na for 96 hr. Cells were then plated into a 96 well plate and stimulated with PMA to produce ROS, which was detected with DHR. The maximum fluorescence values are reported here. The entire fluorescence (AUC) values are provided in **Supplementary Figure S9**. Wells with no cells but with PMA and DHR, and cells receiving no PMA were included as controls. Cells treated with Bis I, a protein kinase C inhibitor, were included as a positive control for inhibition of the respiratory burst. Data shown are from three, combined, independent biological replicates, except for PFHxA, which had 4 biological replicates. Each biological replicate included 8 technical replicates per treatment group. Individual symbols represent individual wells of a 96-well plate. Statistical significance (*, $p<0.05$) was determined by a one-way ANOVA with Dunnett's post-hoc test for pairwise comparisons to the vehicle control.

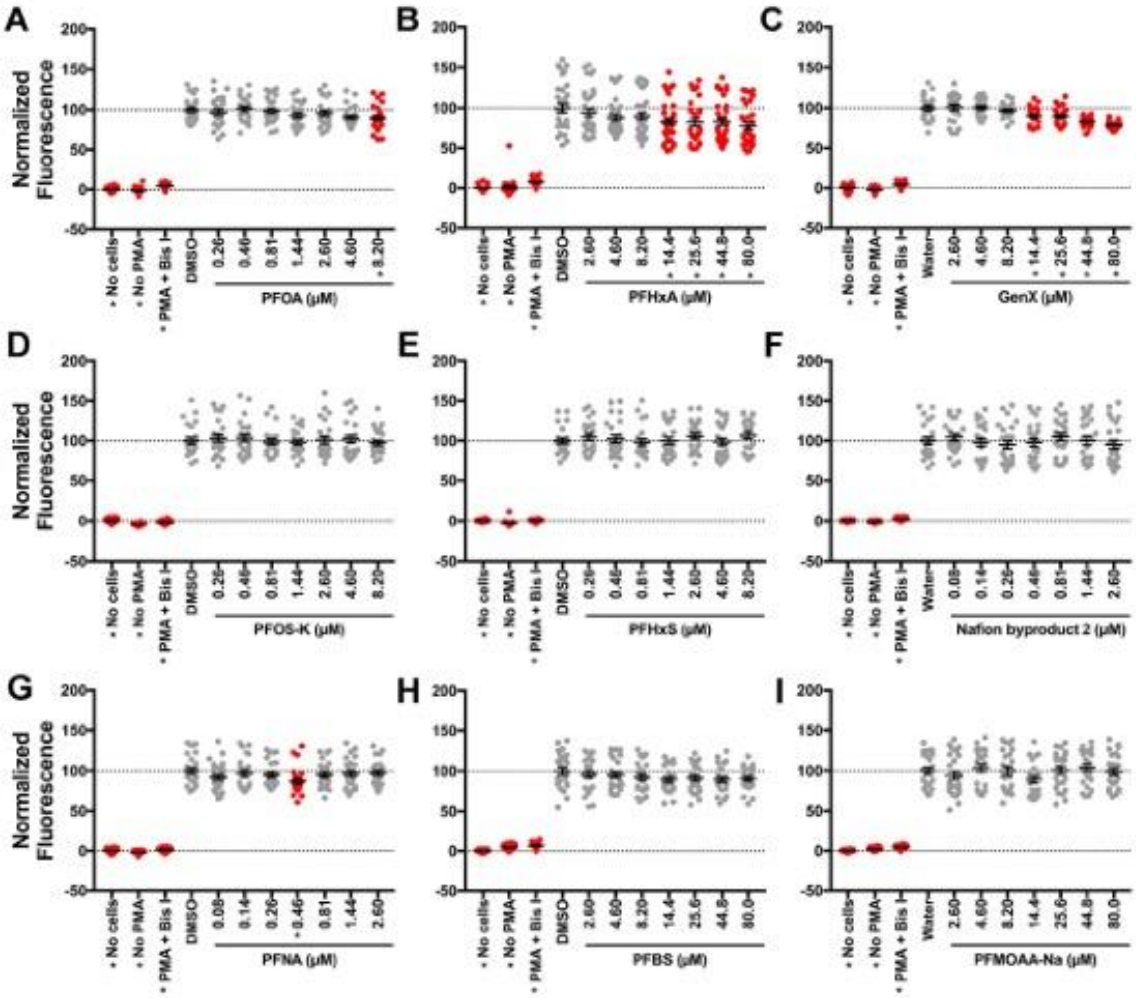
A
B
C
D
E
F
G
H
I
Normalized Fluorescence
200
150
100
50
0
-50
• No cells
• No PMA
• PMA + Bis I
DMSO
Water
0.08
0.14
0.26
0.46
0.81
1.44
2.60
4.60
8.20
14.4
25.6
44.8
80.0
PFOA (μM)
PFHxA (μM)
GenX (μM)
PFOS-K (μM)
PFHxS (μM)
Nafion byproduct 2 (μM)
PFNA (μM)
PFBS (μM)
PFMOAA-Na (μM)

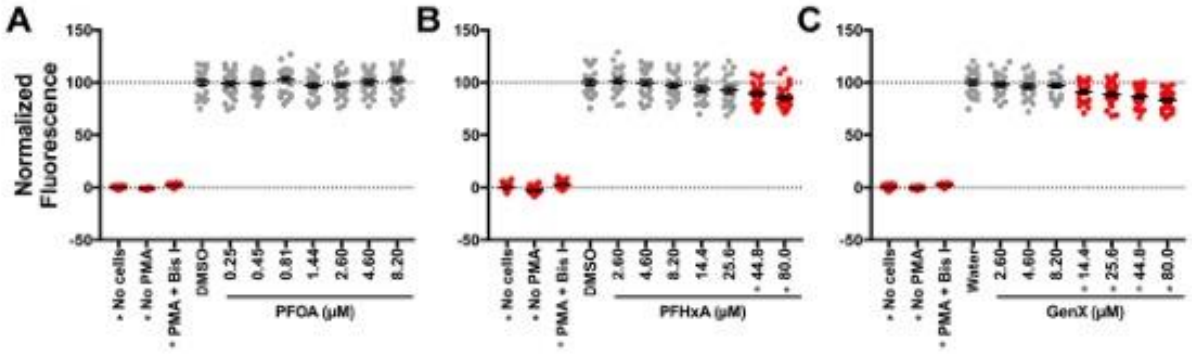

Fig. 7. *In vitro* respiratory burst for select PFASs at 24 hours. After differentiation to nHL-60, cells were dosed with vehicle control or (a) PFOA, (b) PFHxA, or (c) GenX and then plated into a 96 well plate. At 24 hr, cells were stimulated with PMA to produce ROS, which was detected with DHR. The maximum fluorescence values are reported here. The entire fluorescence (AUC) values are provided in **Supplementary Figure S11**. Wells with no cells but with PMA and DHR, and cells receiving no PMA were included as controls. Cells treated with Bis I, a protein kinase C inhibitor, were included as a positive control for inhibition of the respiratory burst. Data shown are from three, combined, independent biological replicates. Each biological replicate included 8 technical replicates per treatment group. Individual symbols represent individual wells of a 96-well plate. Statistical significance (*, $p<0.05$) was determined by a one-way ANOVA with Dunnett's post-hoc test for pairwise comparisons to the vehicle control.

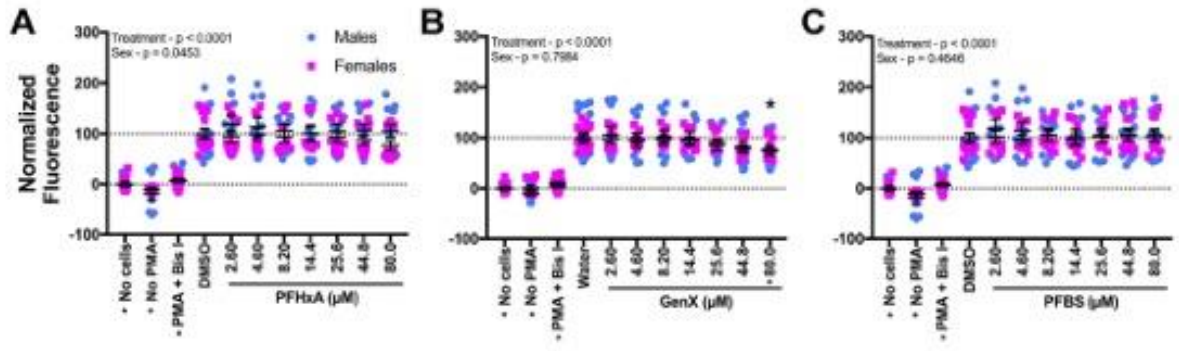

Fig. 8. ***Ex vivo*** **respiratory burst for select PFASs at 24 hours.** After isolation from individual human donors, neutrophils were dosed with vehicle control, (a) PFHxA, (b) GenX, or (c) PFBS and distributed into a 96 well plate. At 24 hours, cells were stimulated with PMA to produce ROS, which was detected with DHR. The maximum fluorescence values are reported here. The entire fluorescence (AUC) values are provided in **Supplementary Figure S15**. Fluorescence of DHR was measured for 2.5 hours on a fluorescent plate reader set to 37 °C. Wells with no cells but with PMA and DHR, and cells receiving no PMA were included as controls. Cells treated with Bis I, a protein kinase C inhibitor, were included as a positive control for inhibition of the respiratory burst. Data shown are from 6 individual human donors (3 males, 3 females). Each biological replicate included 3-6 technical replicates per treatment group. Individual symbols represent individual wells from a 96-well plate. Statistical significance (*, $p<0.05$) was determined by a two-way ANOVA with Dunnett's post-hoc test or Sidak's post-hoc test for pairwise comparisons to the vehicle control.

SUPPLEMENTARY INFORMATION

Note S1. PrestoBlue interacts with specific long-chain PFASs.

To our knowledge, we are the first to report that specific long-chain PFASs are able to directly interact with PrestoBlue Cell Viability Reagent (ThermoFisher Scientific; Catalog number: A13261). Initially, we assumed this was a proliferative phenotype, given that PrestoBlue is sensitive to changes in cell number and because others have previously reported that multiple PFASs can induce cell proliferation in various cell types (Pierozan et al. 2018a; Pierozan et al. 2018b; Jabeen et al. 2020; Williams et al. 2021; Williams et al. 2017). However, upon incubating PFOA with PrestoBlue in the absence of cells, we observed an increase in fluorescence that we interpreted as a reaction of the two compounds (**Supplementary Fig. S6**). Currently, the chemistry underlying this reaction is unknown, and thus, we caution the field at large to avoid using PrestoBlue (or other resazurin-based cytotoxicity reagents) in combination with PFAS exposure unless the cells are washed prior to the addition of PrestoBlue.

Note S2. Maintaining the neutrophil-like phenotype of nHL-60 cells requires DMSO.

Prior to testing PFASs in the cell culture respiratory burst assay, we characterized the differentiated state of nHL-60 cells. Although DMSO is required to differentiate HL-60 cells to a neutrophil-like nHL-60 phenotype (see **Supplementary Note S8**), we asked whether DMSO supplementation was necessary to maintain the neutrophil-like phenotype. We compared undifferentiated HL-60 cells to two different groups of nHL-60 cells; one group of nHL-60s was maintained in media supplemented with DMSO while the other group had DMSO withdrawn after differentiation.

Continuous DMSO treatment of HL-60 cells induced cytomorphological features of neutrophil myeloid differentiation and maturation (**Supplementary Fig. S7**). Undifferentiated

HL-60 cells retained an immature phenotype, and 100% of cells had features of promyelocytes, an immature stage of myeloid differentiation. Cells were in a proliferative state and mitotic figures were present (average 7/300; 2.3%). In contrast, DMSO treatment induced neutrophilic, myeloid differentiation in HL-60 cells. All cells were more mature, displaying features of myelocyte, metamyelocyte, band neutrophil, or mature neutrophil morphology. The cells were smaller and had smaller nuclei that, in more mature cells, had nearly absent mitotic figures (0.3/300; 0.1%). DMSO withdrawal from neutrophil-like HL-60 cells was associated with a return to promyelocyte morphology and to mitotic activity (average 5/300; 1.7%) that was more similar to untreated cells, indicating that continued DMSO exposure was needed to main myeloid differentiation in HL-60 cells.

Functionally, we confirmed these results by performing respiratory burst assays with HL-60 cells in each state of differentiation. Parental, undifferentiated HL-60 cells did not produce ROS when treated with PMA. However, differentiated nHL-60 cells maintained in DMSO produced high levels of ROS (**Supplementary Fig. S8**). nHL-60(-DMSO) cells also produced ROS in response to PMA; however, we observed that this respiratory burst is blunted when compared to nHL-60 cells. To maintain this neutrophil-like phenotype and high dynamic range in subsequent assays, we maintained differentiated cells in the presence of DMSO.

Note S3. PFAS concentrations in drinking water and human serum.

We chose to investigate nine PFASs known to be in surface water, drinking water, and in the serum of residents downstream of a fluorochemical manufacturer. The concentrations at which we tested these PFASs may be higher than those found in these matrices. For example, when Sun et al. (2016) detected GenX in drinking water derived from the Cape Fear River in North Carolina, the maximum concentration measured was 4,560 ppt (=~0.13 μM). In a study of

the human population that consumed this water (Kotlarz et al. 2020), serum levels of PFOS at the 95th percentile were within our testing range (26.8 ppb = ~0.05 μM). Similarly, a cohort living near a fluorochemical plant in China presented with a maximum serum concentration of PFOA to be 5,626 ppb (=~13.59 μM) (Yao et al. 2020), which is well within our *in vivo* testing range and exceeds the concentration at which we observed suppression of the respiratory burst *in vitro*. Their sampling also detected maximum concentrations of PFMOAA at 158.2 ppb (=~0.88 μM), Nafion byproduct 2 at 23.9 ppb (=~0.05 μM), PFHxS at 14.61 ppb (=~0.037 μM), and PFOS at 145.1 ppb (=~0.29 μM); all of these measurements fall within the tested concentrations for at least one of our assays. Similar observations have been made for serum collected from fish in the Cape Fear River, of which the maximum concentration detected of PFOS was 977 ppb (=~1.95 μM). We caution against direct comparisons between our work and these studies as our experimental exposures do not account for the mixtures of PFASs observed in the waterways, fish, and humans in these previous studies. Follow-up studies are necessary to ascertain how PFAS mixtures may further influence the respiratory burst and other components of innate immunity. The exposures in this report also occurred on a relatively short time frame, with a maximum exposure duration of 96 hr. This short window of exposure may not fully account for the complexity of a chronic exposure to persistent, bioaccumulative compounds, of which the absorption, distribution, metabolism, and elimination are not fully understood. Our study may serve as a starting point from which to begin prioritization.

Note S4. Chemicals.

Stock solutions of all PFASs were created at a concentration of 80 mM. Due to solubility limitations, the CAMP stock solution was prepared at a concentration of 15 mM. Because recent reports indicate that DMSO is not a suitable solvent for GenX (Gaballah et al. 2020; Liberatore

et al. 2020; Zhang et al. 2021), the stock solutions for the per- and polyfluorinated ether acids (GenX, Nafion byproduct 2, and PFMOAA-Na) were prepared in molecular biology-grade water; all other stock solutions were prepared in DMSO. All PFASs were stored at -80 °C; CAMP was stored at -20 °C, as recommended by the manufacturer.

Exposure solutions were prepared on the first day of dosing by thawing and diluting aliquots of stock solutions. Exposure solutions were prepared at a 250X concentration in amber glass vials to minimize adsorption. Solutions were prepared using serial dilutions using the solvent in which the compound was originally prepared. Vehicle controls (DMSO at a final concentration of 0.4% or molecular-biology grade water) were also employed.

Note S5. Isolation of primary human neutrophils.

Human blood collection protocols were reviewed and approved by the NC State University Institutional Review Board (approval #616). Whole blood (10-30 mL) was collected from both male and female donors aged 20–45 years using heparinized syringes. Polymorphonuclear leukocytes (PMNs) were isolated from whole blood using Ficoll-Paque Plus (GE Healthcare, Chicago, IL, USA) density gradient centrifugation. Briefly, heparinized whole blood was mixed with 0.6% dextran in a 15 mL polypropylene conical tube and allowed to settle for 45-60 min at room temperature. Up to 10 mL of leukocyte rich plasma was aspirated using a bulb syringe and layered on 5 mL of Ficoll in a separate 15 mL conical tube. Cells were then centrifuged for 20 min at 1800 rpm with no brake. The supernatant was discarded and remaining red blood cells within the cell pellet were depleted by 60 seconds of hypotonic lysis. Isolated PMNs were resuspended and washed in sterile HBSS (Life Technologies, Carlsbad, CA, USA) without additives. Cell number and viability was quantified using trypan blue exclusion (1:1) and a manual hemocytometer count. PMNs isolated by this method typically have >98% viability

and are >95% neutrophils (hereafter referred to as neutrophils). Neutrophils were maintained at 37 °C and 5% CO2 in RPMI-1640 with L-glutamine and without phenol red supplemented with 10% FBS and 1X penicillin/streptomycin, as with the nHL-60 cells above. Media was also supplemented with recombinant human GM-CSF (EMD Millipore; catalog number GF304; final concentration of 100 ng/mL). Data from each human donor was treated as a separate biological replicate for *ex vivo* experiments.

Note S6. Vertebrate animals.

Zebrafish husbandry and experiments involving live animals were approved by the North Carolina State University Institutional Animal Care and Use Committee. Adult zebrafish were maintained in a recirculating aquarium facility (Aquatic Habitats, Apopka, FL) at 28 °C with a 14 hr light/10 hr dark cycle and fed a commercial grade zebrafish diet. Wild-type zebrafish were originally purchased from LiveAquaria (Dayton, OH) and Doctors Foster and Smith (Rhinelander, WI) and maintained and bred in-house for >5 years. Zebrafish embryos were obtained by natural spawning (Westerfield et al. 2007). At 2 hr post fertilization (hpf), embryos were treated with0.06%sodiumhypochlorite(bleach[v/v]) in 10% Hanks saline (Westerfield et al. 2007) in ultra-pure water using two 5 min washes to eliminate extra-ovum microbes. The embryos were then maintained in 100 mm Petri dishes in 10% Hank's saline at 28 °C until use.

Note S7. Developmental Toxicity assays.

Embryos/larvae were exposed to PFASs as described in **Methods and Fig. 2a**. Each day, embryos/larvae were inspected for death and malformations. At 96 hpf, larvae were anesthetized using tricaine methanesulfonate (MS-222; final concentration of 100 mg/L), oriented into the lateral position, and imaged using a Nikon AZ100 macroscope. Images were analyzed using DanioScope (v1.1, Noldus Information Technology, Wageningen, the Netherlands). A

micrometer was imaged concurrently to convert the number of pixels to micrometers. Body length (in μm) and eye area (in μm2) were measured. These endpoints were chosen because they can be measured using non-automated methods, they are quantitative, and they are well-correlated with other measurements of developmental toxicity (Truong et al. 2014; Zhang et al. 2017). Mortality, spinal curvature, pericardial edema, and other overt malformations were also determined qualitatively to measure the percentage of normal larvae. Individual experiments were excluded from this study when ≥25% of the embryos/larvae in the vehicle control group displayed abnormal phenotypes. PFAS concentrations where body length, eye size, or the percentage of normal larvae were significantly different from the vehicle control were considered to be developmentally toxic and excluded from subsequent respiratory burst experiments.

Note S8. HL-60 cell culture and differentiation.

HL-60 cells (ATCC CCL-240) were maintained at 37 °C and 5% CO2 in RPMI-1640 with L-glutamine and without phenol red (Gibco, Waltham, MA, USA; catalog number 11-835-055) supplemented with heat- inactivated fetal bovine serum (Corning, Corning, NY, USA; catalog number 35-010-CV; 10% final concentration) and penicillin/streptomycin (Corning; catalog number 30-002;CI; 1X final concentration). HL- 60 cells were authenticated using STR markers and confirmed to be free of Mycoplasma (IDEXX BioAnalytics, Columbia, MO, USA). HL-60 cells were differentiated to a neutrophil-like phenotype (hereafter referred to as nHL-60) as previously described (Rincón et al. 2018; Karlsson et al. 2011) by passaging cells into fresh media supplemented with DMSO (1.3% final concentration) at a density of 0.3 x 10^6 cells/mL and incubating for five days.

Note S9. Cytological analyses of the differentiated state of HL-60 cells.

For cytological analysis of HL-60 cells, cells were differentiated to a nHL-60 phenotype as described in **Supplementary Note S8** or passaged without differentiation. After 5 days, cells were passaged again to create three groups: undifferentiated HL-60 cells, nHL-60 cells maintained in fresh media supplemented with 1.3% DMSO, and nHL-60 cells maintained in fresh media without DMSO. After four days, cells were collected via centrifugation, counted, and cell counts were normalized. Cells were then transferred to a cytospin funnel attached to a glass microscope slide with 0.5×10^6 cells in each side of the funnel. The cells were then centrifuged in a Shandon CytoSpin 4 (ThermoFisher) at 1000 rpm for 5 min. Microscope slides of cytospin preparations were batch-stained with Wright-Giemsa on a Wescor Aerospray Pro 7151 (Logan, UT, USA) auto-slide staining machine per the manufacturer's instructions.

Cytology preparations of cytospin-prepared cells (undifferentiated HL-60, nHL-60, and nHL-60 with DMSO withdrawn) were evaluated by a board-certified veterinary pathologist (KEL) for morphologic features of neutrophil myeloid differentiation and mitotic activity. Based on cellular differentiation features, cells were classified as having features of promyelocytes, myelocytes, metamyelocytes, band neutrophils, or mature neutrophils. The number of each differentiated myeloid cell stage and the mitotic index were enumerated by a 300-cell differential count of cytology preparations using an Olympus BX43 microscope (Tokyo, Japan) at 100x (oil objective) magnification. Treatments were performed in triplicate, and cell counts were averaged among triplicates.

SUPPLEMENTARY TABLES

Table S1. Names, abbreviations, CAS numbers, vendors, and catalog numbers of PFASs.

Name	Abbreviation	CAS-RN	Vendor	Catalog Number
Perfluorooctanoic acid	PFOA	335-67-1	Sigma	171468
Perfluorooctane sulfonic acid potassium salt	PFOS-K	2795-39-3	Sigma	77282
Perfluorononanoic acid	PFNA	375-95-1	Sigma	394459
Perfluorohexanoic acid	PFHxA	307-24-4	Sigma	29226
Perfluorohexane sulfonic acid	PFHxS	355-46-4	Synquest Laboratories	6164-3-2T
Perfluorobutane sulfonic acid	PFBS	375-73-5	Synquest Laboratories	6164-3-09
Ammonium perfluoro(2-methyl-3-oxahexanoate)	GenX	62037-80-3	Synquest Laboratories	2122-3-09
7H-Perfluoro-4-methyl-3,6-dioxoctanesulfonic acid	Nafion byproduct 2	749836-20-2	Synquest Laboratories	6164-3-3J
Perfluoromethoxyacetic acid sodium salt	PFMOAA-Na	21837-98-9	Fluoryx Labs	FC23-02

SUPPLEMENTARY FIGURES

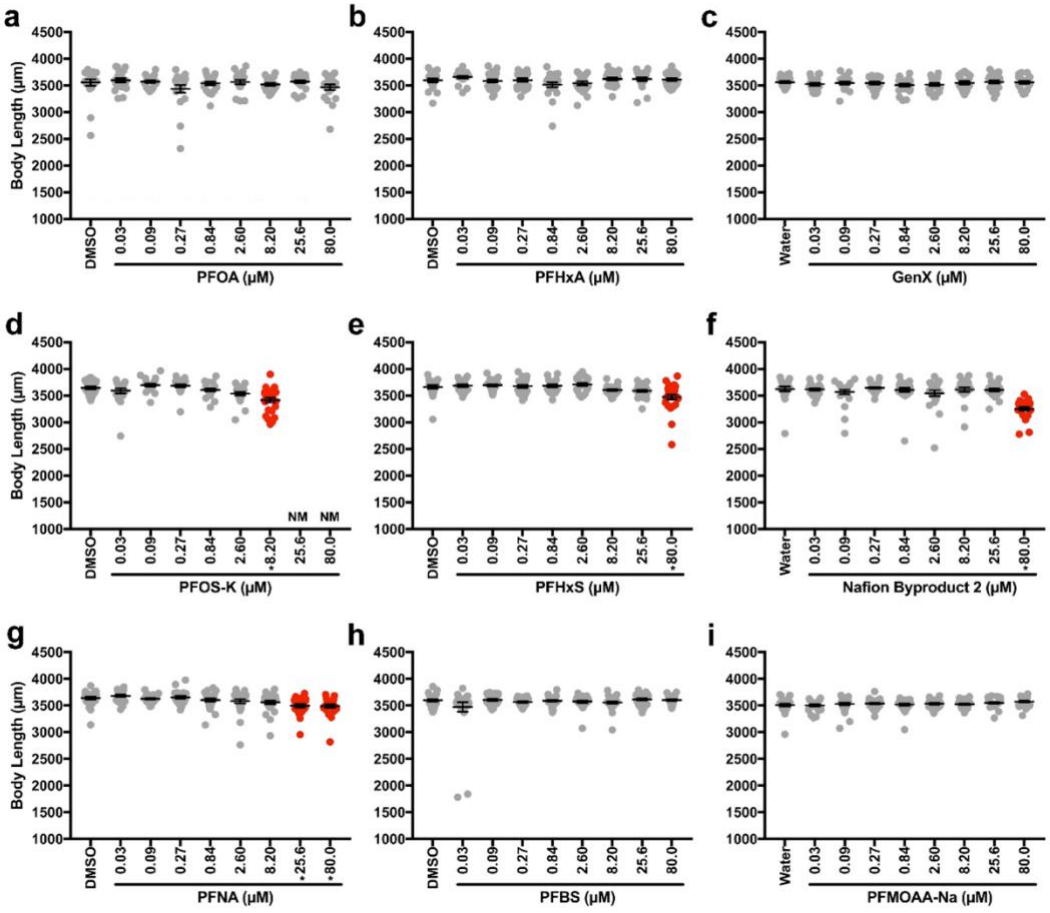

Figure S1. Body length measurements from PFAS-exposed zebrafish larvae. Zebrafish were exposed to (a) PFOA, (b) PFHxA, (c) GenX, (d) PFOS-K, (e) PFHxS, (f) Nafion byproduct 2, (g) PFNA, (h) PFBS or (i) PFMOAA-Na for 96 hr. Images of zebrafish larvae (96 hpf) were taken via brightfield microscopy. Body lengths were measured using DanioScope software (v1.1). Individual symbols represent individual zebrafish larvae. Due to severe death and malformations observed in PFOS-K-exposed larvae, body length was not measured (NM) for the two highest concentrations. Data shown are from three, combined, independent biological replicates. Statistical significance (*, $p<0.05$) was determined by a one-way ANOVA with Dunnett's post-hoc test for pairwise comparisons to the vehicle control.

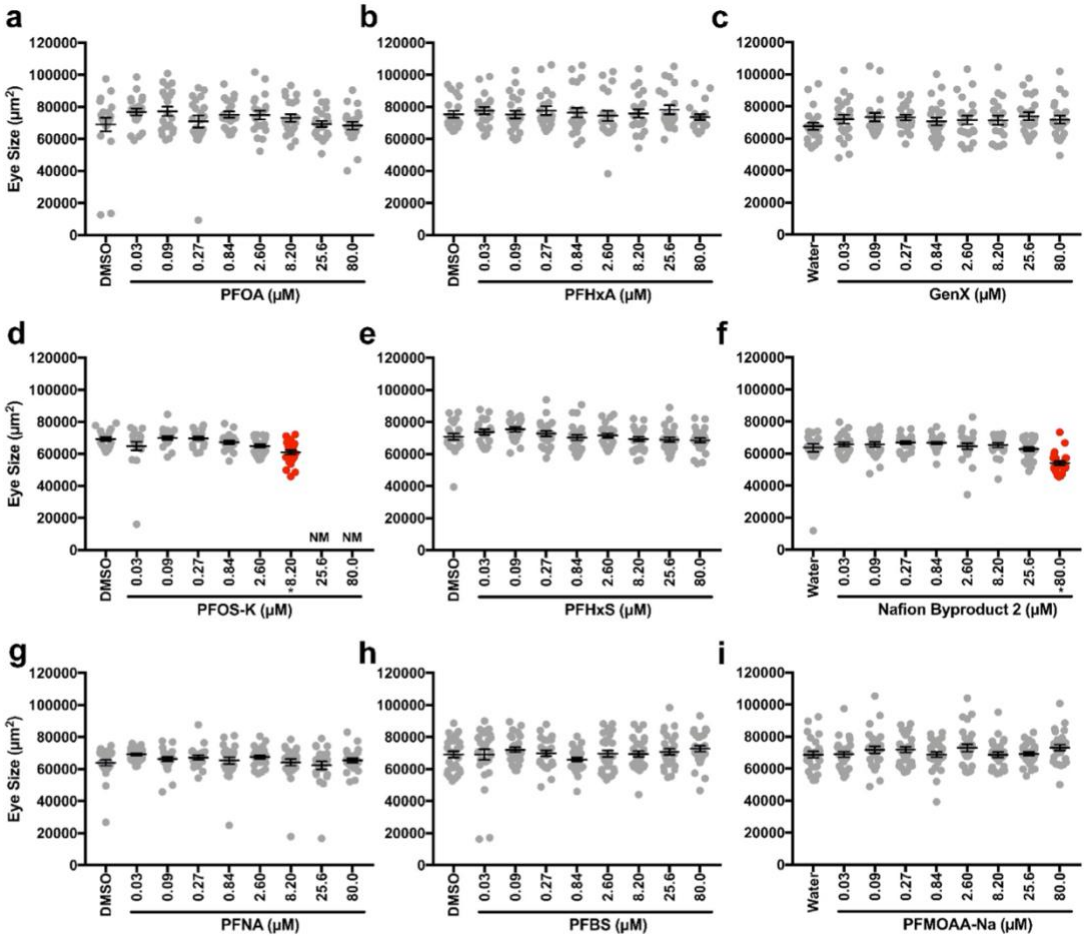

Figure S2. Eye size measurements from PFAS-exposed zebrafish larvae. Zebrafish were exposed to (a) PFOA, (b) PFHxA, (c) GenX, (d) PFOS-K, (e) PFHxS, (f) Nafion byproduct 2, (g) PFNA, (h) PFBS or (i) PFMOAA-Na for 96 hr. Images of zebrafish larvae (96 hpf) were taken via brightfield microscopy. Eye sizes were measured using DanioScope software (v1.1). Individual symbols represent individual zebrafish larvae. Due to severe death and malformations observed in PFOS-K-exposed larvae, eye size was not measured (NM) for the two highest concentrations. Data shown are from three, combined, independent biological replicates. Statistical significance (*, $p<0.05$) was determined by a one-way ANOVA with Dunnett's post-hoc test for pairwise comparisons to the vehicle control.

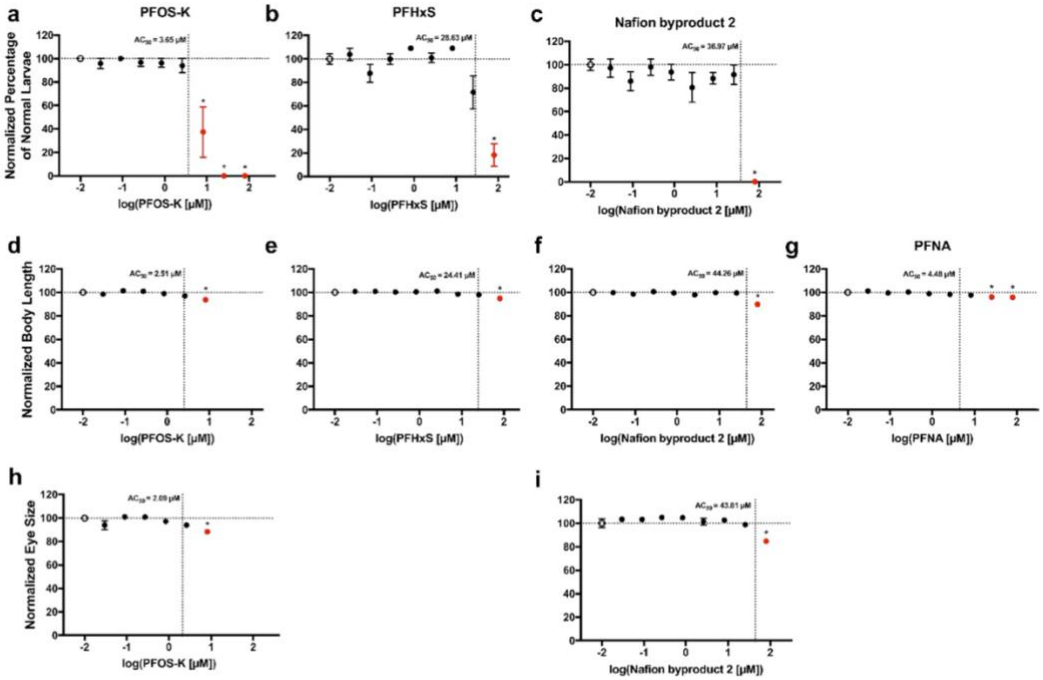

Figure S3. Concentration response analysis of positive hits for developmental toxicity. Exposure (96 hr) to PFOS-K PFHxS, Nafion byproduct 2 and PFNA induced malformation or mortality in zebrafish larval (**Figure 3**) including changes in body length and eye size (**Supplementary Figures S1 and S2**). Based on these results, AC_{50} values were calculated using a two-parameter logistic regression. Data were normalized to the vehicle control, represented by the empty symbol (o). (a-c) Concentration response curves and AC_{50} values for percentage of normal larvae exposed to PFOS-K, PFHxS and Nafion byproduct 2. (d-g) Concentration response curves and AC_{50} values for body length of larvae exposed to PFOS-K, PFHxS, Nafion byproduct 2 and PFNA. (h-i) Concentration response curves and AC_{50} values for eye size of larvae exposed to PFOS-K and Nafion byproduct 2. Red data points and asterisks (*) indicate statistical significance ($p < 0.05$) as determined by a one-way ANOVA with Dunnett's post-hoc test.

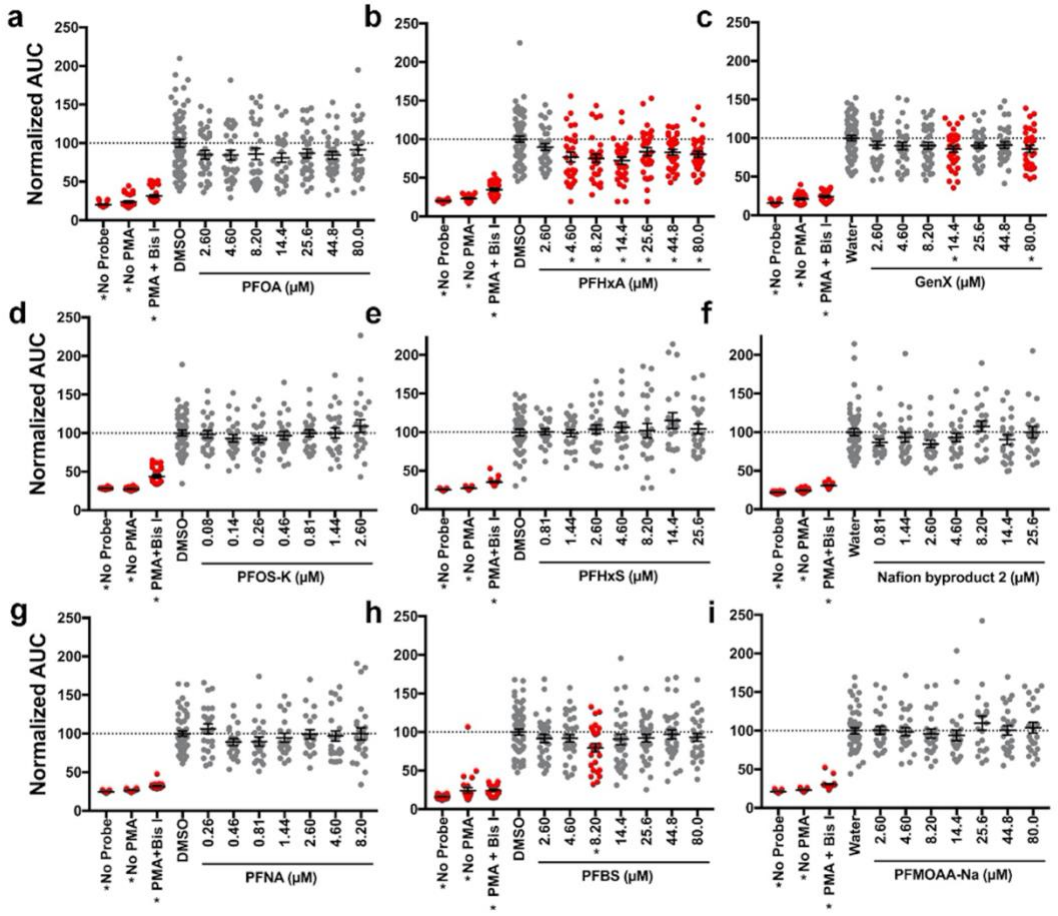

Figure S4. PFHxA and GenX suppressed the respiratory burst *in vivo*. Zebrafish were exposed to (A) PFOA, (B) PFHxA, (C) GenX, (D) PFOS-K, (E) PFHxS, (F) Nafion byproduct 2, (G) PFNA, (H) PFBS or (I) PFMOAA-Na for 96 hr. At 96 hpf, zebrafish larvae were washed and distributed into a 96 well-plate. Larvae were then treated with PMA, to induce ROS production, and H_2DCFDA to measure ROS produced. Fluorescence of H_2DCFDA was measured for 2.5 hours on a fluorescent plate reader set to 28.5°C. Larvae receiving no PMA and no H_2DCFDA were included as controls. Larvae treated with Bis I, a protein kinase C inhibitor, were included as a positive control for inhibition of the respiratory burst. Data shown are from at least three, combined, independent biological replicates and represent the total fluorescence over the entire testing period (Area Under the Curve, AUC). Maximum fluorescence measurements are provided in **Figure 4.**

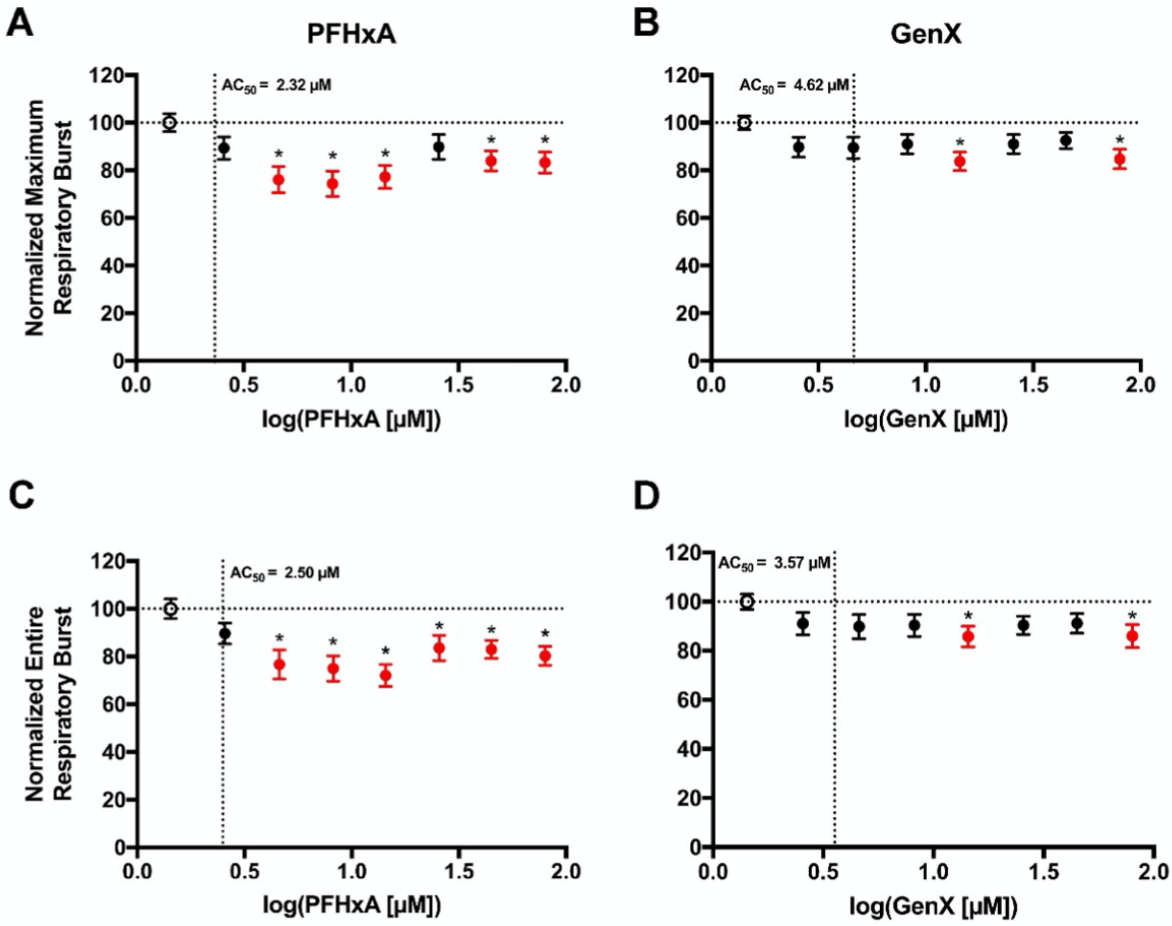

Figure S5. Concentration response analyses for inhibition of in vivo respiratory burst by PFHxA and GenX. Exposure (96 hr) to PFHxA and GenX suppressed the zebrafish larval respiratory burst assay as measured by maximum fluorescence (**Figure 4**) and by total fluorescence (**Supplemental Figure S4**). Based on these results, AC_{50} values were calculated using a two-parameter logistic regression. Data were normalized to the vehicle control, represented by the empty symbol (o). Concentration response curves and AC_{50} values for the maximum respiratory burst for larvae exposed to (A) PFHxA and (B) GenX. Concentration response curves and AC_{50} values for the entire respiratory burst (AUC) for larvae exposed to (C) PFHxA and (D) GenX.

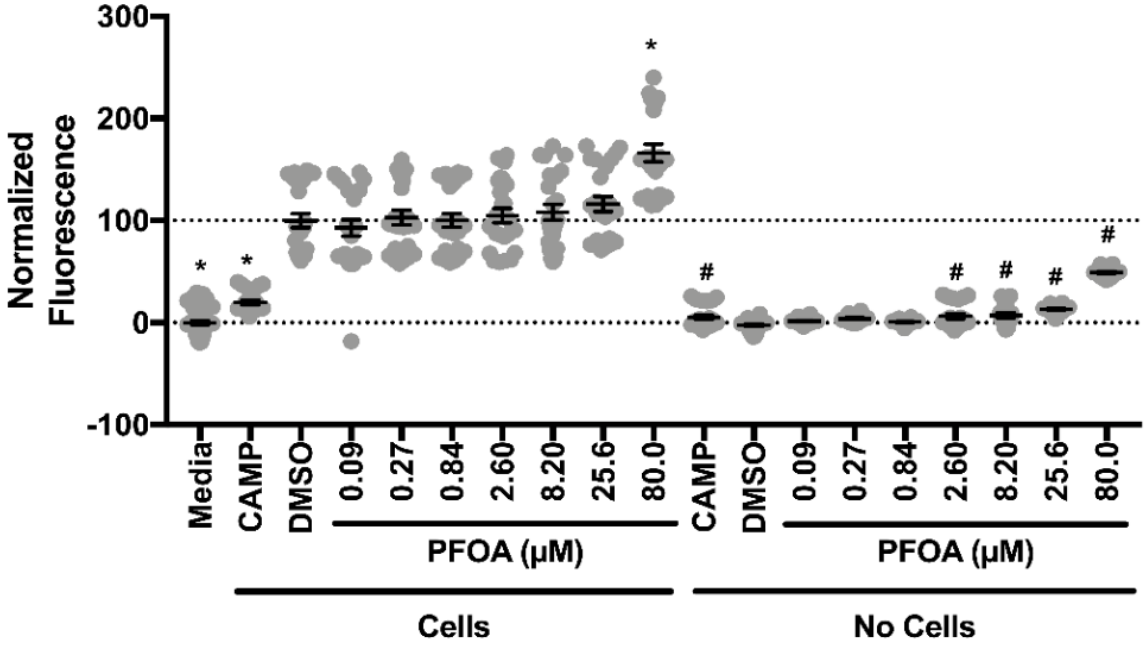

Figure S6. PFOA interacts directly with PrestoBlue, causing increased fluorescence. After differentiation, tubes containing nHL-60 or tubes containing media only were exposed to several concentrations of PFOA and distributed into a 96 well plate. After incubating for 96 hours, PrestoBlue was used to assess viability, as well as auto-fluorescence of PFOA's reaction with PrestoBlue. As a positive control, 10 μM camptothecin (CAMP) was included. Significance from DMSO control with cells is denoted by asterisks (*) while significance from DMSO control without cells is denoted by hash marks (#).

Figure S7. DMSO is required to maintain the neutrophil-like cytological phenotype in nHL-60s after four days in culture. (A-C) Photomicrographs show representative cytospin preparations of cultured HL-60 cells and the effects of DMSO treatment on promotion and maintenance of neutrophilic myeloid differentiation. (A) Untreated HL-60 cells uniformly had cytological differentiation features of promyelocytes (average 300/300; 100%), an immature stage of myelocyte differentiation. The large basophilic cells contained cytoplasmic small clear vacuoles and red primary granules (arrow). Nuclei were large, round, and had coarse chromatin and prominent nucleoli. Mitotic figures (arrowhead) were present. (B) DMSO treatment induced neutrophilic myeloid differentiation in HL-60 cells. Most cells matured to display features of myelocyte (36.3/300; 12.1%), metamyelocyte (127.3/300; 42.4%), band neutrophil (86.7/300; 28.9%), or mature neutrophil morphology (50/300; 16.7%). The cytoplasm was pale and, in more differentiated cells, lost small clear vacuoles and had reduced or absent primary granules. The more mature myeloid cells were smaller and their nuclei had fine pale chromatin, lacked nucleoli, and mitotic figures were rare. Cells with band neutrophil morphology (arrowheads) had deep nuclear indentation and those with mature neutrophil morphology had segmented nuclei (arrows). (C) After withdrawal of DMSO treatment, nHL-60 cells lost neutrophil myeloid differentiation features and reverted to cells with more immature, promyelocyte, morphology (average 293.7/300; 97.9%). The cytoplasm contained small clear spherical vacuoles and abundant red primary granules (arrowhead) and mitotic figures were again present (arrow). 63X Magnification. Wright-Giemsa Stain. (D) 300-cell differential counts across three replicates were averaged and graphed.

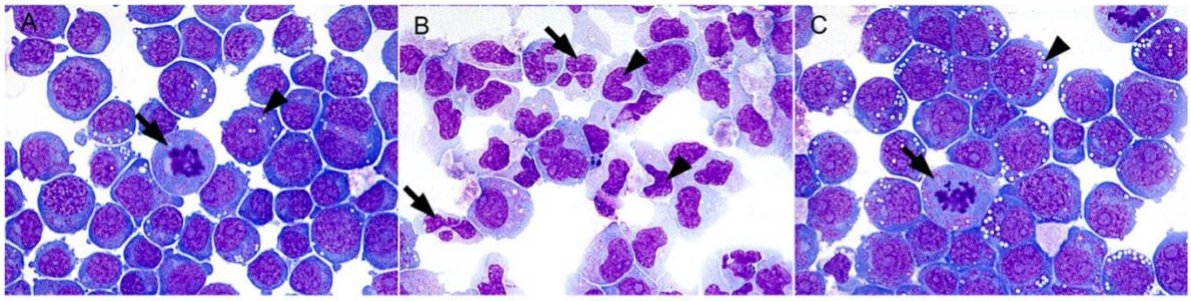
A
B
C

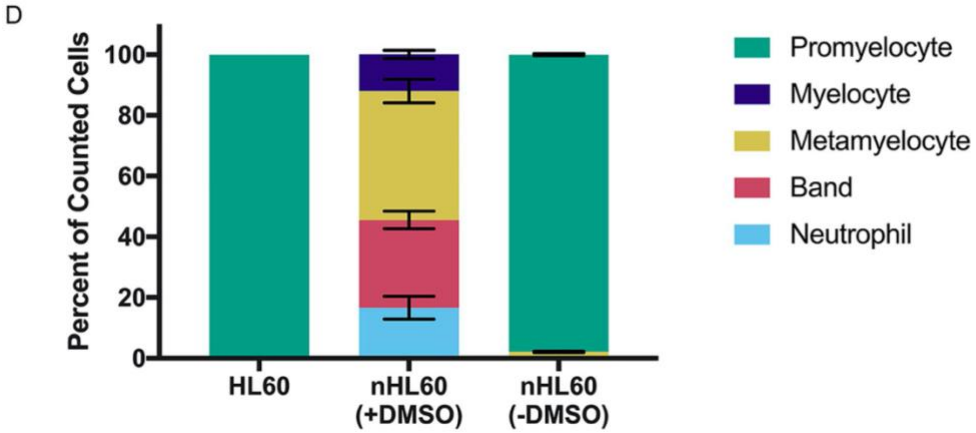
D
Percent of Counted Cells
100
80
60
40
20
0
HL60
nHL60 (+DMSO)
nHL60 (-DMSO)
Promyelocyte
Myelocyte
Metamyelocyte
Band
Neutrophil

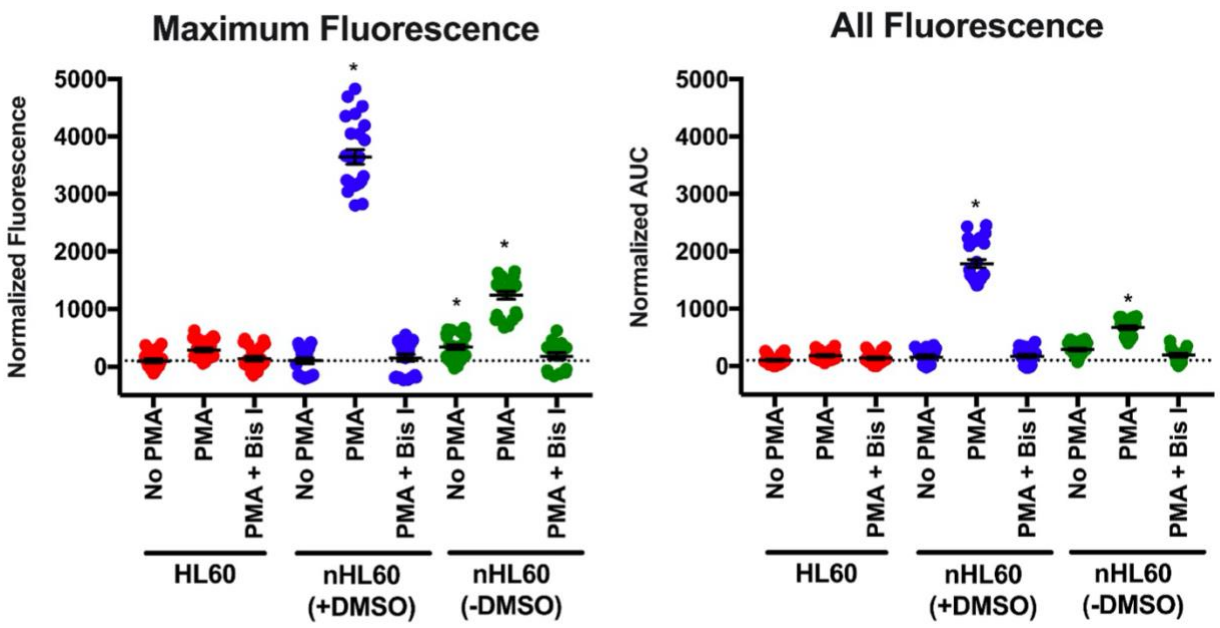

Figure S8. DMSO is necessary to maintain the neutrophil-like functional phenotype in nHL-60s after four days in culture. Using the same experimental design as **Supplemental Figure S7**, after four days in culture, cells from all three treatments were counted and then plated at a concentration of 0.1 x 10^6 cells/mL. Respiratory burst assays were then performed. Bis I was used as a positive control. Each individual symbol represents a different well of a 96-well plate. Data shown are three combined independent experiments. Average background fluorescence of DHR was subtracted from each data point. Data are normalized to HL-60 cells receiving no PMA treatment. Significance (*, $p<0.05$) was determined by one-way ANOVA with Dunnet's post- hoc test for pairwise comparisons to the nHL-60 cells receiving no PMA. Maximum fluorescence (left) and entire (AUC) fluorescence (right) are shown.

Figure S9. *In vitro* respiratory burst after 96 hr PFAS exposure (entire fluorescence). After differentiation to nHL-60, cells were exposed to vehicle control or (A) PFOA, (B) PFHxA, (C) GenX, (D) PFOS-K, (E) PFHxS, (F) Nafion byproduct 2, (G) PFNA, (H) PFBS or (I) PFMOAA-Na for 96 hr and then plated into a 96 well plate. At 96 hr, cells were stimulated with PMA to produce ROS, which was detected with DHR. The entire fluorescence (AUC) values are reported here. The maximum fluorescence values are provided in **Figure 6**. Wells with no cells but with PMA and DHR, and cells receiving no PMA were included as controls. Cells treated with Bis I, a protein kinase C inhibitor, were included as a positive control for inhibition of the respiratory burst. Data shown are from three, combined, independent biological replicates, except for PFHxA, which had 4 biological replicates. Individual symbols represent individual wells of a 96-well plate. Significance (*, $p<0.05$) was determined by a one-way ANOVA with Dunnett's post-hoc test for pairwise comparisons to the vehicle control.

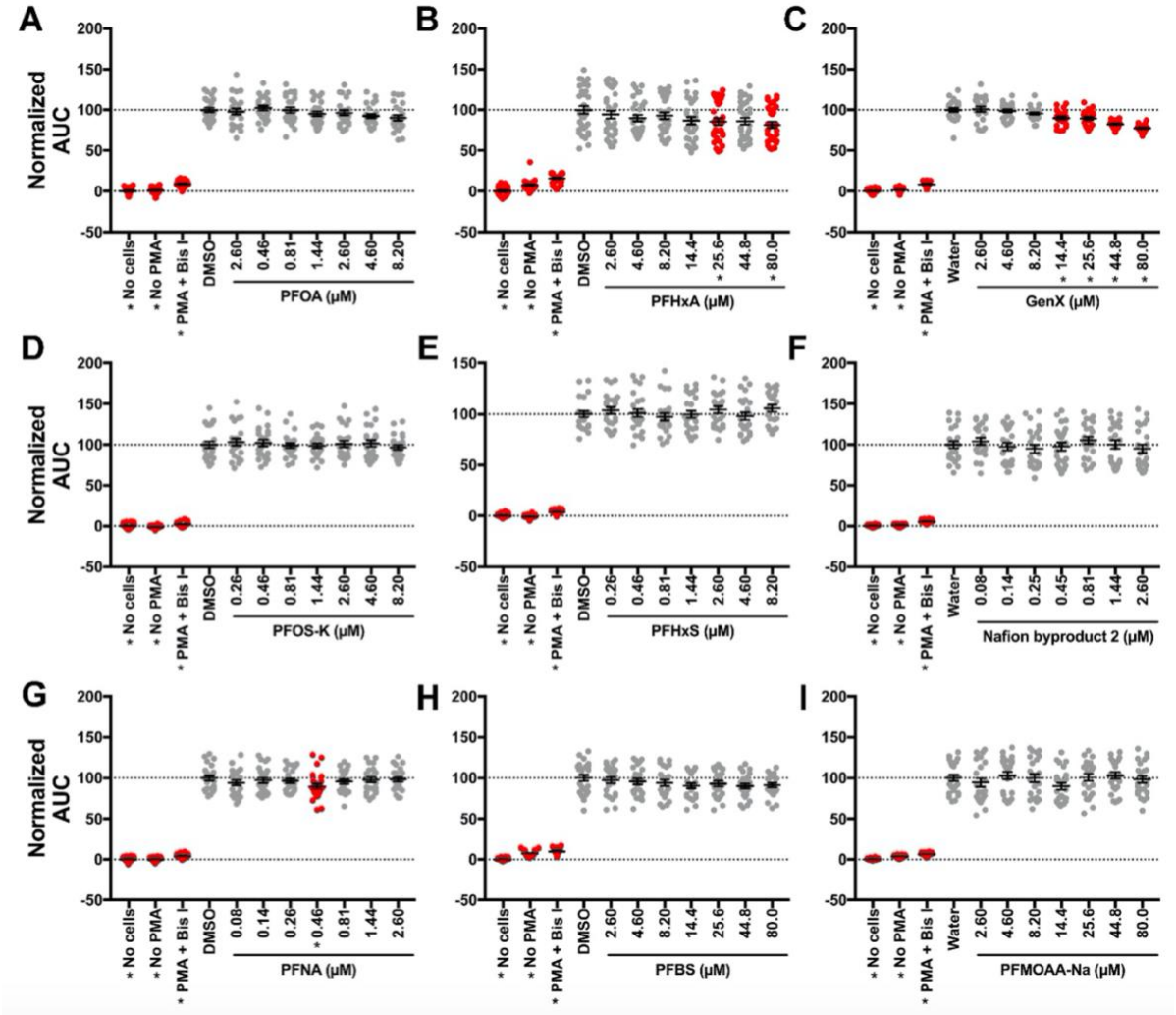
A
B
C
D
E
F
G
H
I
Normalized AUC
200
150
100
50
0
-50
* No cells
* No PMA
* PMA + Bis I
DMSO
Water
2.60
0.46
0.81
1.44
4.60
8.20
4.60
8.20
14.4
* 25.6
44.8
* 80.0
0.26
0.08
0.14
0.25
0.45
* 0.46
PFOA (μM)
PFHxA (μM)
GenX (μM)
PFOS-K (μM)
PFHxS (μM)
Nafion byproduct 2 (μM)
PFNA (μM)
PFBS (μM)
PFMOAA-Na (μM)

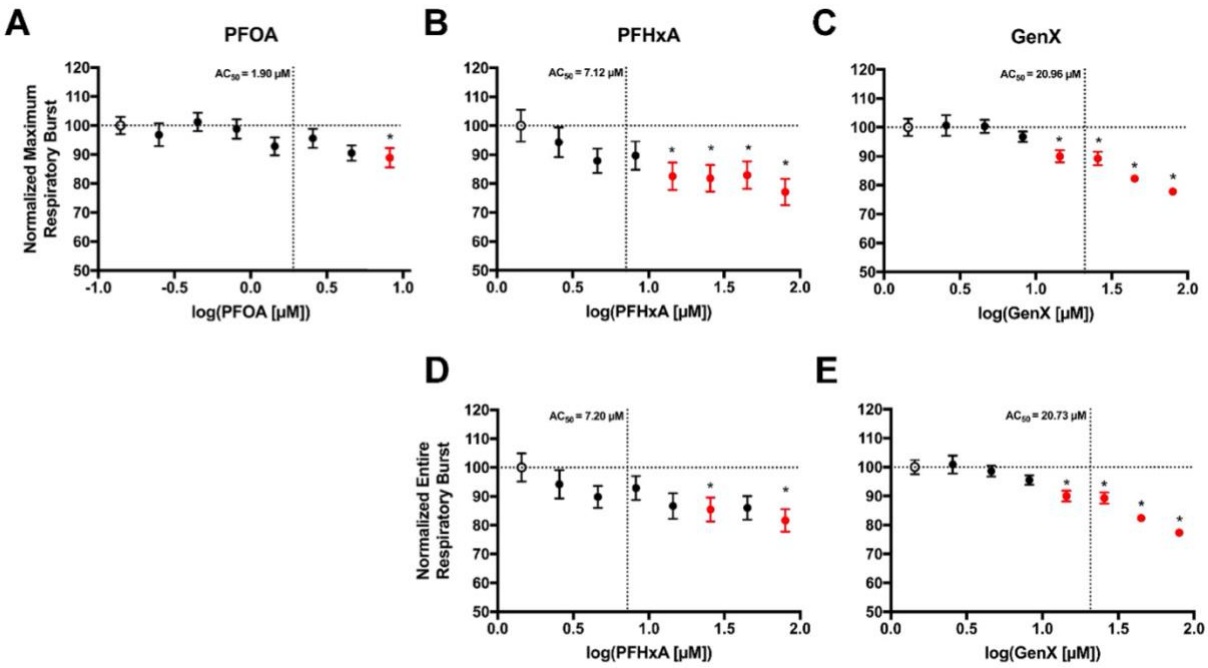

Figure S10. Concentration response analysis for positive *in vitro* hits after 96 hr PFAS exposure. 96 hr exposures to PFOA, PFHxA and GenX suppressed the nHL-60 respiratory burst assay as measured by maximum fluorescence (**Figure 6**) and by total fluorescence (**Supplemental Fig S9**). Based on these results, AC_{50} values were calculated using a two-parameter logistic regression. Data were normalized to the vehicle control, represented by the empty symbol (o). Concentration response curves and AC_{50} values for the maximum respiratory burst respiratory burst as shown for nHL-60 cells after 96 hr exposure to (A) PFOA, (B) PFHxA and (C) GenX. Concentration response curves and AC_{50} values for the entire respiratory burst are shown for nHL-60 cells after a 96 hr exposure to (D) PFHxA and (E) GenX.

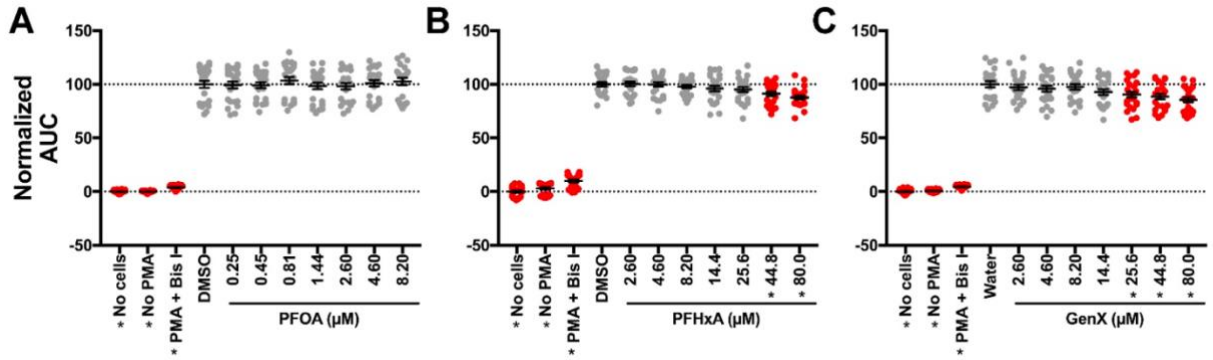

Figure S11. ***In vitro*** **respiratory burst after 24 hr PFAS exposure (entire fluorescence)**. After differentiation to nHL-60, cells were exposed to vehicle control, (A) PFOA, (B) PFHxA or (C) GenX for 24 hr and then plated into a 96 well plate. At 24 hr, cells were stimulated with PMA to produce ROS, which was detected with DHR. The entire fluorescence (AUC) values ares reported here. The maximum fluorescence values are provided in **Figure 7**. Wells with no cells but with PMA and DHR, and cells receiving no PMA were included as controls. Cells treated with Bis I, a protein kinase C inhibitor, were included as a positive control for inhibition of the respiratory burst. Data shown are from three, combined, independent biological replicates. Individual symbols represent individual wells of a 96-well plate. Significance (*, $p<0.05$) was determined by a one-way ANOVA with Dunnett's post-hoc test for pairwise comparisons to the vehicle control.

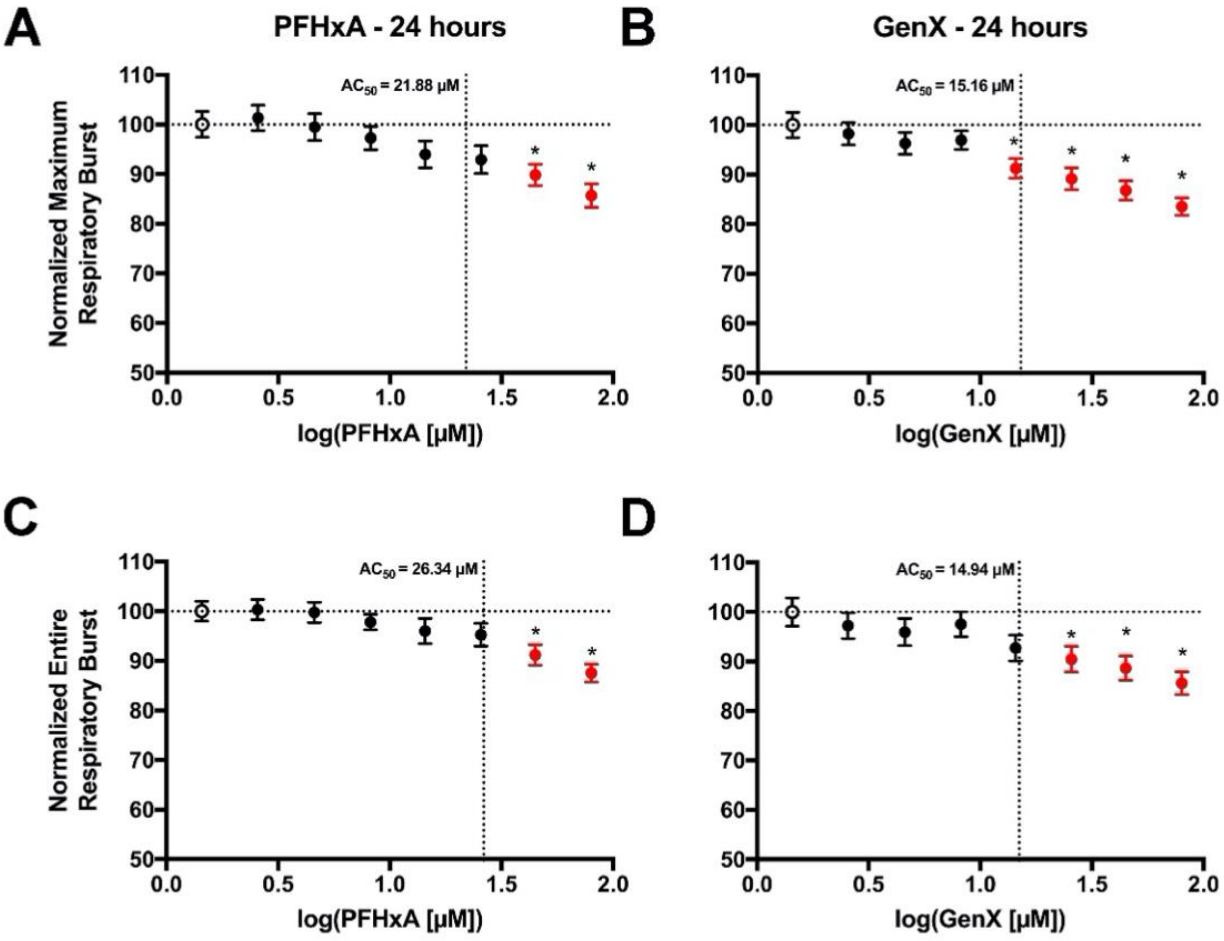

Figure S12. Concentration response analysis for positive *in vitro* hits after 24 hr PFAS exposure. 24 hr exposures to PFHxA and GenX suppressed the nHL-60 respiratory burst assay as measured by maximum fluorescence (**Figure 7**) and by total fluorescence (**Supplemental Fig S11**). Based on these results, AC_{50} values were calculated using a two-parameter logistic regression. Data were normalized to the vehicle control, represented by the empty symbol (o). Concentration response curves and AC_{50} values for the maximum respiratory burst respiratory burst as shown for nHL-60 cells after 24 hr exposure to (A) PFHxA and (B) GenX. Concentration response curves and AC_{50} values for the entire respiratory burst (AUC) are shown for nHL-60 cells after a 24 hr exposure to (C) PFHxA and (D) GenX.

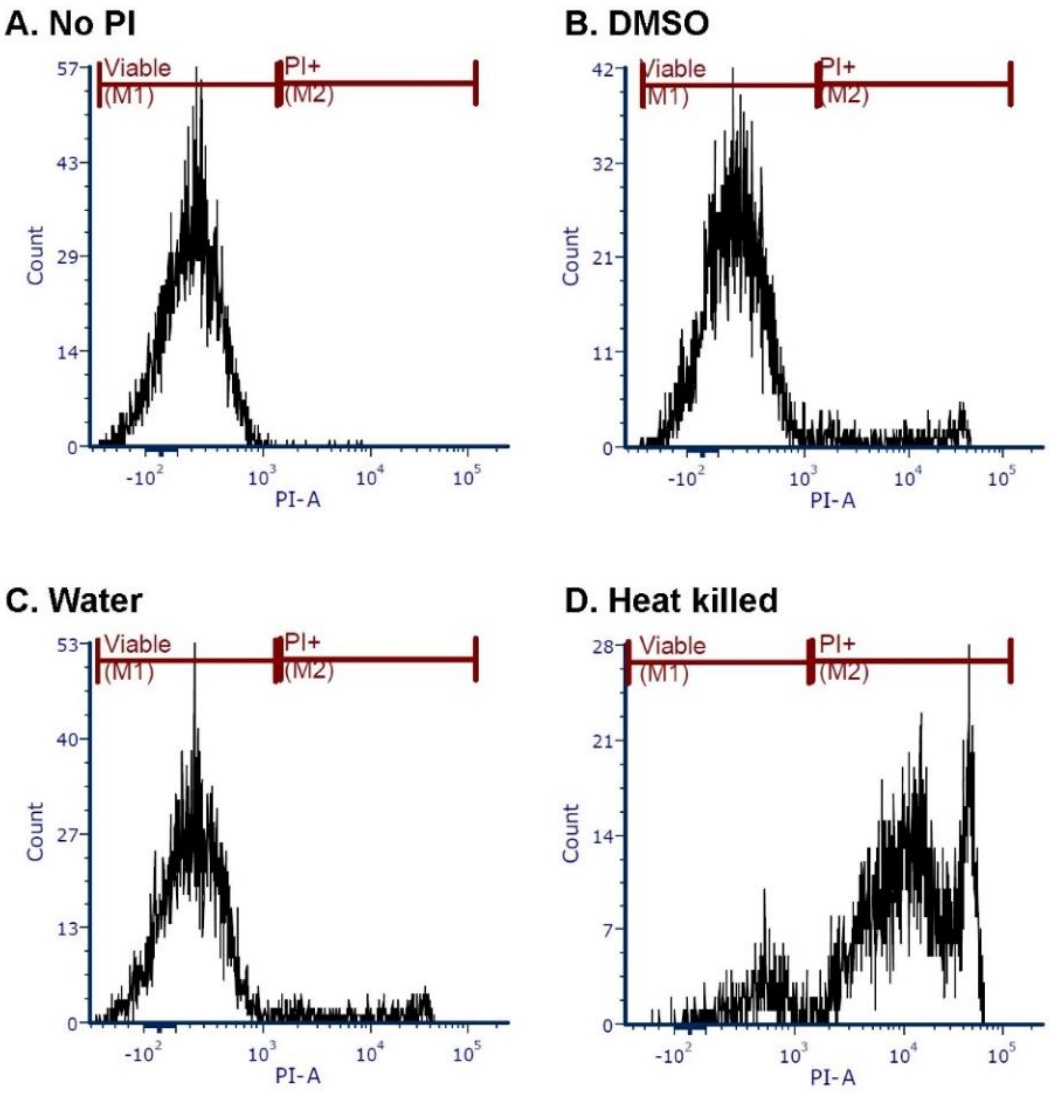

Figure S13. Representative histograms from *ex vivo* cell viability assays. After 24 hours, primary human neutrophils were stained with propidium iodide (PI; which labels non-viable cells) and analyzed using flow cytometry. After gating to exclude cellular debris and clumps of cells, cells were gated to determine the percentage of PI-positive singlets. Representative histograms from (A) unstained cells, (B-C) vehicle-treated cells (DMSO and Water), and (D) heat-killed cells. Unstained cells defined background fluorescence. Histograms from vehicle-treated cells demonstrated no significant increase in non-viable cells. Heat-killed cells served as a positive control for increased PI staining.

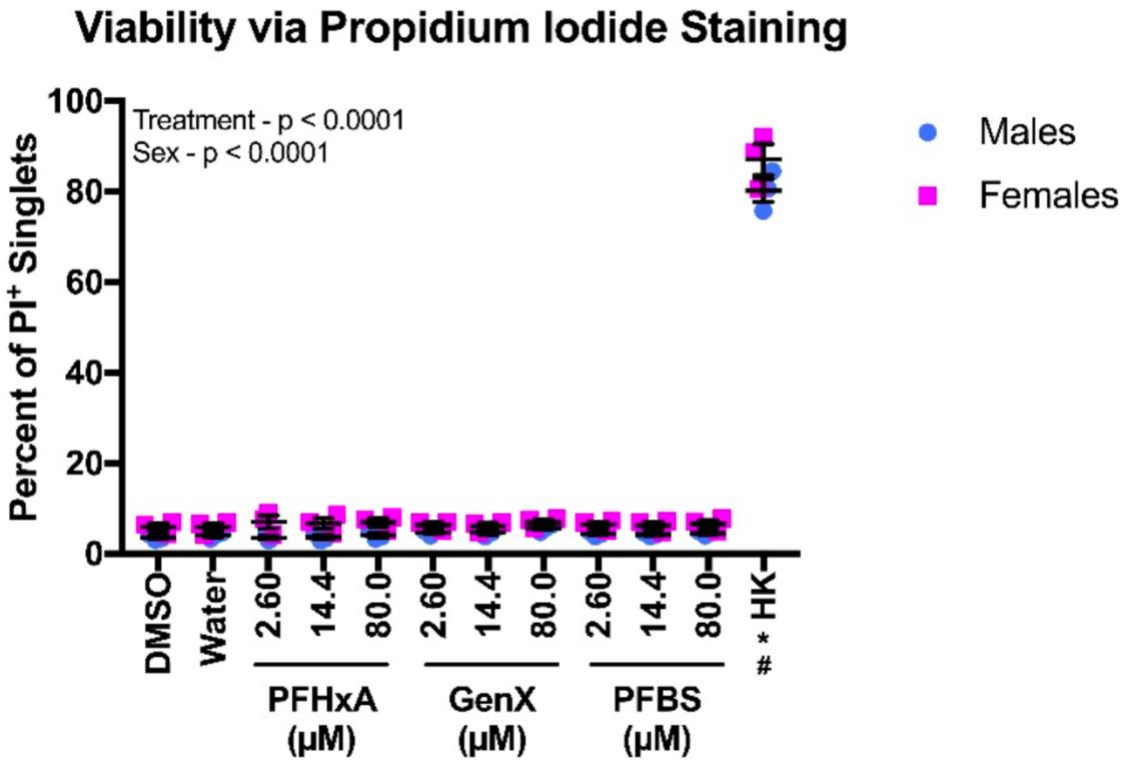

Figure S14. Select PFASs were not cytotoxic *ex vivo*. After 24 hours of PFAS exposure, primary human neutrophils were stained with propidium iodide (PI) and analyzed using flow cytometry. Individual symbols represent the percent of PI+ cells from an individual donor. Heat-killed (HK) cells were included as a positive control for dead cells. Statistical significance was determined by a two-way ANOVA with a Dunnett's post-hoc test for pairwise comparisons to the DMSO and water controls. Significance ($p < 0.05$) from the DMSO control is signified by an asterisk (*) while significance from the water control is signified by a hash mark (#).

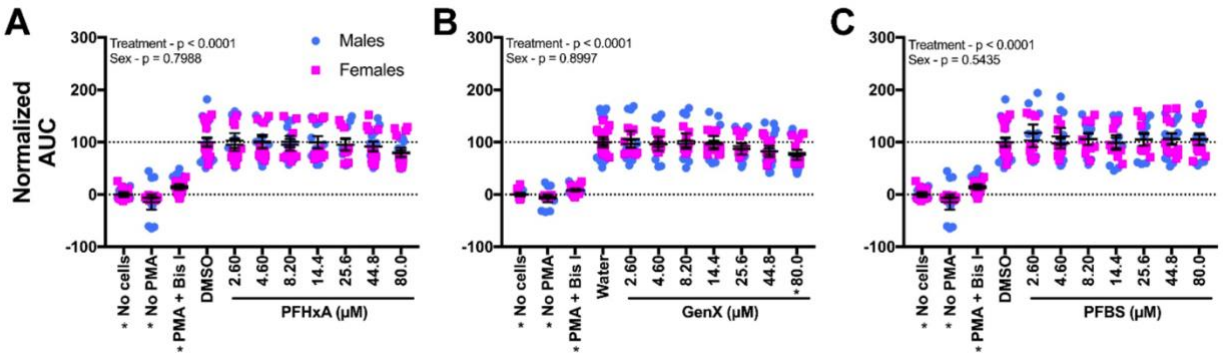

Figure S15. *Ex vivo* respiratory burst after 24 hr PFAS exposure (entire fluorescence). After isolation from individual human donors, neutrophils were dosed with vehicle control, cells were exposed to vehicle control, (A) PFHxA, (B) GenX, or (C) PFBS for 24 hr and then distributed into a 96 well plate. At 24 hr, cells were stimulated with PMA to produce ROS, which was detected with DHR. The entire fluorescence (AUC) values are reported here. The maximum fluorescence values are provided in **Figure 8**. Wells with no cells but with PMA and DHR, and cells receiving no PMA were included as controls. Cells treated with Bis I, a protein kinase C inhibitor, were included as a positive control for inhibition of the respiratory burst. Data shown are from six, individual human donors. Individual symbols represent individual wells of a 96-well plate. Significance (*, $p<0.05$) was determined by a two-way ANOVA with either a Dunnett's post-hoc test or Sidak's post-hoc test for pairwise comparisons to the vehicle control.

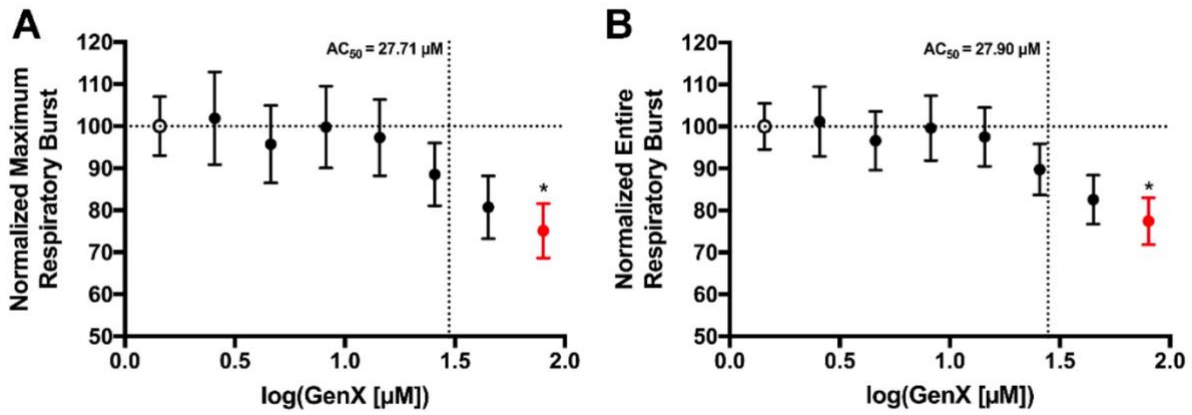

Figure S16. Concentration response analysis for positive *ex vivo* hits after 24 hr PFAS exposure. 24 hr exposure to GenX suppressed the primary human neutrophil respiratory burst assay as measured by maximum fluorescence (**Figure 8**) and by total fluorescence (**Supplemental Figure S15**). Based on these results, AC_{50} values were calculated using a two-parameter logistic regression. Data were normalized to the vehicle control, represented by the empty symbol (o). (A) Concentration response curves and AC_{50} values for the maximum respiratory burst respiratory burst as shown for primary neutrophils after 24 hr exposure to GenX. (B) Concentration response curves and AC_{50} values for the entire respiratory burst (AUC) are shown for primary neutrophils after a 24 hr exposure to GenX.

REFERENCES

1. Ahrens, L, Barber, JL, Xie, Z and Ebinghaus, R. 2009. Longitudinal and latitudinal distribution of perfluoroalkyl compounds in the surface water of the Atlantic Ocean. Environ. Sci. Technol. 43(9):3122-3127. doi: 10.1021/es803507p
2. Ait Bamai, Y, Goudarzi, H, Araki, A, Okada, E, Kashino, I, Miyashita, C and Kishi, R. 2020. Effect of prenatal exposure to per- and polyfluoroalkyl substances on childhood allergies and common infectious diseases in children up to age 7 years: The Hokkaido study on environment and children's health. Environ. Int. 143(105979). doi: 10.1016/j.envint.2020.105979
3. Andrews, DQ and Naidenko, OV. 2020. Population-Wide Exposure to Per- and Polyfluoroalkyl Substances from Drinking Water in the United States. Environ. Sci. Technol. Lett. 7(12):931-936. doi: 10.1021/acs.estlett.0c00713
4. ATSDR. 2021. Toxicological Profile for Perfluoroalkyls. U.S. Department of Health and Human Services.
5. Averina, M, Brox, J, Huber, S, Furberg, A-S and Sørensen, M. 2019. Serum perfluoroalkyl substances (PFAS) and risk of asthma and various allergies in adolescents. The Tromsø study Fit Futures in Northern Norway. Environ. Res. 169(114-121). doi: 10.1016/j.envres.2018.11.005
6. Balik-Meisner, M, Truong, L, Scholl, EH, La Du, JK, Tanguay, RL and Reif, DM. 2018. Elucidating Gene-by-Environment Interactions Associated with Differential Susceptibility to Chemical Exposure. Environ. Health Perspect. 126(6):067010. doi: 10.1289/EHP2662

7. Balik-Meisner, M, Truong, L, Scholl, EH, Tanguay, RL and Reif, DM. 2018. Population genetic diversity in zebrafish lines. Mamm. Genome. 29(1):90-100. doi: 10.1007/s00335-018-9735-x
8. Bangma, J, Szilagyi, J, Blake, BE, Plazas, C, Kepper, S, Fenton, SE and C Fry, R. 2020. An assessment of serum-dependent impacts on intracellular accumulation and genomic response of per- and polyfluoroalkyl substances in a placental trophoblast model. Environ. Toxicol. 35(12):1395-1405. doi: 10.1002/tox.23004
9. Behr, AC, Plinsch, C, Braeuning, A and Buhrke, T. 2020. Activation of human nuclear receptors by perfluoroalkylated substances (PFAS). Toxicol. In Vitro. 62(104700). doi: 10.1016/j.tiv.2019.104700
10. Behr, AC, Lichtenstein, D, Braeuning, A, Lampen, A and Buhrke, T. 2018. Perfluoroalkylated substances (PFAS) affect neither estrogen and androgen receptor activity nor steroidogenesis in human cells in vitro. Toxicol. Lett. 291(51-60). doi: 10.1016/j.toxlet.2018.03.029
11. Berntsen, HF, Bolling, AK, Bjorklund, CG, Zimmer, K, Ropstad, E, Zienolddiny, S, Becher, R, Holme, JA, Dirven, H, Nygaard, UC and Bodin, J. 2018. Decreased macrophage phagocytic function due to xenobiotic exposures in vitro, difference in sensitivity between various macrophage models. Food Chem. Toxicol. 112(86-96). doi: 10.1016/j.fct.2017.12.024
12. Blanter, M, Gouwy, M and Struyf, S. 2021. Studying Neutrophil Function in vitro: Cell Models and Environmental Factors. J. Inflamm. Res. 14(141-162). doi: 10.2147/JIR.S284941

13. Brach, MA, deVos, S, Gruss, HJ and Herrmann, F. 1992. Prolongation of survival of human polymorphonuclear neutrophils by granulocyte-macrophage colony-stimulating factor is caused by inhibition of programmed cell death. Blood. 80(11):2920-2924. doi:
14. Brieger, A, Bienefeld, N, Hasan, R, Goerlich, R and Haase, H. 2011. Impact of perfluorooctanesulfonate and perfluorooctanoic acid on human peripheral leukocytes. Toxicol. In Vitro. 25(4):960-968. doi: 10.1016/j.tiv.2011.03.005
15. Brown, SR, Flynn, RW and Hoverman, JT. 2021. Perfluoroalkyl Substances Increase Susceptibility of Northern Leopard Frog Tadpoles to Trematode Infection. Environ. Toxicol. Chem. 40(3):689-694. doi: 10.1002/etc.4678
16. Buser, MC and Scinicariello, F. 2016. Perfluoroalkyl substances and food allergies in adolescents. Environ. Int. 88(74-79). doi: 10.1016/j.envint.2015.12.020
17. Calafat, AM, Wong, L-Y, Kuklenyik, Z, Reidy, JA and Needham, LL. 2007. Polyfluoroalkyl chemicals in the U.S. population: data from the National Health and Nutrition Examination Survey (NHANES) 2003-2004 and comparisons with NHANES 1999-2000. Environ. Health Perspect. 115(11):1596-1602. doi: 10.1289/ehp.10598
18. CDC. 2019. Fourth National Report on Human Exposure to Environmental Chemicals Updated Tables. US Department of Health and Human Services. https://www.cdc.gov/exposurereport/pdf/FourthReport_UpdatedTables_Volume1_Jan2019-508.pdf
19. Collins, SJ, Ruscetti, FW, Gallagher, RE and Gallo, RC. 1979. Normal functional characteristics of cultured human promyelocytic leukemia cells (HL-60) after induction of differentiation by dimethylsulfoxide. J. Exp. Med. 149(4):969-974. doi:

20. Conder, JM, Hoke, RA, De Wolf, W, Russell, MH and Buck, RC. 2008. Are PFCAs bioaccumulative? A critical review and comparison with regulatory criteria and persistent lipophilic compounds. Environ. Sci. Technol. 42(4):995-1003. doi: 10.1021/es070895g
21. Conley, JM, Lambright, CS, Evans, N, Medlock-Kakaley, E, Hill, D, McCord, J, Strynar, MJ, Wehmas, LC, Hester, S, MacMillan, DK and Gray, LE, Jr. 2022. Developmental toxicity of Nafion byproduct 2 (NBP2) in the Sprague-Dawley rat with comparisons to hexafluoropropylene oxide-dimer acid (HFPO-DA or GenX) and perfluorooctane sulfonate (PFOS). Environ. Int. 160(107056). doi: 10.1016/j.envint.2021.107056
22. Dalsager, L, Christensen, N, Husby, S, Kyhl, H, Nielsen, F, Host, A, Grandjean, P and Jensen, TK. 2016. Association between prenatal exposure to perfluorinated compounds and symptoms of infections at age 1-4years among 359 children in the Odense Child Cohort. Environ. Int. 96(58-64. doi: 10.1016/j.envint.2016.08.026
23. DeWitt, JC, Blossom, SJ and Schaider, LA. 2019. Exposure to per-fluoroalkyl and polyfluoroalkyl substances leads to immunotoxicity: epidemiological and toxicological evidence. J. Expo. Sci. Environ. Epidemiol. 29(2):148-156. doi: 10.1038/s41370-018-0097-y
24. Dewitt, JC, Copeland, CB, Strynar, MJ and Luebke, RW. 2008. Perfluorooctanoic acid-induced immunomodulation in adult C57BL/6J or C57BL/6N female mice. Environ. Health Perspect. 116(5):644-650. doi: 10.1289/ehp.10896
25. Dupré-Crochet, S, Erard, M and Nüβe, O. 2013. ROS production in phagocytes: why, when, and where? J. Leukoc. Biol. 94(4):657-670. doi: 10.1189/jlb.1012544
26. Evich, MG, Davis, MJB, McCord, JP, Acrey, B, Awkerman, JA, Knappe, DRU, Lindstrom, AB, Speth, TF, Tebes-Stevens, C, Strynar, MJ, Wang, Z, Weber, EJ,

Henderson, WM and Washington, JW. 2022. Per- and polyfluoroalkyl substances in the environment. Science. 375(6580):eabg9065. doi: 10.1126/science.abg9065

27. Fenton, SE, Ducatman, A, Boobis, A, DeWitt, JC, Lau, C, Ng, C, Smith, JS and Roberts, SM. 2021. Per- and Polyfluoroalkyl Substance Toxicity and Human Health Review: Current State of Knowledge and Strategies for Informing Future Research. Environ. Toxicol. Chem. 40(3):606-630. doi: 10.1002/etc.4890
28. Fingerhut, L, Dolz, G and de Buhr, N. 2020. What Is the Evolutionary Fingerprint in Neutrophil Granulocytes? Int. J. Mol. Sci. 21(12):doi: 10.3390/ijms21124523
29. Gaballah, S, Swank, A, Sobus, JR, Howey, XM, Schmid, J, Catron, T, McCord, J, Hines, E, Strynar, M and Tal, T. 2020. Evaluation of Developmental Toxicity, Developmental Neurotoxicity, and Tissue Dose in Zebrafish Exposed to GenX and Other PFAS. Environ. Health Perspect. 128(4):47005. doi: 10.1289/EHP5843
30. Gallagher, R, Collins, S, Trujillo, J, McCredie, K, Ahearn, M, Tsai, S, Metzgar, R, Aulakh, G, Ting, R, Ruscetti, F and Gallo, R. 1979. Characterization of the continuous, differentiating myeloid cell line (HL-60) from a patient with acute promyelocytic leukemia. Blood. 54(3):713-733. doi:
31. Goudarzi, H, Miyashita, C, Okada, E, Kashino, I, Chen, C-J, Ito, S, Araki, A, Kobayashi, S, Matsuura, H and Kishi, R. 2017. Prenatal exposure to perfluoroalkyl acids and prevalence of infectious diseases up to 4years of age. Environ. Int. 104(132-138). doi: 10.1016/j.envint.2017.01.024
32. Grandjean, P, Heilmann, C, Weihe, P, Nielsen, F, Mogensen, UB and Budtz-Jorgensen, E. 2017. Serum Vaccine Antibody Concentrations in Adolescents Exposed to

Perfluorinated Compounds. Environ. Health Perspect. 125(7):077018. doi: 10.1289/EHP275

33. Grandjean, P, Heilmann, C, Weihe, P, Nielsen, F, Mogensen, UB, Timmermann, A and Budtz-Jorgensen, E. 2017. Estimated exposures to perfluorinated compounds in infancy predict attenuated vaccine antibody concentrations at age 5-years. J. Immunotoxicol. 14(1):188-195. doi: 10.1080/1547691X.2017.1360968
34. Guillette, TC, McCord, J, Guillette, M, Polera, ME, Rachels, KT, Morgeson, C, Kotlarz, N, Knappe, DRU, Reading, BJ, Strynar, M and Belcher, SM. 2020. Elevated levels of per- and polyfluoroalkyl substances in Cape Fear River Striped Bass (Morone saxatilis) are associated with biomarkers of altered immune and liver function. Environ. Int. 136(105358). doi: 10.1016/j.envint.2019.105358
35. Guruge, KS, Hikono, H, Shimada, N, Murakami, K, Hasegawa, J, Yeung, LWY, Yamanaka, N and Yamashita, N. 2009. Effect of perfluorooctane sulfonate (PFOS) on influenza A virus-induced mortality in female B6C3F1 mice. J. Toxicol. Sci. 34(6):687-691. doi: 10.2131/jts.34.687
36. Herb, M and Schramm, M. 2021. Functions of ROS in Macrophages and Antimicrobial Immunity. Antioxidants (Basel). 10(2):doi: 10.3390/antiox10020313
37. Howe, K, Clark, MD, Torroja, CF, Torrance, J, Berthelot, C, Muffato, M, Collins, JE, Humphray, S, McLaren, K, Matthews, L, McLaren, S, Sealy, I, Caccamo, M, Churcher, C, Scott, C, Barrett, JC, Koch, R, Rauch, GJ, White, S, Chow, W, Kilian, B, Quintais, LT, Guerra-Assuncao, JA, Zhou, Y, Gu, Y, Yen, J, Vogel, JH, Eyre, T, Redmond, S, Banerjee, R, Chi, J, Fu, B, Langley, E, Maguire, SF, Laird, GK, Lloyd, D, Kenyon, E, Donaldson, S, Sehra, H, Almeida-King, J, Loveland, J, Trevanion, S, Jones, M, Quail, M,

Willey, D, Hunt, A, Burton, J, Sims, S, McLay, K, Plumb, B, Davis, J, Clee, C, Oliver, K, Clark, R, Riddle, C, Elliot, D, Threadgold, G, Harden, G, Ware, D, Begum, S, Mortimore, B, Kerry, G, Heath, P, Phillimore, B, Tracey, A, Corby, N, Dunn, M, Johnson, C, Wood, J, Clark, S, Pelan, S, Griffiths, G, Smith, M, Glithero, R, Howden, P, Barker, N, Lloyd, C, Stevens, C, Harley, J, Holt, K, Panagiotidis, G, Lovell, J, Beasley, H, Henderson, C, Gordon, D, Auger, K, Wright, D, Collins, J, Raisen, C, Dyer, L, Leung, K, Robertson, L, Ambridge, K, Leongamornlert, D, McGuire, S, Gilderthorp, R, Griffiths, C, Manthravadi, D, Nichol, S, Barker, G, Whitehead, S, Kay, M, Brown, J, Murnane, C, Gray, E, Humphries, M, Sycamore, N, Barker, D, Saunders, D, Wallis, J, Babbage, A, Hammond, S, Mashreghi-Mohammadi, M, Barr, L, Martin, S, Wray, P, Ellington, A, Matthews, N, Ellwood, M, Woodmansey, R, Clark, G, Cooper, J, Tromans, A, Grafham, D, Skuce, C, Pandian, R, Andrews, R, Harrison, E, Kimberley, A, Garnett, J, Fosker, N, Hall, R, Garner, P, Kelly, D, Bird, C, Palmer, S, Gehring, I, Berger, A, Dooley, CM, Ersan-Urun, Z, Eser, C, Geiger, H, Geisler, M, Karotki, L, Kirn, A, Konantz, J, Konantz, M, Oberlander, M, Rudolph-Geiger, S, Teucke, M, Lanz, C, Raddatz, G, Osoegawa, K, Zhu, B, Rapp, A, Widaa, S, Langford, C, Yang, F, Schuster, SC, Carter, NP, Harrow, J, Ning, Z, Herrero, J, Searle, SM, Enright, A, Geisler, R, Plasterk, RH, Lee, C, Westerfield, M, de Jong, PJ, Zon, LI, Postlethwait, JH, Nusslein-Volhard, C, Hubbard, TJ, Roest Crollius, H, Rogers, J and Stemple, DL. 2013. The zebrafish reference genome sequence and its relationship to the human genome. Nature. 496(7446):498-503. doi: 10.1038/nature12111

38. Hu, XC, Andrews, DQ, Lindstrom, AB, Bruton, TA, Schaider, LA, Grandjean, P, Lohmann, R, Carignan, CC, Blum, A, Balan, SA, Higgins, CP and Sunderland, EM.

2016. Detection of Poly- and Perfluoroalkyl Substances (PFASs) in U.S. Drinking Water Linked to Industrial Sites, Military Fire Training Areas, and Wastewater Treatment Plants. Environ Sci Technol Lett. 3(10):344-350. doi: 10.1021/acs.estlett.6b00260

39. Humblet, O, Diaz-Ramirez, LG, Balmes, JR, Pinney, SM and Hiatt, RA. 2014. Perfluoroalkyl chemicals and asthma among children 12-19 years of age: NHANES (1999-2008). Environ. Health Perspect. 122(10):1129-1133. doi: 10.1289/ehp.1306606
40. Jabeen, M, Fayyaz, M and Irudayaraj, J. 2020. Epigenetic Modifications, and Alterations in Cell Cycle and Apoptosis Pathway in A549 Lung Carcinoma Cell Line upon Exposure to Perfluoroalkyl Substances. Toxics. 8(4):doi: 10.3390/toxics8040112
41. Karlsson, T, Glogauer, M, Ellen, RP, Loitto, V-M, Magnusson, K-E and Magalhães, MAO. 2011. Aquaporin 9 phosphorylation mediates membrane localization and neutrophil polarization. J. Leukoc. Biol. 90(5):963-973. doi: 10.1189/jlb.0910540
42. King, MA and Radicchi-Mastroianni, MA. 2002. Effects of caspase inhibition on camptothecin-induced apoptosis of HL-60 cells. Cytometry. 49(1):28-35. doi: 10.1002/cyto.10141
43. Kotlarz, N, McCord, J, Collier, D, Lea, CS, Strynar, M, Lindstrom, AB, Wilkie, AA, Islam, JY, Matney, K, Tarte, P, Polera, ME, Burdette, K, DeWitt, J, May, K, Smart, RC, Knappe, DRU and Hoppin, JA. 2020. Measurement of Novel, Drinking Water-Associated PFAS in Blood from Adults and Children in Wilmington, North Carolina. Environ. Health Perspect. 128(7):77005. doi: 10.1289/EHP6837
44. Lang, JR, Strynar, MJ, Lindstrom, AB, Farthing, A, Huang, H, Schmid, J, Hill, D and Chernoff, N. 2020. Toxicity of Balb-c mice exposed to recently identified 1,1,2,2-

tetrafluoro-2-[1,1,1,2,3,3-hexafluoro-3-(1,1,2,2-tetrafluoroethoxy)propan-2-yl]oxyethane-1-sulfonic acid (PFESA-BP2). Toxicology. 441(152529). doi: 10.1016/j.tox.2020.152529

45. Liang, L, Pan, Y, Bin, L, Liu, Y, Huang, W, Li, R and Lai, KP. 2022. Immunotoxicity mechanisms of perfluorinated compounds PFOA and PFOS. Chemosphere. 291(2):132892. doi: 10.1016/j.chemosphere.2021.132892
46. Liberatore, HK, Jackson, SR, Strynar, MJ and McCord, JP. 2020. Solvent Suitability for HFPO-DA ("GenX" Parent Acid) in Toxicological Studies. Environ Sci Technol Lett. 7(7):477-481. doi: 10.1021/acs.estlett.0c00323
47. Martin, EM, Till, RL, Sheats, MK and Jones, SL. 2017. Misoprostol Inhibits Equine Neutrophil Adhesion, Migration, and Respiratory Burst in an In Vitro Model of Inflammation. Front Vet Sci. 4(159). doi: 10.3389/fvets.2017.00159
48. Marvel, SW, To, K, Grimm, FA, Wright, FA, Rusyn, I and Reif, DM. 2018. ToxPi Graphical User Interface 2.0: Dynamic exploration, visualization, and sharing of integrated data models. BMC Bioinformatics. 19(1):80. doi: 10.1186/s12859-018-2089-2
49. McCord, J and Strynar, M. 2019. Identification of Per- and Polyfluoroalkyl Substances in the Cape Fear River by High Resolution Mass Spectrometry and Nontargeted Screening. Environ. Sci. Technol. 53(9):4717-4727. doi: 10.1021/acs.est.8b06017
50. Mylroie, JE, Wilbanks, MS, Kimble, AN, To, KT, Cox, CS, McLeod, SJ, Gust, KA, Moore, DW, Perkins, EJ and Garcia-Reyero, N. 2021. Perfluorooctanesulfonic Acid-Induced Toxicity on Zebrafish Embryos in the Presence or Absence of the Chorion. Environ. Toxicol. Chem. 40(3):780-791. doi: 10.1002/etc.4899

51. Neagu, M, Constantin, C, Bardi, G and Duraes, L. 2021. Adverse outcome pathway in immunotoxicity of perfluoroalkyls. Current Opinion in Toxicology. 25(23-29). doi: 10.1016/j.cotox.2021.02.001

52. Neehus, A-L, Moriya, K, Nieto-Patlán, A, Le Voyer, T, Lévy, R, Özen, A, Karakoc-Aydiner, E, Baris, S, Yildiran, A, Altundag, E, Roynard, M, Haake, K, Migaud, M, Dorgham, K, Gorochov, G, Abel, L, Lachmann, N, Dogu, F, Haskologlu, S, İnce, E, El-Benna, J, Uzel, G, Kiykim, A, Boztug, K, Roderick, MR, Shahrooei, M, Brogan, PA, Abolhassani, H, Hancioglu, G, Parvaneh, N, Belot, A, Ikinciogullari, A, Casanova, J-L, Puel, A and Bustamante, J. 2021. Impaired respiratory burst contributes to infections in PKCδ-deficient patients. J. Exp. Med. 218(9):doi: 10.1084/jem.20210501

53. Ng, CA and Hungerbühler, K. 2014. Bioaccumulation of perfluorinated alkyl acids: observations and models. Environ. Sci. Technol. 48(9):4637-4648. doi: 10.1021/es404008g

54. NTP. 2016. Monograph on Immunotoxicity Associated with Exposure to Perfluorooctanoic acid (PFOA) and perfluorooctane sulfonate (PFOS). National Toxicology Program. https://ntp.niehs.nih.gov/ntp/ohat/pfoa_pfos/pfoa_pfosmonograph_508.pdf

55. OECD. 2018. Environment Directorate Joint Meeting of the Chemicals Committee and the Working Party on Chemicals, Pesticides and Biotechnology. Toward a New Comprehensive Global Database of Per- and Polyfluoroalkyl Substances (PFASs): Summary Report On Updating The OECD 2007 List Of Per- and Polyfluoroalkyl Substances (PFASs). Organisation for Economic Co-operation and Development.

https://www.oecd.org/env/ehs/risk-management/series-on-risk-management-publications-by-number.htm

56. Phelps, DW, Fletcher, AA, Rodriguez-Nunez, I, Balik-Meisner, MR, Tokarz, DA, Reif, DM, Germolec, DR and Yoder, JA. 2020. In vivo assessment of respiratory burst inhibition by xenobiotic exposure using larval zebrafish. J. Immunotoxicol. 17(1):94-104. doi: 10.1080/1547691X.2020.1748772
57. Pierozan, P, Jerneren, F and Karlsson, O. 2018. Perfluorooctanoic acid (PFOA) exposure promotes proliferation, migration and invasion potential in human breast epithelial cells. Arch. Toxicol. 92(5):1729-1739. doi: 10.1007/s00204-018-2181-4
58. Pierozan, P and Karlsson, O. 2018. PFOS induces proliferation, cell-cycle progression, and malignant phenotype in human breast epithelial cells. Arch. Toxicol. 92(2):705-716. doi: 10.1007/s00204-017-2077-8
59. Reif, DM, Martin, MT, Tan, SW, Houck, KA, Judson, RS, Richard, AM, Knudsen, TB, Dix, DJ and Kavlock, RJ. 2010. Endocrine profiling and prioritization of environmental chemicals using ToxCast data. Environ. Health Perspect. 118(12):1714-1720. doi: 10.1289/ehp.1002180
60. Rice, PA, Aungst, J, Cooper, J, Bandele, O and Kabadi, SV. 2020. Comparative analysis of the toxicological databases for 6:2 fluorotelomer alcohol (6:2 FTOH) and perfluorohexanoic acid (PFHxA). Food Chem. Toxicol. 138(111210). doi: 10.1016/j.fct.2020.111210
61. Rincón, E, Rocha-Gregg, BL and Collins, SR. 2018. A map of gene expression in neutrophil-like cell lines. BMC Genomics. 19(1):573. doi: 10.1186/s12864-018-4957-6

62. Ritz, C, Baty, F, Streibig, JC and Gerhard, D. 2015. Dose-Response Analysis Using R. PLoS One. 10(12):e0146021. doi: 10.1371/journal.pone.0146021

63. Rosenmai, AK, Taxvig, C, Svingen, T, Trier, X, van Vugt-Lussenburg, BMA, Pedersen, M, Lesné, L, Jégou, B and Vinggaard, AM. 2016. Fluorinated alkyl substances and technical mixtures used in food paper-packaging exhibit endocrine-related activity in vitro. Andrology. 4(4):662-672. doi: 10.1111/andr.12190

64. Rushing, BR, Hu, Q, Franklin, JN, McMahen, R, Dagnino, S, Higgins, CP, Strynar, MJ and DeWitt, JC. 2017. Evaluation of the immunomodulatory effects of 2,3,3,3-tetrafluoro-2-(heptafluoropropoxy)-propanoate in C57BL/6 mice. Toxicol. Sci. 156(1):179–189. doi: 10.1093/toxsci/kfw251

65. Shane, HL, Baur, R, Lukomska, E, Weatherly, L and Anderson, SE. 2020. Immunotoxicity and allergenic potential induced by topical application of perfluorooctanoic acid (PFOA) in a murine model. Food Chem. Toxicol. 136(111114). doi: 10.1016/j.fct.2020.111114

66. Signorell, A. 2021. DescTools: Tools for descriptive statistics. R package. https://andrisignorell.github.io/DescTools/

67. Steenland, K, Zhao, L, Winquist, A and Parks, C. 2013. Ulcerative colitis and perfluorooctanoic acid (PFOA) in a highly exposed population of community residents and workers in the mid-Ohio valley. Environ. Health Perspect. 121(8):900-905. doi: 10.1289/ehp.1206449

68. Sun, M, Arevalo, E, Strynar, M, Lindstrom, A, Richardson, M, Kearns, B, Pickett, A, Smith, C and Knappe, DRU. 2016. Legacy and Emerging Perfluoroalkyl Substances Are Important Drinking Water Contaminants in the Cape Fear River Watershed of North

Carolina. Environmental Science & Technology Letters. 3(12):415-419. doi: 10.1021/acs.estlett.6b00398

69. Truong, L, Reif, DM, St Mary, L, Geier, MC, Truong, HD and Tanguay, RL. 2014. Multidimensional in vivo hazard assessment using zebrafish. Toxicol. Sci. 137(1):212-233. doi: 10.1093/toxsci/kft235
70. USEPA. 1998. Health Effects Test Guidelines OPPTS 870.7800 Immunotoxicity. United States Environmental Protection Agency.
71. USEPA. 2020. PFAS Master List of PFAS Substances. https://comptox.epa.gov/dashboard/chemical-lists/PFASMASTER
72. Verdon, R, Gillies, SL, Brown, DM, Henry, T, Tran, L, Tyler, CR, Rossi, AG, Stone, V and Johnston, HJ. 2021. Neutrophil activation by nanomaterials in vitro: comparing strengths and limitations of primary human cells with those of an immortalized (HL-60) cell line. Nanotoxicology. 15(1):1-20. doi: 10.1080/17435390.2020.1834635
73. Wang, Z, DeWitt, JC, Higgins, CP and Cousins, IT. 2017. A Never-Ending Story of Per- and Polyfluoroalkyl Substances (PFASs)? Environ. Sci. Technol. 51(5):2508-2518. doi: 10.1021/acs.est.6b04806
74. Westerfield, M. 2007. The zebrafish book. A guide for the laboratory use of zebrafish (Danio rerio). Univ. of Oregon Press.
75. Westerman, TL, Bogomolnaya, L, Andrews-Polymenis, HL, Sheats, MK and Elfenbein, JR. 2018. The Salmonella type-3 secretion system-1 and flagellar motility influence the neutrophil respiratory burst. PLoS One. 13(9):e0203698. doi: 10.1371/journal.pone.0203698

76. Williams, AJ, Grulke, CM, Edwards, J, McEachran, AD, Mansouri, K, Baker, NC, Patlewicz, G, Shah, I, Wambaugh, JF, Judson, RS and Richard, AM. 2017. The CompTox Chemistry Dashboard: a community data resource for environmental chemistry. J. Cheminform. 9(1):61. doi: 10.1186/s13321-017-0247-6

77. Williams, AJ, Lambert, JC, Thayer, K and Dorne, J-LCM. 2021. Sourcing data on chemical properties and hazard data from the US-EPA CompTox Chemicals Dashboard: A practical guide for human risk assessment. Environ. Int. 154(106566). doi: 10.1016/j.envint.2021.106566

78. Yang, Q, Abedi-Valugerdi, M, Xie, Y, Zhao, X-Y, Möller, G, Nelson, BD and DePierre, JW. 2002. Potent suppression of the adaptive immune response in mice upon dietary exposure to the potent peroxisome proliferator, perfluorooctanoic acid. Int. Immunopharmacol. 2(2-3):389-397. doi: 10.1016/s1567-5769(01)00164-3

79. Yao, J, Pan, Y, Sheng, N, Su, Z, Guo, Y, Wang, J and Dai, J. 2020. Novel Perfluoroalkyl Ether Carboxylic Acids (PFECAs) and Sulfonic Acids (PFESAs): Occurrence and Association with Serum Biochemical Parameters in Residents Living Near a Fluorochemical Plant in China. Environ. Sci. Technol. 54(21):13389-13398. doi: 10.1021/acs.est.0c02888

80. Zhang, C, McElroy, AC, Liberatore, HK, Alexander, NLM and Knappe, DRU. 2021. Stability of Per- and Polyfluoroalkyl Substances in Solvents Relevant to Environmental and Toxicological Analysis. Environ. Sci. Technol. doi: 10.1021/acs.est.1c03979

81. Zhang, G, Roell, KR, Truong, L, Tanguay, RL and Reif, DM. 2017. A data-driven weighting scheme for multivariate phenotypic endpoints recapitulates zebrafish

developmental cascades. Toxicol. Appl. Pharmacol. 314(109-117). doi: 10.1016/j.taap.2016.11.010

82. Zheng, X-M, Liu, H-L, Shi, W, Wei, S, Giesy, JP and Yu, H-X. 2011. Effects of perfluorinated compounds on development of zebrafish embryos. Environ. Sci. Pollut. Res. Int. 19(7):2498-2505. doi: 10.1007/s11356-012-0977-y

CHAPTER 4

Conclusions, Recommendations, and Future Directions

Drake W. Phelps[1,2,3]

[1]Department of Molecular Biomedical Sciences, College of Veterinary Medicine, North Carolina State University, Raleigh, NC, USA

[2]Comparative Medicine Institute, North Carolina State University, Raleigh, NC, USA

[3]Center for Environmental and Health Effects of PFAS, North Carolina State University, Raleigh, NC, USA

In Chapter 1, I examined the issue of how little is known about the effects of per- and polyfluoroalkyl substances (PFASs) impact on innate immunity. The existing data in the literature are often contradictory, raising more questions than they answer. Still there is sufficient evidence demonstrating that PFAS exposure impacts innate immunity of humans, experimental animals, and wildlife. These data support the growing field of evidence that has concluded that these compounds are immunotoxic. However, data gaps remain, given that thousands of PFASs have been registered globally, and only a handful of the registered compounds have been investigated for immunotoxicity. Of course, it must also be noted that unregistered PFASs may also exist and have not been studied for immunotoxic outcomes. Even with compounds where immunotoxicity has been studied, there lacks uniformity in the overall findings among different studies, which makes drawing definitive conclusions difficult.

In Chapter 2, I sought to ask whether the larval zebrafish could be used as a screening tool to identify compounds that inhibit one aspect of innate immune function. In doing so, I successfully identified five compounds that suppress the respiratory burst in larval zebrafish. The immunotoxicity of these compounds was supported by studies in mammalian models, validating that the larval zebrafish is a versatile model that can serve as a model for human and ecological health. I also showed that none of these immunotoxic compounds suppressed the number of phagocytes present in the larvae; in fact, benzo[a]pyrene increased the numbers of macrophages. While this mechanism would have been a simple explanation for the observed phenotype, it demonstrates that other, currently-unknown molecular mechanisms are at play. These immunotoxic compounds were also structurally diverse, indicating that many classes of compounds have the potential to disrupt this critical response of the innate immune system. Given that the exposures in this study occurred during embryonic hematopoiesis and the

complex signaling cascade required to initiate the respiratory burst, it is likely that multiple mechanisms are at play for the phenotype observed after exposure to these compounds.

In Chapter 3, I asked whether my previous work could be expanded upon to determine if the respiratory burst assay could be applied to screen structurally similar compounds in several experimental models. As in Chapter 2, I utilized larval zebrafish to screen nine PFASs and identified two PFASs (PFHxA and GenX) that were able to inhibit the respiratory burst with statistical significance. I adapted my *in vivo* methods for use *in vitro* with a human neutrophil-like cell line. In doing so, I was able to recapitulate my results in this model, again identifying PFHxA and GenX as immunotoxic while also observing that PFOA was immunotoxic. These results validated the models and supported the notion that they should be used in tandem given that they were not in total agreement. In following up on these findings with primary human neutrophils *ex vivo*, only GenX suppressed the respiratory burst with statistical significance among the compounds tested. This testing paradigm is an ideal example of how high-throughput screening can be used with libraries of compounds and prioritize positive hits for studies in more complex and costly models, whether they be primary cells or *in vivo* rodent models.

This dissertation set out to explore whether the neutrophil respiratory burst could be a target of xenobiotics. Using high-throughput methods such as larval zebrafish and a neutrophil-like cell line, I was able to identify eight compounds that suppress the respiratory burst in at least one of these models. While these compounds were identified using a successful and conclusive screening-based approach, hypothesis-driven work is necessary to follow up on the above findings. Indeed, the findings reported here are a starting point, not a final conclusion. The compounds identified as suppressive of the respiratory burst still present a hazard, but future

studies should extend beyond hazard identification to determine biological relevancy and mechanism in order to inform risk assessment and risk management of these compounds.

The question remains regarding the relevancy of what these results mean for the field at large and for protection of human and environmental health. While defects in the respiratory burst have been observed in genetic disorders of human patients, my work did not identify compounds that result in complete or near-complete ablation of the respiratory burst. I observed anywhere from 10-50% suppression of the respiratory burst depending on the test compound, its concentration, and the model of interest. Notably, compounds that did not suppress the respiratory burst may be able to suppress this innate immune function at higher concentrations that were developmentally toxic to zebrafish larvae or cytotoxic to cells. Regardless, while statistically significant, it remains to be seen whether this level of respiratory burst suppression is biologically significant. I have begun to address this by developing an assay to assess whether this suppression confers susceptibility to infectious disease *in vivo* (See **Appendix B**), and it will be interesting to compare the results of these two assays once it is developed. Future studies should seek to determine the sensitivity and specificity of the *in vivo* and *in vitro* respiratory burst assays. In all of the screened compounds, this work has also yet to identify compounds that potentiate or activate the respiratory burst. Future studies focused on identifying compounds with this phenotype may open new avenues of exploration into xenobiotic-induced autoimmunity.

Once relevancy has been addressed, mechanisms must be established for these compounds' immunotoxicity. Future experiments are already in progress to address this on two fronts. First, transcriptomics and metabolomics will be performed on neutrophil-like HL-60 cells after exposure to PFOA, PFHxA, or GenX to identify potential pathways disrupted after exposure to these compounds. The integration of these datasets, along with other potential omics

analyses, will be a novel approach allowing for a wide-reaching investigation of how these compounds inhibit innate immune function. Experiments exploring mechanisms outside of these data are also being explored as the experiments I proposed during my Preliminary Exam were funded. These experiments will explore the interaction of thyroid disruption, PFAS exposure, and innate immune function while also expanding the suite of assays in the Yoder Lab to include natural killer (NK) cell function.

I would encourage future researchers to return to the results of Chapter 2. The initial study that began this work was foundational in identifying compounds that share immunotoxicity between larval zebrafish and mammalian models. These compounds should be re-examined using the *in vitro* and *in vivo* models established in Chapter 3. Further study of these compounds remains important, and may establish new mechanisms for their immunotoxicity. Ultimately, I would encourage this dissertation, along with ongoing and recommended experiments, to serve as a starting point for identifying molecular initiating events to contribute to the development of adverse outcome pathways to aid in hazard identification, risk assessment, and risk management of immunotoxic xenobiotics.

Finally, I have discussed the risk management of the xenobiotics in this dissertation throughout as the policy decisions made regarding xenobiotics directly impact human and environmental health. Many compounds from Chapter 2 have been regulated at the federal level to prevent exposure and/or cease manufacture. However, to date, there are no federal laws in the US regulating PFASs in drinking water. While some states have acted on their own, this is insufficient as most PFASs have gone unregulated. Due to the sheer number of compounds in this class, it is not rational or feasible to test each one individually. PFASs should be regulated as a class to prevent further harm of these compounds to the environment and communities around

the globe. While I can appreciate that these compounds are not all equally toxic, as demonstrated in Chapter 3, there is sufficient data to show that these compounds, as a class, can result in toxic outcomes. There is also precedent for a class-based approach, as was the case for polychlorinated biphenyls (PCBs). The PFAS crisis will continue to worsen if swift, broad, and effective actions are not taken and enforced.

APPENDICES

Appendix A: Investigation of Proliferation in Neutrophil-like HL-60 Cells

Drake W. Phelps[1,2] and Jeffrey A. Yoder[1,2,3]

[1]Department of Molecular Biomedical Sciences, College of Veterinary Medicine, North Carolina State University, Raleigh, NC, USA

[2]Comparative Medicine Institute, North Carolina State University, Raleigh, NC, USA

[3]Center for Human Health and the Environment, North Carolina State University, Raleigh, NC, USA

INTRODUCTION

In Chapter 3, I showed that perfluorooctanoic acid (PFOA) interacts directly with PrestoBlue to convert PrestoBlue from its non-fluorescent to its fluorescent form. As noted in the Discussion of that Chapter, I initially thought that this was a proliferative phenotype. I attempted to show proliferation through various methods outlined below. Ultimately, however, once I discovered that PFOA can interact directly with PrestoBlue, I abandoned these assays since proliferation did not seem likely. Still, the experiments described below outline the steps taken to assess the potential proliferation that was observed.

MATERIALS AND METHODS

Cell culture and exposure

HL-60 cells were maintained, differentiated to a neutrophil-like phenotype (nHL-60), and exposed to PFOA as described in Chapter 3.

Automated cell counting

After exposure to PFOA, cells were centrifuged at 0.4 x g for 10 min. Cells were resuspended in 100 µL of media. Cells were then counted using a media and counted using a Cellometer Vision (Nexcelom Biosciences, Lawrence, MA, USA) using trypan blue exclusion to determine the concentration and viability of the cells.

Counting via flow cytometry

After exposure to PFOA, cells were counted using only forward-scatter and side-scatter via flow cytometry using a CytoFLEX (Beckman Coulter; Brea, CA, USA). Wells with no cells were also included as a control.

Carboxyfluorescein succinimidyl ester (CFSE) staining for proliferation

Staining with carboxyfluorescein succinimidyl ester (CFSE) is a common immunological method used to detect cellular proliferation. CellTrace CFSE (ThermoFisher; Waltham, MA) was prepared fresh for each experiment and used according to the manufacturer's instructions. After differentiation, cells were centrifuged at 0.4 x g for 10 min. Cells were then resuspended in sterile phosphate-buffered saline (PBS). Cells were counted via counted using a Cellometer Vision using trypan blue exclusion to determine the concentration and viability of the cells. Cells were normalized to a concentration of 0.1 x 10^6 cells/mL in PBS. CFSE was then added to the cells at final concentrations of 5 µM, 2.5 µM, 1.25 µM, and 0.625 µM. Unstained cells were included as well as undifferentiated HL-60 cells, which were included as a positive control for proliferation. Cells were incubated at 37 °Celsius for 20 minutes. 10 mL of cell culture media was then added to neutralize any extracellular CFSE. Cells were centrifuged at 0.4 x g for 10 min. After aspirating the supernatant, cells were resuspended in 10 mL media, exposed to PFOA, and plated.

Cells were analyzed using flow cytometry using a CytoFLEX. Cells were gated on forward-scatter and side-scatter to exclude acellular debris and doublets. Cells were then gated on whether they were $CFSE^+$.

Cell cycle staining

Pierozan et al. (2018a, 2018b) reported that PFOA and PFOS alter the cell cycle and induce proliferative phenotypes. Using Vybrant Dye Cycle Green (ThermoFisher; Waltham, MA, USA), I attempted to reproduce their results in HL-60 and nHL-60 cells. Vybrant Dye Cycle Green was used according to manufacturer's instructions. Due to technical changes in protocols, cells were cultured and exposed in T25 flasks, rather than 96 well plates. Different

timepoints of exposure were also prepared (24hr, 48 hr, 96 hr). After exposure to PFOA, cells were centrifuged at 0.4 x g for 10 min and resuspended in 1 mL media. Cells were then stained with 2 µL of Vybrant Dye Cycle Green and incubated for 30 min at 37 °Celsius. Cells were then analyzed via flow cytometry using a LSRII (Becton Dickinson; Franklin Lakes, NJ, USA). Cells were gated on forward-scatter and side-scatter to exclude acellular debris and doublets. Cells were then gated on whether they were Vybrant^{+} using a linear scale. Once collected, data were analyzed using FCS Express 6 (De Novo Software, Pasadena, CA, USA).

RESULTS

Automated cell counting was not sensitive enough to detect proliferation

Counting using only automated cell counting proved unreliable. The cells were not concentrated enough to be reliably detected, even when resuspended at 100 µL, with concentrations with no group reaching 1 x 10^6 cells (**Figure 1a**). From the initial experiments in Chapter 3, a doubling of cell number was expected with PFOA treatment. Viability was also low among all groups (**Figure 1b**), raising questions about the validity of these data. Ultimately, even though only one experiment was performed, I decided that this method was not sensitive enough to detect proliferation.

Counting via flow cytometry was sensitive but not specific

Counting via flow cytometry also proved unfruitful in this work. While sensitive in detecting events, the method proved non-specific because cellular events were detected in the wells where no cells were present (**Figure 2**). This method was also deemed unable to detect proliferation.

CFSE staining was inconsistent among groups

Initial experiments revealed that manufacturer-recommended concentrations of CFSE were too high, resulting in CFSE fluorescence that was off-scale for the flow cytometer. Subsequent experiments found that 1.25 µM and 0.625 µM CFSE were sufficient. However, upon analyzing cells via flow cytometry, I determined that there were differences in the uptake of CFSE between HL-60 cells and nHL-60 cells, indicating that the HL-60 cells are a poor positive control. In the nHL-60 cells, staining efficiency was too low for valid data, thus peaks of CFSE staining could not be determined.

Cell cycle staining revealed no differences in the cell cycle after PFOA exposure

Between two replicates, cell cycle plots were successfully generated. However, as was the case for CFSE staining, Vybrant staining was inefficient for nHL-60 cells. Similarly, HL-60 cells had high staining efficiency (**Figure 3**). Upon investigating the cell cycle in both replicates, nHL-60 cells exposed to DMSO or PFOA were mostly in the G0/G1 phase while undifferentiated HL-60 cells were largely in S phase (**Figure 4**). Interestingly, there were few cells among all treatments that were in G2/M phase. These data show that while there are differences between HL-60 and nHL-60 cells, exposure to PFOA did not alter the cell cycle when compared to the DMSO control.

DISCUSSION

In this Appendix, I explore the rationale behind experiments wherein I investigated a potential proliferative phenotype in nHL-60 cells after exposure to PFOA. This phenotype was interesting, given that it had been observed previously by others in the literature albeit it in other cell types (Pierozan et al. 2018a; Pierozan et al. 2018b; Jabeen et al. 2020; Williams et al. 2021; Williams et al. 2017). However, I was unable to recapitulate the findings of others in these

experiments. This was later found to be due to direct interactions between PrestoBlue and PFOA (and other long-chain PFASs) that were misidentified as proliferation (see **Chapter 3**). It is worth noting in these previously published studies did not use PrestoBlue or other resazurin-based reagents in their analysis of proliferation, indicating that their results are valid, especially given that three of these studies confirmed their proliferation through other methods, including cell cycle analysis (Pierozan et al. 2018a; Pierozan et al. 2018b; Jabeen et al. 2020).

While frustrating, these experiments were illuminating and allowed for exercises in troubleshooting and experimental design, especially with regards to flow cytometry. It was also interesting that HL-60 and nHL-60 cells possessed different staining efficiencies with both CFSE and Vybrant Dye Cycle Green. I would urge future researchers pursuing the use of these reagents in HL-60 cells and nHL-60 cells to use caution because of this while also working to understand why this occurs.

ACKNOWLEDGEMENTS

I would like to thank Javid Mohammed (NC State University) for the assistance in the flow cytometry experiments.

FIGURES

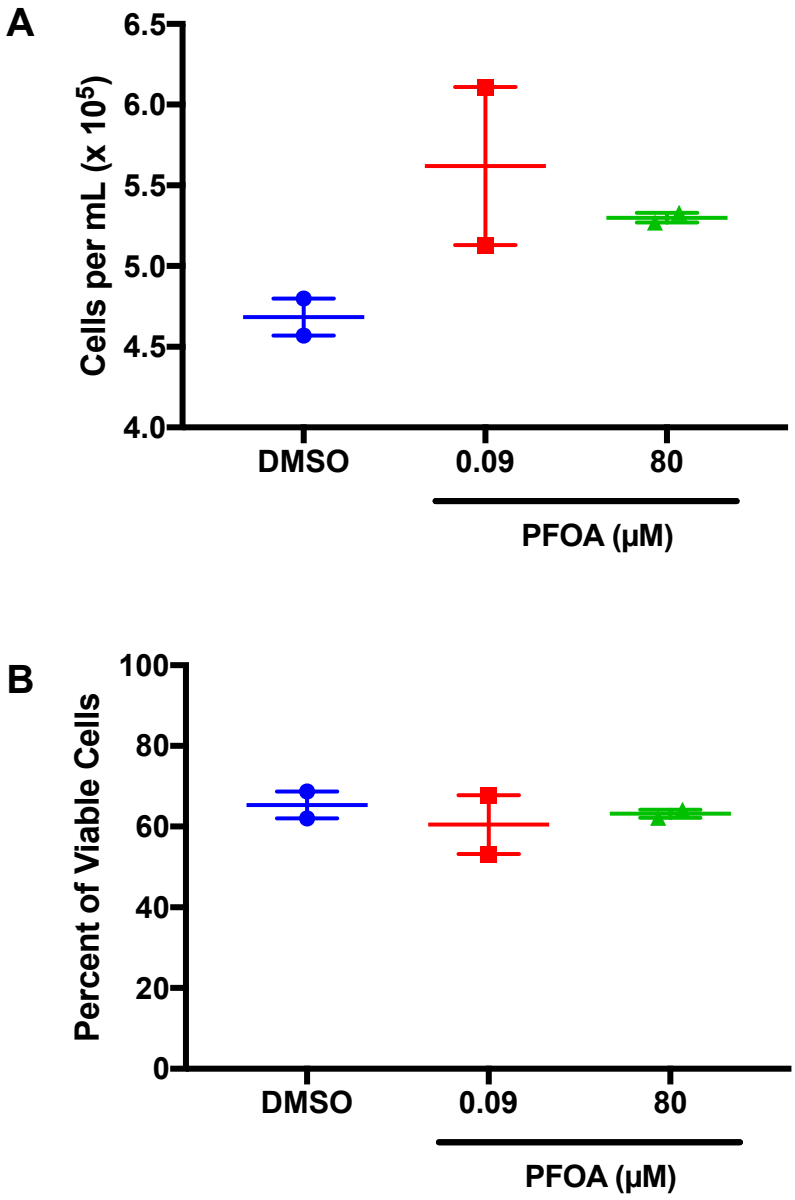

Figure 1. Counting cells via an automated cell counter. HL-60 cells were differentiated to nHL-60 cells and exposed to PFOA. (A) Cells were then counted using a Nexcelom Cellometer Vision. (B) Viability was determined using using trypan blue exclusion. Individual symbols represent individual counts from the same culture.

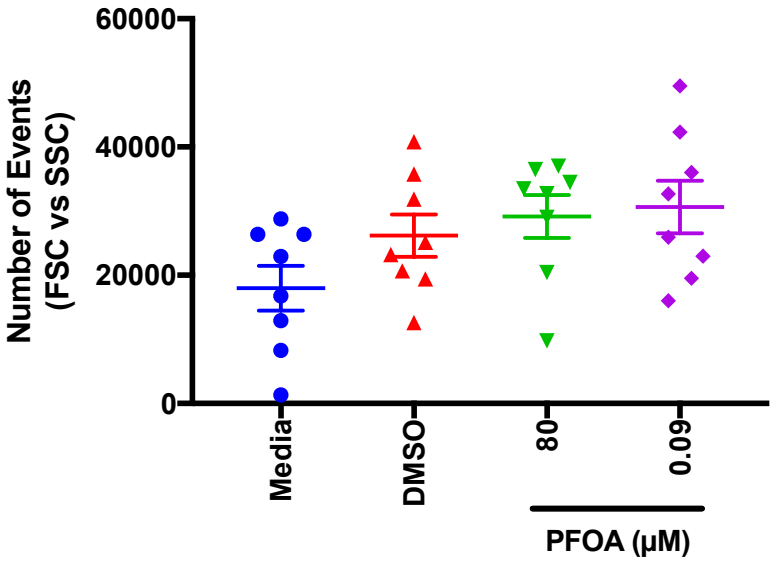

Figure 2. Counting cells via flow cytometry. HL-60 cells were differentiated to nHL-60 cells and exposed to PFOA. (A) Cells were then counted using forward- and side-scatter on a Becton Dickinson CytoFLEX. Individual symbols represent individual wells of a 96-well plate.

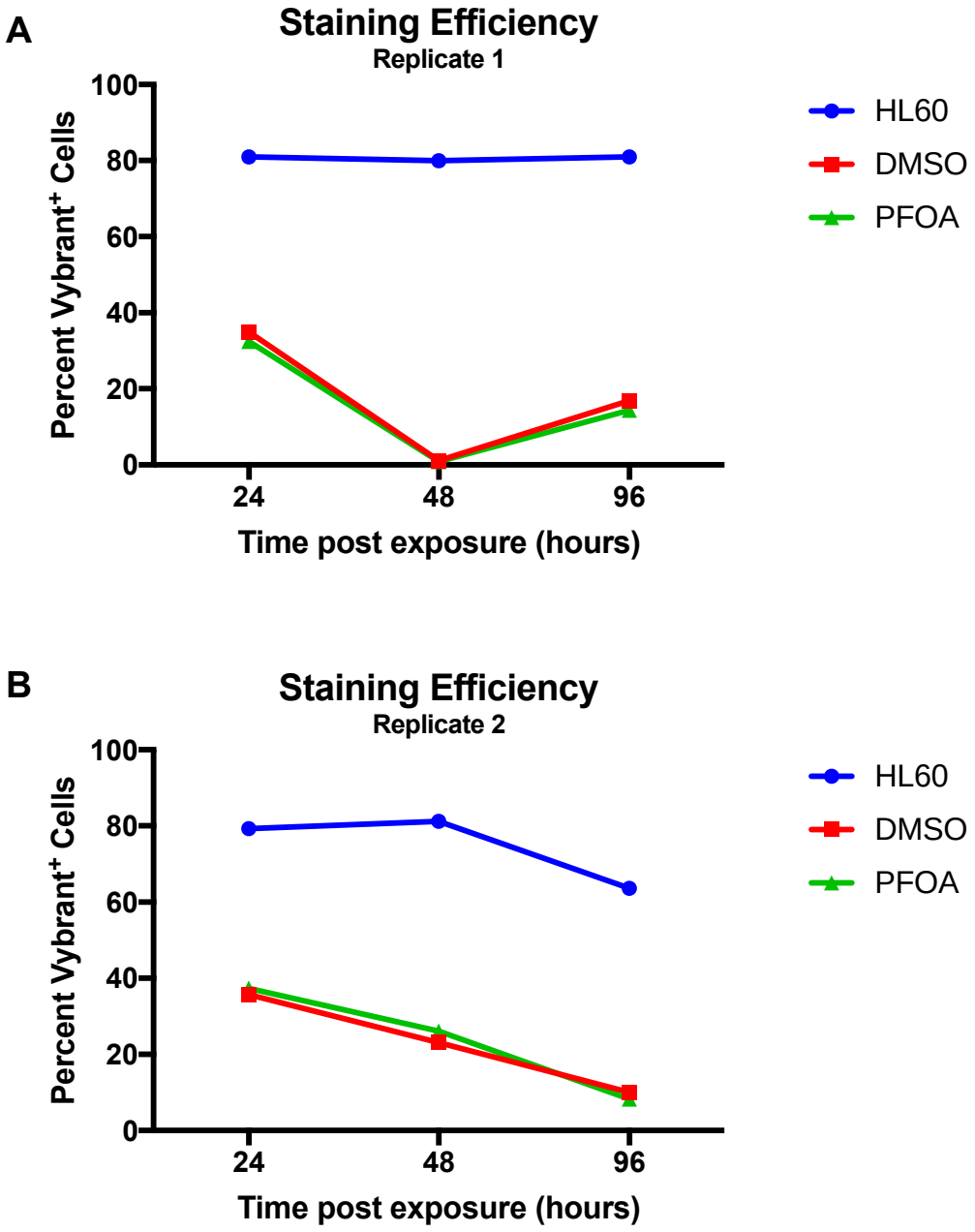

Figure 3. Staining efficiency of Vybrant Dye Cycle in HL-60 and nHL-60 cells. HL-60 cells were differentiated to nHL-60 cells and exposed to PFOA for 24, 48, or 96 hours after which they were stained with Vybrant Dye Cycle and analyzed on a Becton Dickinson LSRII. (A,B) Staining efficiency of Vybrant Dye Cycle was determined by the number of Vybrant^{+} singlets across two replicates.

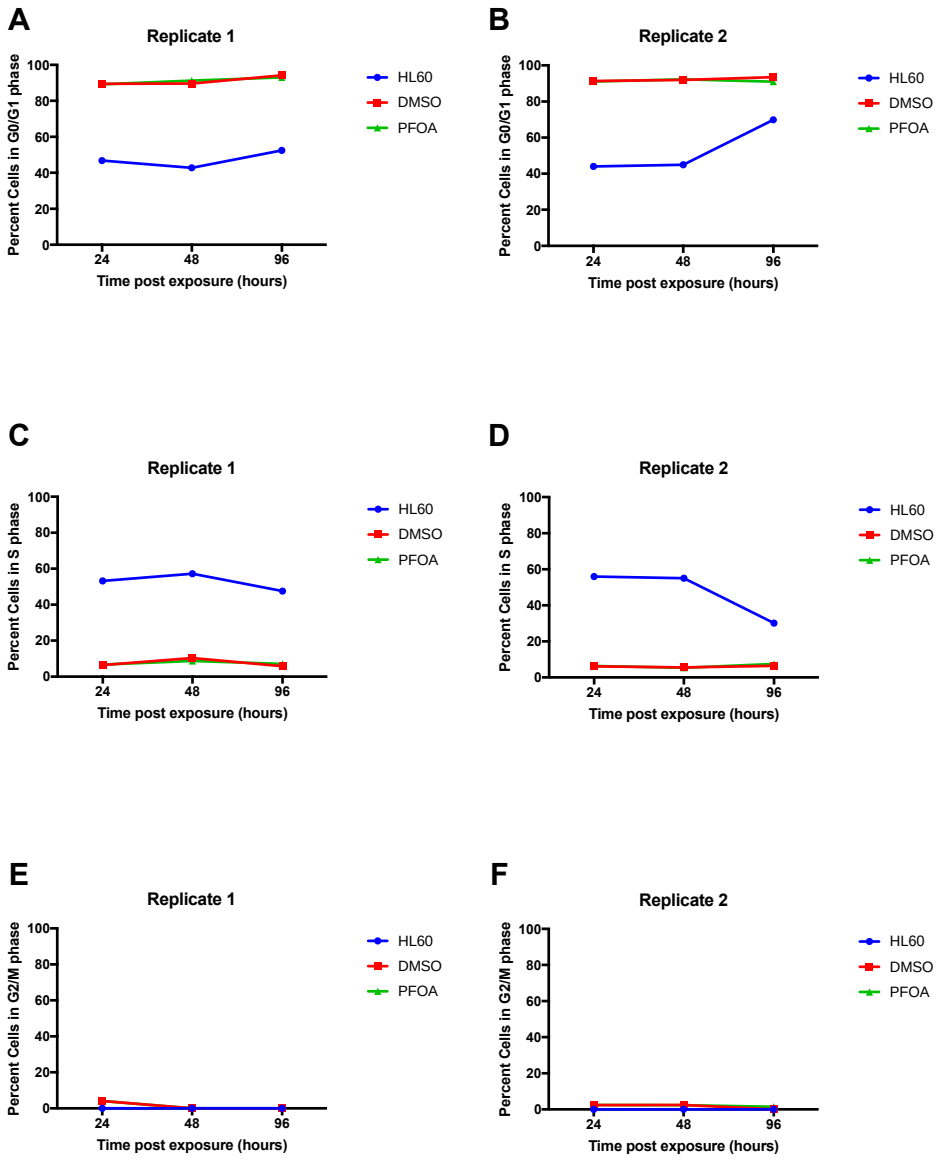

Figure 4. Cell cycle analysis in HL-60 and nHL-60 cells. HL-60 cells were differentiated to nHL-60 cells and exposed to PFOA for 24, 48, or 96 hours after which they were stained with Vybrant Dye Cycle and analyzed on a Becton Dickinson LSRII. Cell cycle analysis was performed in FCS Express 6. (A,B) Percent of cells in G0/G1 phase in two different replicates. (C,D) Percent of cells in S phase in two different replicates. (E,F) Percent of cells in G2/M phase in two different replicates

REFERENCES

1. Pierozan, P, Jerneren, F and Karlsson, O. 2018. Perfluorooctanoic acid (PFOA) exposure promotes proliferation, migration and invasion potential in human breast epithelial cells. Arch. Toxicol. 92(5):1729-1739. doi: 10.1007/s00204-018-2181-4
2. Pierozan, P and Karlsson, O. 2018. PFOS induces proliferation, cell-cycle progression, and malignant phenotype in human breast epithelial cells. Arch. Toxicol. 92(2):705-716. doi: 10.1007/s00204-017-2077-8
3. Jabeen, M, Fayyaz, M and Irudayaraj, J. 2020. Epigenetic Modifications, and Alterations in Cell Cycle and Apoptosis Pathway in A549 Lung Carcinoma Cell Line upon Exposure to Perfluoroalkyl Substances. Toxics. 8(4):doi: 10.3390/toxics8040112
4. Williams, AJ, Grulke, CM, Edwards, J, McEachran, AD, Mansouri, K, Baker, NC, Patlewicz, G, Shah, I, Wambaugh, JF, Judson, RS and Richard, AM. 2017. The CompTox Chemistry Dashboard: a community data resource for environmental chemistry. J. Cheminform. 9(1):61. doi: 10.1186/s13321-017-0247-6
5. Williams, AJ, Lambert, JC, Thayer, K and Dorne, J-LCM. 2021. Sourcing data on chemical properties and hazard data from the US-EPA CompTox Chemicals Dashboard: A practical guide for human risk assessment. Environ. Int. 154(106566). doi: 10.1016/j.envint.2021.106566

Appendix B: Preliminary Development of a High-Throughput Infection Assay in Larval Zebrafish

Drake W. Phelps[1,2,3], Jacob H. Driggers[1], and Jeffrey A. Yoder[1,2,3,4]

[1]Department of Molecular Biomedical Sciences, College of Veterinary Medicine, North Carolina State University, Raleigh, NC, USA

[2]Comparative Medicine Institute, North Carolina State University, Raleigh, NC, USA

[3] Center for Environmental and Health Effects of PFAS, North Carolina State University, Raleigh, NC, USA

[4]Center for Human Health and the Environment, North Carolina State University, Raleigh, NC, USA

INTRODUCTION

As mentioned in Chapters 3 and 4, there is a critical need to develop high-throughput *in vivo* infection assays in order to determine if per- and polyfluoroalkyl substances (PFASs) confer susceptibility to infectious disease. Previous attempts in the Yoder Lab have been successful in infecting larval zebrafish and reisolating the inoculum. However, experiments were not reproducible among biological replicates, likely due to genetic variability among larvae within a clutch as well as genetic variability among different clutches. Here, I set out to establish a high-throughput infection assay in larval zebrafish using *Edwardsiella tarda*, an opportunistic fish pathogen that can infect larval zebrafish through immersion (Pressley 2005). In contrast to initial development of the assay in our lab, instead of testing individual larvae, I pooled groups of larvae to minimize variability within a clutch.

MATERIALS AND METHODS

Zebrafish

Adult zebrafish were maintained as described in Chapter 3. Embryos were collected via natural spawning and bleached as described in Chapter 3. After bleaching, embryos were incubated at 28 °C until ~6 hpf. Embryos were then sorted into a 6-well plate with 10 embryos per well in 5 mL of 10% Hank's Buffered Saline Solution (HBSS). Plates were wrapped in parafilm and incubated at 28.5 °C with a 14 h light/10 h dark cycle. Each day, embryos were inspected for dead or malformed embryos, which were removed. The plates then received a 99% media change by performing two separate 90% media changes. At 96 hpf, prior to infection, larvae were inspected once more and then received 3 separate 80% media changes to wash the larvae. Zebrafish husbandry and experiments involving live animals were approved by the North Carolina State University Institutional Animal Care and Use Committee.

Bacterial culture

Edwardsiella tarda, originally isolated from catfish, was provided as a gift from Carol Kim (University of Maine). Glycerol stocks of the bacterium were maintained at -80 °Celsius. *E. tarda* was grown in tryptic soy broth (TSB) liquid media (BD Biosciences catalog number 211825). TSB was prepared according to the manufacturer's instructions. *Edwardsiella* Isolation Media (EIM) agar plates were prepared for isolation of *E. tarda* from infected larvae as described previously (Shotts et al. 1990). Each week, the glycerol stock was streaked onto an EIM agar plate. This media is selective for *Edwardsiella* species, thus minimizing the chance of contamination of non-*Edwardsiella* spp. EIM also changes color from green to blue in the presence of *Edwardsiella*, and only colonies where this color change was observed were used.

Infection of larval zebrafish with *E. tarda*

The overall experimental design for infection can be seen in **Figure 1**. The day prior to infection, a single colony was grown overnight in TSB media at 28.5 °Celsius shaking at 200 RPM. On the morning of infection, 5 mL of the overnight culture was added to 45 mL of TSB in a volumetric flask, resulting in a 1:10 dilution. This culture was grown for 200 minutes at 28.5 degrees Celsius shaking at 200 RPM. Previous experiments determined that the bacterium is in a logarithmic growth phase at this time. After 200 minutes, the culture was transferred to a 50 mL conical tube and centrifuged at 4000 x g for 10 minutes. The supernatant was aspirated, and the pellet was resuspended in 1 mL of 10% HBSS and serially diluted. The initial dilutions were $5x10^9$, $5x10^8$, and $5x10^7$ colony forming units (CFU)/mL, and 100 µL of these dilutions were transferred into wells containing 5 mL 10% HBSS. This results in nominal concentrations of $1x10^8$, $1x10^7$, and $1x10^6$ CFU/mL. A well of uninfected larvae receiving only 10% HBSS was included as a negative control. Wells containing no larval zebrafish were also included as

controls for each dilution of the inoculum to assess background growth of *E. tarda* in the absence of a host. Once infected, plates were swirled to disperse the bacteria, and the plates were wrapped in parafilm. The plates were incubated at 28.5 °C for 4 hours. After four hours, all wells were washed by performing three separate 80% media changes with 10% HBSS. Plates were then wrapped in parafilm and incubated overnight at 28.5 °C.

Calculating CFU/mL to verify nominal inoculum concentrations

The dilutions created for the infection of the zebrafish were verified via growth on EIM to ensure nominal concentrations were the intended concentrations; these concentrations are referred to as "nominal" concentrations because their measured concentrations may vary slightly among experiments. However, since measured concentrations are within a log-fold of each other, we have chosen to describe them using this nomenclature. Using a 96 well plate, each initial dilution was diluted further to a dilution factor of 10^{-6}. Dilutions with dilution factors of 10^{-4}, 10^{-5}, and 10^{-6} were then plated on EIM. The EIM plates were wrapped in parafilm and incubated at 28.5 °C for 24 hours. Colonies were then counted to calculate CFU/mL.

Re-isolation of *E. tarda* from larval zebrafish

After overnight infection, larvae were anesthetized by adding MS-222 to each well at a final concentration of 100 mg/L. Larvae were then rinsed in 0.03% bleach for approximately 30 seconds. This bleaching step was included to kill any *E. tarda* that were external to the larvae. Larvae were then washed using three separate 80% media changes in 10% HBSS. After washing, larvae were anesthetized with MS-222 again prior to homogenization.

Larval zebrafish were homogenized using two different methods. Initial experiments used a manual homogenization that was modified from a method used for flow cytometry as described previously (Phelps et al. 2020). The methods for these experiments used only 10% HBSS and did

not use flow cytometry buffer, and larvae were not de-yolked prior to homogenization. Follow-up experiments used a bead beater. In a deep-well 96-well plate, wells were filled to half their volume with 1 milliliter glass beads. Groups of larvae were transferred to the wells. Final volume was consistent among all wells. The plate was then sealed and placed on the bead beater set to 3500 oscillations per minute for 1 minute.

After homogenization, the samples were transferred to a 96 well plate and were serially diluted by a factor of 100. The dilutions were plated, in triplicate, onto an EIM plate. Plates were then wrapped in parafilm and incubated for 24 hours at 28.5 °C. CFU/mL was calculated as described above. To obtain CFU per larva, CFU was divided by the number of larvae that were homogenized. This was done to account for any embryos or larvae that were removed due to death or malformation throughout the experiment. In the described experiments, death was not observed after infection at any concentration of *E. tarda.*

RESULTS

Verification of nominal concentrations

Initial experiments attempted to create a standard curve between optical density of the bacterial culture and CFU/mL. However, I observed that these two measures are not well-correlated in our system (data not shown). For this reason, I sought to grow the culture for a consistent amount of time (200 min) and ask if reproducible growth could be observed among biological replicates. As part of each experiment, the nominal inoculum concentration was verified through serial dilution, plating, and calculation of CFU/mL. CFU/mL were within the expected range for these nominal concentrations, and results were reproducible across 3 biological replicates (**Figure 2a**). This indicated that reproducible growth could be achieved across experiments.

Manual homogenization results in variable re-isolation of *E. tarda*

After infection with the nominal concentrations from **Figure 2a**, *E. tarda* was re-isolated from zebrafish larvae that were manually homogenized. From these infections, growth was observed among all three concentrations of inoculum (**Figure 2b**). The uninfected controls and control wells containing no fish had no growth, as expected. However, among the three replicates, the amount of re-isolated *E. tarda* was variable and inconsistent. For this reason, I hypothesized that this homogenization method was not sufficient for consistent re-isolation of the pathogen in this assay.

Homogenization via bead beater provides increased re-isolation of *E. tarda*

To ask whether a different homogenization approach improved re-isolation of *E. tarda*, we used a bead beater to homogenize pooled larvae after infection. It is worth noting that, at this time, only two biological replicates have been completed for these data. As with the first study, nominal concentrations of bacteria were confirmed and were reproducible between the two experiments (**Figure 3a**). Using the bead beater resulted in almost a log-fold increase in the amount of inoculum isolated per larva (**Figure 3b**) when compared to manual homogenization. Between both replicates, however, there exists a large difference in the amount of re-isolated bacteria in the $1x10^8$ CFU/mL treatment group (~3000 CFU per larva in Experiment 1 vs ~500 CFU per larva in Experiment 2). In the $1x10^7$ CFU/mL treatment group, though, growth was more consistent (~700 CFU per larva in Experiment 1 vs ~550 CFU per larva in Experiment 2). While no growth was detected in the controls where no larvae were present, growth was observed in the uninfected controls in one of these experiments.

DISCUSSION

In this study, I sought to begin optimizing a high-throughput *in vivo* infection assay in larval zebrafish. I have concluded that growing the inoculum for a consistent amount of time (200 min) allows for reproducible growth among three biological replicates, indicating the methods for growth are viable and that the larvae are infected with consistent and reproducible amounts of bacteria. Therefore, it can be concluded that issues with reproducibility do not lie with the bacteria and are likely due to genetic differences among clutches of larvae.

In infection experiments using manual homogenization, the three inoculum concentrations measured showed varied results among the experiments. The 10^8 CFU/mL concentration from each of the experiments, decreased over the course of this study (**Figure 2b**). For the 10^7 and 10^6 CFU/mL concentrations, the CFU per larva remained low among the experiments (**Figure 2b**), calling into question the sensitivity of this method. Upon testing the bead beater for homogenization (**Figure 3b**), I was able to re-isolate more of the inoculum than manual homogenization, thus improving sensitivity of the assay. However, variability between biological replicates remained at the highest concentration. This may indicate that the highest concentration is not suitable for this assay. From the perspective of high-throughput assay development, the "signal" (CFU per larva) in this assay may become saturated with too much "input" (inoculum) into the "system" (zebrafish larvae). Future work should work to identify an optimal concentration of inoculum for infection that provides reliable results.

The detection of growth from uninfected larvae was not entirely surprising for several reasons. First, the bead beater is a more sensitive method for homogenization, likely allowing for the enumeration and detection of bacteria of which there are very small amounts. Secondly, *Edwardsiella* spp. have been identified as part of the microbiome of zebrafish (Roeselers et al.

2011); because it is an opportunistic pathogen, it is likely present at low levels within our fish facility without causing harm. Lastly, EIM is specific media, but it is only specific to members of the genus *Edwardsiella*; there are many members of this species, which may mean we have isolated a microbe other than *E. tarda* in this approach. Regardless, future experiments will use a polymerase chain reaction (PCR) and DNA-sequencing approach to identify this microbe, based on strategies performed by previous researchers (Dubey et al. 2019). Accounting for background levels of *Edwardsiella* in this assay will be useful for future data analysis and determining the viability of this assay moving forward.

ACKNOWLEDGEMENTS

I would like to thank Mitsu Suyemoto (NC State University) for expert advice and insight that helped in the development of this assay.

FIGURES

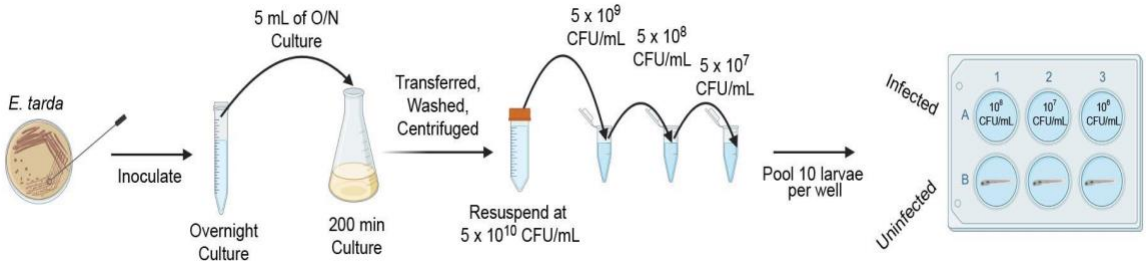

Figure 1. Protocol for *E. tarda* infections of zebrafish larvae. *E. tarda* are grown in tryptic soy broth (TSB) overnight to stationary phase and 5 mL are used to seed a 50 mL culture. After 200 min the culture is transferred to a 50 mL conical tube and centrifuged. The bacterial pellet is washed and resuspended at a density of 5 x 10^{10} colony forming units (CFU)/mL, and diluted to infect zebrafish larvae.

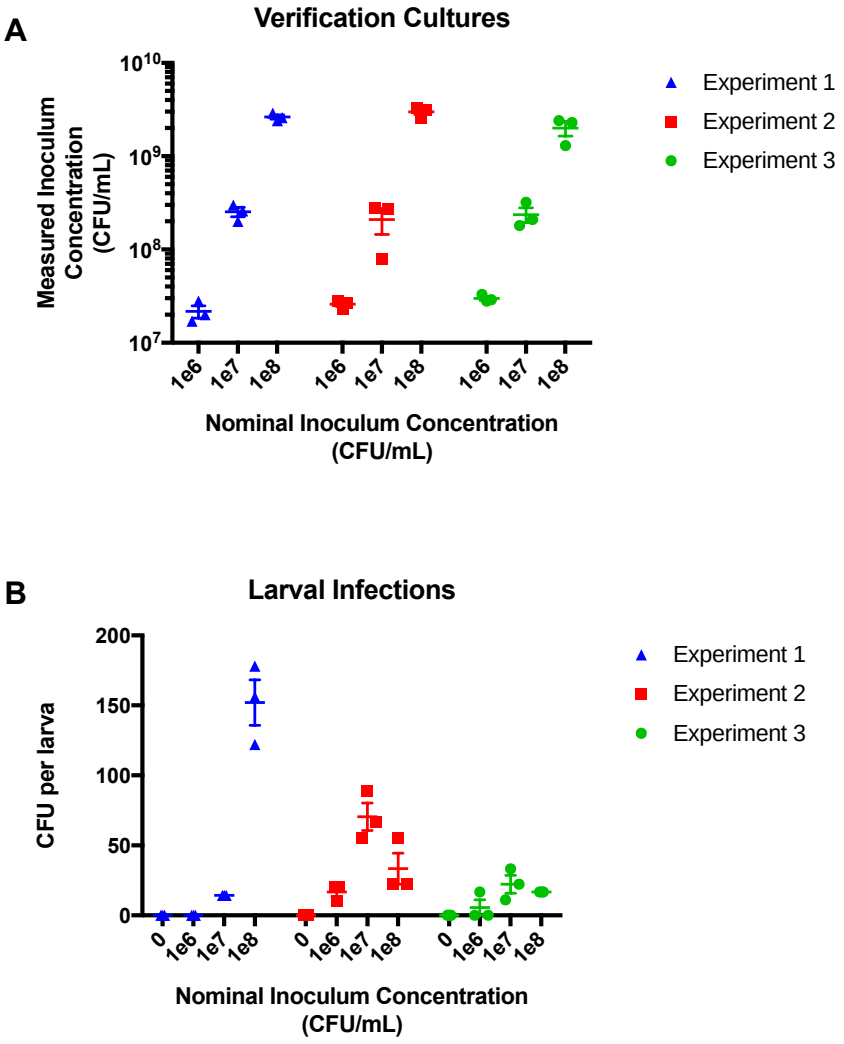

Figure 2. Manual homogenization re-isolated *E. tarda* from larval zebrafish with variability. (A) CFU/mL were measured for inoculum solutions used to infect zebrafish larvae in order to verify the accuracy of the nominal concentrations. Individual symbols represent technical replicates of plated spots that were counted. (B) After infection with *E. tarda*, zebrafish larvae were homogenized manually. Homogenates were plated on EIM and incubated at 28.5 °C for 24 hours. Colonies were then counted to calculate the CFU/mL per larva. Individual symbols represent technical replicates of plated homogenates that were counted.

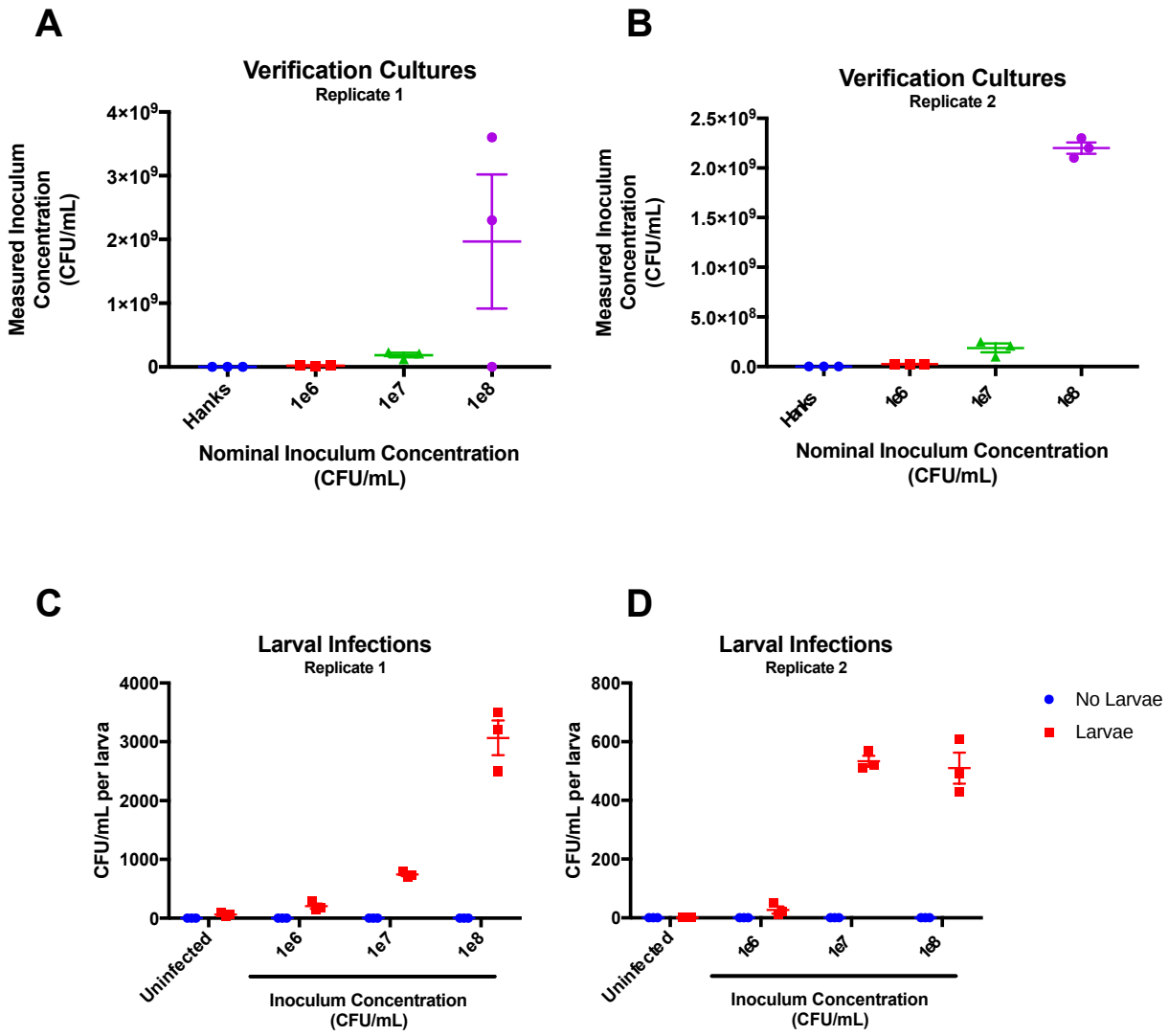

Figure 3. Homogenization via bead beater may re-isolate *E. tarda* from larval zebrafish reliably. (A,B) CFU/mL were measured for inoculum solutions used to infect zebrafish larvae in order to verify the accuracy of the nominal concentrations. Individual symbols represent technical replicates of plated spots that were counted. (C,D) After infection with *E. tarda*, zebrafish larvae were homogenized manually. Homogenates were plated on EIM and incubated at 28.5 °C for 24 hours. Colonies were then counted to calculate the CFU/mL per larva. Individual symbols represent technical replicates of plated homogenates that were counted.

REFERENCES

1. Dubey, S, Maiti, B, Kim, S-H, Sivadasan, SM, Kannimuthu, D, Pandey, PK, Girisha, SK, Mutoloki, S, Chen, S-C, Evensen, Ø, Karunasagar, I and Munang´andu, HM. 2019. Genotypic and phenotypic characterization of Edwardsiella isolates from different fish species and geographical areas in Asia: Implications for vaccine development. Journal of Fish Diseases. 42(6):835-850. doi: 10.1111/jfd.12984
2. Phelps, DW, Fletcher, AA, Rodriguez-Nunez, I, Balik-Meisner, MR, Tokarz, DA, Reif, DM, Germolec, DR and Yoder, JA. 2020. In vivo assessment of respiratory burst inhibition by xenobiotic exposure using larval zebrafish. J. Immunotoxicol. 17(1):94-104. doi: 10.1080/1547691X.2020.1748772
3. Pressley, ME, Phelan, PE, 3rd, Witten, PE, Mellon, MT and Kim, CH. 2005. Pathogenesis and inflammatory response to Edwardsiella tarda infection in the zebrafish. Dev Comp Immunol. 29(6):501-13. doi: 10.1016/j.dci.2004.10.007
4. Roeselers, G, Mittge, EK, Stephens, WZ, Parichy, DM, Cavanaugh, CM, Guillemin, K and Rawls, JF. 2011. Evidence for a core gut microbiota in the zebrafish. Isme j. 5(10):1595-608. doi: 10.1038/ismej.2011.38
5. Shotts, EB and Waltman, WD, 2nd. 1990. A medium for the selective isolation of Edwardsiella ictaluri. J Wildl Dis. 26(2):214-8. doi: 10.7589/0090-3558-26.2.21